CLIMATE CHANGE IMPACTS ON HYDROLOGIC COMPONENTS AND OCCURRENCE OF DROUGHT IN AN AGRICULTURAL WATERSHED

_____

A Dissertation

presented to

the Faculty of the Graduate School

at the University of Missouri

_____

In Partial Fulfillment

of the Requirements for the Degree

Doctor of Philosophy

_____

by

SAGAR GAUTAM

Dr. Christine Costello, Dissertation Supervisor

DECEMBER 2018

_____

The undersigned, appointed by the dean of the Graduate School, have examined the dissertation entitled

CLIMATE CHANGE IMPACTS ON HYDROLOGIC COMPONENTS AND OCCURRENCE OF DROUGHT IN AN AGRICULTURAL WATERSHED

presented by

SAGAR GAUTAM

a candidate for the degree of

DOCTOR OF PHILOSOPHY

and hereby certify that, in their opinion, it is worthy of acceptance.

_____

Dr. Christine Costello

Department of Industrial & Manufacturing Systems Engineering

_____

Dr. Allen L. Thompson

Department of Bioengineering

_____

Dr. Claire Baffaut

Soil, Environmental and Atmospheric Sciences and USDA ARS

_____

Dr. John Sadler

Department of Bioengineering and USDA ARS

ACKNOWLEDGMENTS

LIST OF TABLES

LIST OF FIGURES

ABSTRACT

CLIMATE CHANGE IMPACTS ON HYDROLOGIC COMPONENTS AND OCCURRENCE OF DROUGHT IN AN AGRICULTURAL WATERSHED

SAGAR GAUTAM

2018

The study on potential acceleration of future hydrologic cycle due to change in precipitation and increase in temperature are essential for managing natural resources and setting policy. The impact of future climate change on hydrologic components of Goodwater Creek Experimental Watershed (GCEW) and experimental field (Field1) were assessed using climate datasets from the Coupled Model Intercomparison Project Phase 5 (CMIP5), Soil and Water Assessment Tool (SWAT) and Agricultural Policy Environmental Extender (APEX). SWAT and APEX models were setup and calibrated for watershed and field scale using observed hydrology data at their respective outlets. The study identified future (2016-2075) occurrence of meteorological, hydrological, agricultural droughts, and extreme events based on projections of future climate in the GCEW and SWAT simulations. Standardized Precipitation Index, Standardized Streamflow Index, and Soil Moisture Index were used to represent the three types of drought. CMIP5 data were downscaled to watershed and field scale using quantile mapping for precipitation and delta method for temperature. Historical and future ensembles of downscaled precipitation and temperature, and modeled water yield, surface runoff, and evapotranspiration were compared. At the watershed scale, ensemble SWAT simulated results indicated increased springtime precipitation, water yield, surface runoff and a shift in evapotranspiration peak one month earlier in the future. At field scale, two management system business-As-Usual (BAU) and Aspirational (ASP) management system were compared to access the environmental benefits of improved management

system using APEX model. Simulated results indicated that the change in management alone from BAU to ASP during historic period resulted in 25% (162 mm to 120 mm) reduction in surface runoff. The simulated average annual runoff loss was reduced by 16.5% (192 mm to 160 mm) and 18.8% (203 mm to 165 mm) in ASP scenario compared to BAU for ensemble of RCP 8.5 for near and far future respectively. The average ensemble annual soluble nitrogen loss was 8 kg/ha for BAU compared to 3.9 kg/ha for ASP management for baseline historic period. Result indicated the inclusion of no-till and winter cover crop resulted in increased subsurface flow. The result indicates the environmental benefit of crop rotation and cover crop with reduction in runoff and nutrient losses. The ASP management provides surface cover all year round and improves soil quality resulting in lower runoff.

At watershed scale, the outputs from SWAT model and downscaled climate data were used for drought projection and extreme analysis. Historical drought events were calculated based on observed precipitation and SWAT simulated streamflow and soil moisture datasets for the period of 1980-2015. The physical values corresponding to the indices used to identify drought in the past were used to characterize drought in the future. The analysis of multiple drought types provides multiple perspectives for evaluating drought under future climate. All three drought indices indicate increased projected drought occurrence for the future in this region for both RCP 4.5 and RCP 8.5 emission pathways. Seven different indices developed by the Expert team on Climate Change Detection Monitoring Indices (ETCCDMI) were calculated on an annual scale for extreme analysis. The simulated results based on extreme indices indicated increased warm spell duration along with projected decline in summer precipitation favoring summer drought for study region. To evaluate the performance

of model spatial resolution, gridded surface runoff estimated by Lund–Potsdam–Jena managed Land (LPJmL) and Jena Diversity-Dynamic Global Vegetation model (JeDi-DGVM) were compared to SWAT. Long-term comparison shows 6-8% higher average annual runoff estimation for LPJmL and 5-30% estimation prediction for JeDi-DGVM compared to SWAT simulated average annual runoff. Although annual runoff estimation showed little change for LPJmL, monthly runoff projection under estimated peak runoff and over-estimated low runoff for LPJmL compared to SWAT simulated runoff. The reasons for these differences include difference in spatial resolution of model inputs and mathematical representation of physical processes. Results indicate benefits of impact assessments at local scales with heterogeneous sets of parameters to adequately represent extreme conditions that are muted in global gridded model studies by spatial averaging over large study domains. An overall result based on simulation study indicated increased extreme precipitation and temperature resulting in increased runoff and change in evapotranspiration peak. Drought projection results indicated increased frequency of drought months for future. Field scale simulation results indicates management change to ASP is beneficial for reduction of runoff and nutrient under changing future with more extremes.

CHAPTER 1

INTRODUCTION

Increased pressure on natural and environmental systems is a major global challenge with world population heading toward 9.7 billion by 2050. There is a scientific consensus that climate change is occurring primarily due to increased greenhouse gas (GHG) emissions with 97% of peer-reviewed scientific literature indicating that humans are the cause (Cook et al., 2013). Climate, defined as long-term patterns of day-to-day weather, is a major driver of hydrological processes, therefore climate change will ultimately affect hydrology, water resources and agriculture. Uncertainty still exists with regard to how a warming climate and corresponding changes in weather patterns will impact Earth systems that humans utilize in order to sustain life. Increased GHG concentrations alter the radiative balance of the Earth's atmosphere, causing an increase in average temperature and change in precipitation patterns (Cubasch et al., 2013). Additionally, the impacts of this change in climate has been widely reported in literature, observation and simulation results indicate an increased probability of extreme precipitation in response to the changing climate (O'Gorman, 2015). The Intergovernmental Panel on Climate Change (IPCC) fourth assessment report (IPCC, 2007) and the fifth assessment report (IPCC, 2014) document the comprehensive modeling effort for simulating future climate. The potential impact of climate change is a major concern, as we have witnessed frequent hydrologic extremes in past few decades.

The uncertainty regarding the future impact of climate change has become an important topic for water resource managers around the world as climate change is projected to have significant impacts on hydrologic components (Vetter et al., 2017).

One way to understand the relationship between climate change and hydrology includes the use of process-based models to simulate the various components of the hydrologic cycle. Process models calibrated based on historic data can be perturbed with future climate projection to understand the impacts of future change. There is a plethora of hydrologic models available to simulate hydrology at different scales. The Agricultural Policy Environmental eXtender (APEX) and the Soil Water Assessment Tool (SWAT) are the two most widely used models applied for climate change impact assessment at small and large scales, respectively. Both of these models include algorithms for predicting how precipitation, temperature, and CO_2 concentration affect plant growth and hydrologic components. The expected change in precipitation and temperature under elevated CO_2 future can impact the hydrologic cycle and can ultimately impact crop production. Understanding how these changes impact future water availability and, correspondingly, potential influences to agricultural productivity are very important for policy decision making.

The climate projections from General Circulation Models (GCM) can be used as an input to hydrologic models to simulate the impact of climate change on water resources. The hurdles for climate change impact assessment on hydrology are associated with uncertainty from both the hydrologic modeling approaches and the climate projections. The climate data are the product of GCMs, which are three-dimensional numerical models built to represent the physical dynamics of the Earth's atmosphere, land surface, ocean surface and to predict system behavior under increasing GHG concentration in the atmosphere (IPCC, 2013). Major sources of uncertainty when coupling climate and hydrologic models are climate model uncertainty and uncertainty in downscaling of available GCM output to spatial resolutions required for hydrologic models (Praskievicz and Bartlein, 2014). GCM

temperature and precipitation outputs are provided at a very large spatial resolution (87.5 km × 87.5 km) making it difficult to apply to local geospatial scales in order to model more localized systems. Even the resolution provided through the Coupled Model Intercomparison Project (12 km × 12 km) is often too coarse for assessing impacts on hydrologic components at small basin scale. Although a few studies have focused on quantifying the impact of future climate on hydrologic processes at a regional scale in the Midwestern United States (Jha et al., 2004b; Stone et al., 2003), there have been minimal studies at smaller scales. Climate scenarios downscaled from GCM using either dynamical or statistical downscaling, provide the best available information for assessing future impacts of climate change on water resources (Ayar et al., 2016; Gleick, 1989). The greatest challenge for planning for adaptation to climate change is lack of certainty, particularly with respect to time, about the impacts of climate change. In order to make the best adaption plan, it is very important to improve the accuracy and reliability of analysis regarding the possible impacts on key systems due to future climate change.

The potential acceleration of the hydrologic cycle due to changes in precipitation and increases in temperature is likely to result in increased occurrence of hydrologic extremes such as excessive wet and dry periods. These changes in climate alter the dry/wet conditions, which ultimately impact agriculture. The climate extreme study based on observed data at global scale suggests that the changes in precipitation are amplified for both tails and change in temperature extremes have been observed (Meehl et al., 2000). Both lack of and excess precipitation will impact agriculture; lack of precipitation during the growing season leads to stress in plants and excess precipitation hinders field operations. Future projection of extreme conditions can be

helpful for decision making for policy makers as future projection help to design better mitigation strategy.

Drought can have significant impacts on crop yield. For an instance, the 2012 drought event in the United States alone resulted in $17.3 billion damages due to lost crop production (O'Connor, 2013). Drought is the condition of prolonged deficiency of water below normal (Redmond, 2002). Drought is a natural hazard that occurs due to prolonged dry spells resulting in reduction of soil water and ultimately low river flow. Drought characterization using real-time data and short-term projection of weather can help to provide early drought warning and drought risk analysis, which can help for drought preparedness (Zargar et al., 2011). In addition, the drought can be anticipated for future using future projection of hydrologic components. Droughts definitions differ based on disciplinary perspective; meteorological, agricultural, and hydrological droughts are the major types of biophysical drought of interest from environmental and agriculture perspectives (Wilhite and Glantz, 1985). Multiple drought indices are used within this dissertation to quantify different drought types acknowledging uncertainty in climate model and indices itself. The use of multiple indices, defined using different critical variables, can help better understand drought and its associated impacts. A previous study on drought modeling suggests the use of multiple drought indices is necessary to quantitatively evaluate drought conditions (Tian et al., 2018).

Climate change impact assessments using simulation models applied at global, regional and local scales are abundant in recent literature (Al-Mukhtar et al., 2014; Ficklin et al., 2013; Giuntoli et al., 2015; Jha et al., 2004a; Panagopoulos et al., 2014; Stone et al., 2003). However, there have not been many attempts to compare results and their implications at different scales to identify how differences in the aggregation

of weather and geographically defined elements of the physical environment, e.g., soil data, model assumptions, and extent of calibration affects simulated results. This study is conducted at Goodwater Creek Experimental Watershed (GCEW) and field (Field 1) located within the watershed to simulate the impact of future climate change on hydrology and future extreme using hydrologic model and climate model outputs. Simulating and projecting future hydrology and extremes using multiple models can help evaluate and recommend solutions appropriate for particular risk and adaption question.

Objectives

In this dissertation, analysis is conducted to represent two different scales within the same geographic location, the watershed scale (GCEW) and field scale (Field 1 located within GCEW). GCEW is a headwater watershed in the Salt River Basin and the geophysical context of the study area represents the Central Claypan region, which includes Northeast Missouri, Southeast Iowa and Southern Illinois (Baffaut et al., 2015; Sadler et al., 2015). The information gained from this study on hydrologic changes in the face of climate change is instrumental for the region characterized by claypan soils and generally contributes to understanding how modeling at different scales reflects the impact of climate change on hydrology, and relatedly on agriculture. The projection can be useful for policy makers as future projections of hydrologic conditions and extremes help to design better mitigation strategies. The overall study was divided into three sub-studies (mentioned below), and separate objectives were developed for each study.

Study 1. This study was entitled "Assessing Long-Term Hydrological Impact of Climate Change Using an Ensemble Approach and Comparison with Global Gridded Model-A Case Study on Goodwater Creek Experimental Watershed" with the specific objectives to contribute to the body of knowledge developed in conjunction with the Long-Term Agroecosystem Research (LTAR) project in the GCEW, to characterize the potential hydrological impacts in relation to climate change in the GCEW, and to compare hydrological outputs from models of different spatial resolution, as well as with and without localized downscaling of weather data.

Study 2. This study was entitled "Multi-index Evaluation of Future Drought and Climate Extreme Occurrence in an Agricultural Watershed" with the specific objectives to project how drought and climate extremes may change in the future relative to historic trends using the hydro-model outputs (soil water, streamflow) from a calibrated hydrologic model (Soil and Water Assessment Tools (SWAT)).

Study 3. This study was entitled "Assessing the Climate Change Impacts on Hydrology and Water Quality: A case study on a field located at Central Missouri." with the specific objectives of determining the environmental benefits of application of alternative management practices including no-till, cover crops and longer crop rotation on a field compared to business as usual.

References

Al-Mukhtar, M., Dunger, V., and Merkel, B. (2014). Assessing the Impacts of Climate Change on Hydrology of the Upper Reach of the Spree River: Germany. *Water Resources Management* **28**, 2731-2749.

Ayar, P. V., Vrac, M., Bastin, S., Carreau, J., Déqué, M., and Gallardo, C. (2016). Intercomparison of Statistical and Dynamical Downscaling Models under the Euro-and Med-Cordex Initiative Framework: Present Climate Evaluations. *Climate Dynamics* **46**, 1301-1329.

Baffaut, C., John Sadler, E., Ghidey, F., and Anderson, S. H. (2015). Long-Term Agroecosystem Research in the Central Mississippi River Basin: Swat Simulation of Flow and Water Quality in the Goodwater Creek Experimental Watershed. *Journal of Environmental Quality* **44**, 84-96.

Cook, J., Nuccitelli, D., Green, S. A., Richardson, M., Winkler, B., Painting, R., Way, R., Jacobs, P., and Skuce, A. (2013). Quantifying the Consensus on Anthropogenic Global Warming in the Scientific Literature. *Environmental Research Letters* **8**, 024024.

Cubasch, U., D. Wuebbles, D. Chen, M.C. Facchini, D. Frame, N. Mahowald, and Winther, J. G. (2013). Introduction: The Physical Science Basis. Contribution of Working Group I to the Fifth Assessment Report of the Intergovernmental Panel on Climate Change [Stocker, T.F., D. Qin, G.-K. Plattner, M. Tignor, S.K. Allen, J. Boschung, A. Nauels, Y. Xia, V. Bex and P.M. Midgley (Eds.)]. *Climate Change*.

Ficklin, D., Stewart, I., and Maurer, E. (2013). Effects of Projected Climate Change on the Hydrology in the Mono Lake Basin, California. *Climatic Change* **116**, 111-131.

Giuntoli, I., Vidal, J.-P., Prudhomme, C., and Hannah, D. M. (2015). Future Hydrological Extremes: The Uncertainty from Multiple Global Climate and Global Hydrological Models. *Earth System Dynamics* **6**, 267.

Gleick, P. H. (1989). Climate Change, Hydrology, and Water Resources. *Reviews of Geophysics* **27**, 329-344.

IPCC (2007). (Intergovermental Panal on Climate Change), Working Group I. Climate Change 2007: The Physical Science Basis. In : Solomon, S., D. Qin, M. Manning, Z. Chen, M. Marquis, K.B. Averyt, M. Tignor and H.L. Miller (Eds.), Contribution of Group I to the Fourth Assessment Report of the Intergovernental Panael on Climate Change.

IPCC (2013). What Is a GCM? *In* "Guidance on the use of data". Data Distribution Centre.

IPCC (2014). "Climate Change 2014: Mitigation of Climate Change.," Cambridge University Press, Cambridge, United Kingdom and New York, NY, USA.

Jha, M., Pan, Z., Takle, E. S., and Gu, R. (2004a). Impacts of Climate Change on Streamflow in the Upper Mississippi River Basin: A Regional Climate Model Perspective. *Journal of Geophysical Research: Atmospheres* **109**, 1-12.

Jha, M. K., Arnold, J. G., Gassman, P. W., and Gu, R. R. (2004b). Climate Change Sensitivity Assessment on Upper Mississippi River Basin Streamflows Using Swat. *Journal of the American Water Resources Association* **42**, 997-1015.

Meehl, G. A., Zwiers, F., Evans, J., Knutson, T., Mearns, L., and Whetton, P. (2000). Trends in Extreme Weather and Climate Events: Issues Related to Modeling Extremes in Projections of Future Climate Change. *Bulletin of the American Meteorological Society* **81**, 427-436.

O'Connor, C. (2013). Soil Matters: How the Federal Crop Insurance Program Should Be Reformed to Encourage Low-Risk Farming Methods with High-Reward Environmental Outcomes. *In* "Agricultural & Applied Economics Association's 2013 Crop Insurance and the Farm Bill Symposium, Louisville, Kentucky".

O'Gorman, P. A. (2015). Precipitation Extremes under Climate Change. *Current Climate Change Reports* **1**, 49-59.

Panagopoulos, Y., Gassman, P., Arritt, R., Herzmann, D., Campbell, T., Jha, M., Kling, C., Srinivasan, R., White, M., and Arnold, J. (2014). Surface Water Quality and Cropping Systems Sustainability under a Changing Climate in the Upper Mississippi River Basin. *Journal of Soil and Water Conservation* **69**, 483-494.

Praskievicz, S., and Bartlein, P. (2014). Hydrologic Modeling Using Elevationally Adjusted Narr and Narccap Regional Climate-Model Simulations: Tucannon River, Washington. *Journal of Hydrology* **517**, 803-814.

Redmond, K. T. (2002). The Depiction of Drought: A Commentary. *Bulletin of the American Meteorological Society* **83**, 1143-1147.

Sadler, E. J., Lerch, R. N., Kitchen, N. R., Anderson, S. H., Baffaut, C., Sudduth, K. A., Prato, A. A., Kremer, R. J., Vories, E. D., and Myers, D. B. (2015). Long-Term Agroecosystem Research in the Central Mississippi River Basin: Introduction, Establishment, and Overview. *Journal of Environmental Quality* **44**, 3-12.

Stone, M. C., Hotchkiss, R. H., and Mearns, L. O. (2003). Water Yield Responses to High and Low Spatial Resolution Climate Change Scenarios in the Missouri River Basin. *Geophysical Research Letters* **30**.

Tian, L., Yuan, S., and Quiring, S. M. (2018). Evaluation of Six Indices for Monitoring Agricultural Drought in the South-Central United States. *Agricultural and Forest Meteorology* **249**, 107-119.

Vetter, T., Reinhardt, J., Flörke, M., van Griensven, A., Hattermann, F., Huang, S., Koch, H., Pechlivanidis, I. G., Plötner, S., and Seidou, O. (2017). Evaluation of Sources of Uncertainty in Projected Hydrological Changes under Climate Change in 12 Large-Scale River Basins. *Climatic Change* **141**, 419-433.

Wilhite, D. A., and Glantz, M. H. (1985). Understanding: The Drought Phenomenon: The Role of Definitions. *Water International* **10**, 111-120.

Zargar, A., Sadiq, R., Naser, B., and Khan, F. I. (2011). A Review of Drought Indices. *Environmental Reviews* **19**, 333-349.

CHAPTER 2

LITERATURE REVIEW

Climate Change Impact on Hydrology

The major reason for climate change is the emission of greenhouse gases (GHG) due to extensive use of fossils fuels and other anthropogenic activities, such as deforestation. Increased GHG concentrations are altering the radiative balance of the Earth's atmosphere, causing an increase in average surface temperature and change in precipitation patterns and intensity (Cubasch et al., 2013). GHGs emissions have increased significantly since the pre-industrial era, driven largely by population and economic growth (Pachauri et al., 2014). These trends are projected to continue and intensify in the future. Climatic shift due to global warming has been linked to water supply shortages (De Wit and Stankiewicz, 2006), declining biodiversity (Gregory et al., 2009) and other ecosystem damage (Walther et al., 2002). It is very important to understand how these changes could affect hydrologic components and, correspondingly, potential influences to agricultural productivity. Climate change, especially the changes in precipitation and temperature have been found to impact the hydrology and ultimately the water availability at local and regional scales (Barnett et al., 2005). Outputs from climate models are widely used in hydrologic simulation models to assess the climate change impacts on streamflow (Ficklin et al., 2013a; Ouyang et al., 2015), nutrient loading (Jha et al., 2015), and crop productivity (Panagopoulos et al., 2014), and to ultimately assist farm decision-making processes. Climate changes also affect the snowmelt dynamics. Many studies have found a shift in the timing of peak streamflow as increased temperatures cause snowmelt in early spring and result the drier streams in summer (Ficklin et al., 2013a; Ficklin et al., 2013b), which may directly impact the agricultural activity and the aquatic life.

Results from climate change impact assessment studies on hydrology suggest that climate change will have more impact on hydrologic extremes rather than on mean conditions. A study conducted by (Huang et al., 2014) in Europe to assess the impact of climate change on drought and flood event indicates frequent occurrences of 50-year floods and droughts.

Management Impacts on Hydrology

Management change includes any kind of structural and non-structural change in an agricultural management system, including tillage operations and the sequence of crop. Agriculture is managed with diverse management systems that include tillage (no-till, plow-till and conservation till), diverse cropping system including rotation, cover crop, hay pasture and grazing. Crop rotation includes rotation of crop every year in a sequence, for example corn-soybean rotation where corn and soybean are planted alternatively year after. The major benefits of a crop rotation include: improved soil fertility and structure, inclusion of legume in rotation ensure the nitrogen supply for preceding crop and control weed, pest and disease infestation to crop (FAO, 2006). In addition to crop rotation, incorporation of cover crop and conservation tillage such as no-till can provide environmental benefits such as improved soil structure and carbon sequestration leading to improved water quality (Hoorman, 2009; Reeves, 1997). Management system applied in a field impact the physical and biological properties of soil such as soil organic carbon, bulk density, and alter the year-to-year surface cover (Bari et al., 1993; Bhattacharyya et al., 2006; Dabney, 1998). The surface cover and soil properties affect the movement of water through soil by infiltration and evaporation. Therefore, the management system directly affects the hydrologic cycle.

Hydrologic Simulation Models

Hydrologic simulation models are useful tools to assess cause and effect relation. Simulation models are frequently used for assessing management and climate change impacts on hydrologic components. Outputs from climate models are widely used in hydrologic simulation models to assess the bounds of a system and to assist decision-making processes toward a sustainable future (Moss et al., 2010). The impacts of these changes on water quantity and quality are a major question as it affects crop productivity, environmental sustainability and economic benefits. Models are important tools for evaluating the movement of water and the transport of nutrient across complex land surfaces given weather conditions to analyse the potential benefits of alternative management systems (Dabney et al., 2001). The model based approach of simulating the impact of alternative management and future projection is a cost effective method. However, model results need to be compared with observed set of data to have trust in the simulation results. The well-calibrated and validated hydrologic model can be readily used for scenario analysis for decision-making. Hydrologic simulation studies are cost effective tool for impact assessment with availability of data required for hydrologic modeling over space and time in geographic information system (GIS) including climate, soil, land use land cover and hydrology data (Gurtz et al., 2005). In past few decade, many hydrologic models were developed and used for modeling the hydrologic component at different spatial scales. Hydrologic models combined with Geographic Information System (GIS) and improved computational capability provide options for long term simulation, data management and visualization during modeling (Suia and Maggiob, 1999). The widely used models for simulating water quantity and quality at different scales include; Environmental Policy Integrated Climate (EPIC) model (Williams et al.,

1984), Soil and Water Integrated Model (SWIM) (Krysanova et al., 2000), Dynamic Watershed Simulation Model (DWSM) (Borah et al., 2002), Chemicals, Runoff, and Erosion from Agricultural Management Systems (CREAMS) (Knisel, 1980), Soil and Water Assessment Tool (SWAT) (Arnold et al., 1998), Agricultural Non-Point source pollution model (Young et al., 1987), Agricultural Land Management Alternatives with Numerical Assessment Criteria (ALMANAC) (Kiniry et al., 1992) and Variable Infiltration Capacity (VIC) (Liang, 1994). Although there are many models available for impact assessment, uncertainties are major hurdles for impact assessment studies using hydrologic models; uncertainties associated with the hydrologic model parameterization, where modelers have to assign a value to unmeasurable model parameters based on model evaluation, and uncertainties in model structure. However, for application of hydrologic models for climate change impact assessment, climate model uncertainty is higher than model parameter uncertainty (Bennett et al., 2012; Sellami et al., 2016).

Agricultural Policy/Environmental eXtender

Agricultural Policy Environmental eXtender (APEX) is an extended version of the crop and soil productivity simulation model (Environmental Policy Integrated Climate (EPIC)) , built to simulate the effect of soil erosion on crop productivity (Williams and Izaurralde, 2005). APEX model was designed to enhance the capability of EPIC to extend its scope as a watershed and land management simulation model. APEX model is capable to simulate multiple land management systems; furrowing diking, buffer strips, terraces, waterways, lagoons, manure management, crop rotation, fertilizer and chemical application and grazing management on hydrology (Williams et al., 2000). The major components of the APEX model includes climate, hydrology, pesticide fate, crop growth, erosion-sedimentation, carbon cycling, management

practices, soil temperatures, nutrient fate, plant control environment, subarea/routing and economic (Gassman et al., 2010). Climate inputs to the APEX model include daily weather variable: precipitation, temperature (minimum and maximum), solar radiation, wind speed and relative humidity. APEX model is capable to simulate both water quantity and water quality. It has been used extensively for both fields and small watersheds for assessing the impact of different management options; for instance, simulating fate of herbicide (Harman et al., 2004), simulating forested watersheds (Wang et al., 2007), simulating the impact of buffer width and stocking density (Kumar et al., 2011), and impact of grass waterways (Anomaa Senaviratne et al., 2013) and climate change (Gautam et al., 2015) on runoff and water quality.

Soil and Water Assessment Tool

The Soil and Water Assessment Tool (SWAT) is a process based daily time step distributed watershed scale hydrologic simulation model (Santhi et al., 2001). SWAT has the capability to simulate stream flow as a function of land management, soil, climate and topography. Similar to APEX, the components of SWAT include climate, hydrology, pesticide fate, nutrient fate, plant growth, erosion-sedimentation, carbon cycling, management practices, and soil temperatures. In SWAT , the watershed is subdivided into the sub watersheds, and these sub-watersheds are further divided into hydrologic response units (HRU), which consist of homogeneous soil, management and topography (Arnold et al., 2012). These subdivisions enable better representation of the heterogeneity of the watershed and better prediction of hydrology. SWAT is one of the intensively used models to study the management, climate change and other alternative on the stream flow (Bekele and Knapp, 2010; Jayakrishnan et al., 2005; Parajuli, 2010; Wang et al., 2014). The SWAT model has been widely used to assess the climate change impacts on nutrient loading (Jha et al., 2015), crop

productivity (Panagopoulos et al., 2014), and streamflow (Ficklin et al., 2013a; Ouyang et al., 2015). The SWAT model is one of the most widely used decision-making tools among hydrologists for predicting the impact of agricultural land use, climate change and management on sediment, water and chemical yields. Although the model is data intensive, SWAT coupled with GIS interface has provided an opportunity to integrate readily available GIS datasets to simulate hydrology.

Scaling Issue in Hydrologic Modeling

Models can be used to predict and forecast different phenomena at different spatio-temporal scales in which the experimal measurement are not possible due to economical and resource limitation. These changes in scale involve some sort of exteraploation and transfer of infromation across the scale. The potential of inappropriate representation of processess increases with changes in spatial and temproal dimension of hydrologic model (Baffaut et al., 2015). Hydrological processes occur at a wide range of scales, from unsaturated flow in soil layer to flood in river system of a multiple acerage (Blöschl and Sivapalan, 1995). The transfer of information from one scale to another is known as scaling and problems associated during this process are refered as scaling issues. In hydrologic prospective, upscaling refers to transfering information from a given scale to large scale, conversly downscaling refers to transfering information to smaller scale. For example, measuring soil moisture content at a point within a field and assuming it applies to the surrounding area involves upscaling. The observed hydrologic measurements are coarser spaced in space compare to time, therefore most of the extrapolation schemes are carried in the space domain (Blöschl and Sivapalan, 1995). In the past few years the importance of issue of scaling in hydrology has increased due to increased environmental awareness. The challenges on simulating hydrology include the

adequacy of mathematical description to represent the multiple processes occurring in the system (Freeze and Harlan, 1969). How to best represent the small scale heterogeneities on large-scale fluxes, and the movement of water across landscape and soil are major research challenges (Clark et al., 2017). Additionally, determining the scale for impact modeling is still a big question. Modeling multiple scales and comparing the knowledge from one scale to another can be an option to determine the impact of scale on hydrologic simulation.

Global Climate Models

Climate change research has been well supported since the early 1980s by the development of General Circulation Models (GCMs). GCMs are the most advanced and readily available tools for simulating the response of the Earth's climate to changing atmospheric composition. GCMs are numerical models coupled with ocean models, land-use models, economic and future development models, and provide an arena for the study of climate change impacts on different processes involved in the atmosphere (Fowler et al., 2007). The work on climate models started in 1960, with release of first (1990), second (1995), third (2001), fourth (2007) and fifth (2013) assessment reports (IPCC, 2001; Wang, 2005). The spatial resolution has improved over this period; the first assessment report data resolution was 500 km^2 compared to 87.5 km^2 in the fifth assessment report . In the fifth assessment report the emission scenarios are based on radiative forcing known as representative concentratation pathways (RCPs). These radiative forcing scenarios are based on the change in radiative forcing at the end of 2100 relative to the preindusturial period. The fifth assessment reports consist of four different RCPs, which are named based on change in radiative forcing by 2100; 2.6, 4.5, 6.0 and 8.5 watts per square meter (W/m^2) (Hayhoe et al., 2017). Although there is ample data available from GCMs,

uncertainity are still there. Major sources of uncertainties of climate model outputs include downscaling of available GCM output to spatial resolutions required for hydrologic models (Praskievicz and Bartlein, 2014) and uncertainty between Global Climate Models (GCMs) and within a GCM (Peel et al., 2014).

Climate Bias, Downscaling Need and Ensemble Approach

The climate projection from general circulation models (GCM) are used as an input to hydrologic models to simulate the impact of climate change on water quality and quantity at multiple scale. Coupled Model Intercomparison projects from fourth and fifth assessment reports (CMIP3 and CMIP5) of IPCC have opened a wide space for impact assessment research. Climate output from multiple, well-established Global Circulation Models (GCMs) are available for both CMIP3 and CMIP5. CMIP3 simulations of the 21st century were based on emission scenarios from the Special Report on Emissions Scenarios (SRES) (IPCC, 2000) and CMIP5 emission scenarios are based on representative concentration pathways (RCPs) (van Vuuren et al., 2011). GCM bias for the application in hydrologic model is a major challenge due to its coarse resolution, which involves the spatial averaging. When these biased data are used in hydrologic model, it leads to the uncertainties in impact assessment. There is a need to bridge the gap between the coarse resolution of climate models and the resolution needed for impact assessment for application of climate change scenarios to hydrological models. As defined in earlier section there is still uncertainty in climate model output based on scale of operation. Thus, a widely used approach in the climate community has focused on developing a technique to bridge the gap known as 'bias correction'. Bias corrections include adjusting GCM outputs, basically temperature and precipitation results, based on the bias found between observed and predicted value during period of observation. Ensemble modeling is widely adopted in

16

impact assessment studies; multimodal ensemble modeling can help to present the result as median surrounded band of possible range (Perez et al., 2014). The better prediction of multimodal ensemble average to any individual GCM has been already found for global study for examining the mean climate as the ensemble model shows range of possible case along with median (GCM) (Pierce et al., 2009b)**.** In use of a single model, predictions may be highly influenced by predictive error associated with selected GCM (Pierce et al., 2009b).

Climate Change and Future Extreme Weather Events

Anthropogenic GHG emission to atmosphere is a factor for rapid warming of Earth (IPCC, 2007). Major concerns of climate change include extreme weather events as majority of effects are due to these events. The major impacts of climate change include increased temperature and change in precipitation extremes, which result in intensification of hydrological cycle leading to more floods and drought (Rosenzweig et al., 2001). In some areas, more winter precipitation is projected to fall as rain instead of snow, decreasing snowpack and spring runoff and potentially exacerbating spring and summer droughts. The Intergovernmental Panel on Climate Change (IPCC) points out increased risk of drought and extreme events during the 21st century across the globe (IPCC, 2007, 2014). Majority of study for projecting drought are conducted using drought indices where variable like precipitation, streamflow and soil water are used as proxy for drought quantification. Studies on drought projection have been conducted using climate scenarios and process based hydrologic models and studies have been conducted at different scale; global scale (Hirabayashi et al., 2008; Sheffield and Wood, 2008; Touma et al., 2015; Wang, 2005), regional scale (Huang et al., 2015; Romanowicz and Wong, 2016), and watershed scale (Liu et al., 2012; Vu et al., 2015; Wang et al., 2011). The majority of these studies indicate projected

increases in spatial and temporal distribution of drought for future. There is a strong need of projecting drought and climate-induced risk at small scale as global and regional scale projection misrepresent local scale details.

Uncertainty in Climate Change Impact Assessment

Major sources of uncertainty in predicting climate change on hydrologic response in future includes uncertainty associated with climate model emission scenarios. These scenarios are very hypothetical and reality totally depends on global, political, and economic conditions that will define how future of emission will look like. Other sources include; uncertainty associated with general circulation models (GCMs) (as we know model will not be able to represent the system completely and it will be even harder to model dynamic system like atmosphere); uncertainty caused by the bias correction/downscaling technique used for converting the coarse scale GCM output to regional scale by matching with the observed trends; and finally uncertainty associated with hydrological model where user have to define the unknown parameters, uncertainty in observed data used for model validation and uncertainty in model representation of different processes (Beven and Binley, 1992; Maurer, 2007). One of the ways to deal with these uncertainties is ensemble modeling, which involves running two or more related models and synthesizing the results. The study reports better prediction of multimodel ensemble average to any individual GCM for examining the mean climate as the ensemble model cancels errors associated with individual models (GCM) (Pierce et al., 2009a)**.** Although some studies have explored the use of multiple models, for example Ahmadi et al. (2014) used 112 different climate scenarios from 16 GCM (CMIP3) to simulate hydrologic and water quality processes. However, the majority of the impact assessment studies focus on use of the

single/few GCM due to time and resources constrain. Different sets of climate model outputs are introduced in hydrologic model to see the impact of different climate models on simulated results. This will give the range of possibilities for future instead of a single one. Although increasing use of climate model ensembles for impact assessment research presents opportunities for understanding uncertainties, again it does have challenges for interpreting the results and to make a right decision (Falloon et al., 2014).

References

Ahmadi, M., Records, R., and Arabi, M. (2014). Impact of Climate Change on Diffuse Pollutant Fluxes at the Watershed Scale. *Hydrological Processes* **28**, 1962-1972.

Anomaa Senaviratne, G. M. M. M., Udawatta, R. P., Baffaut, C., and Anderson, S. H. (2013). Agricultural Policy Environmental Extender Simulation of Three Adjacent Row-Crop Watersheds in the Claypan Region. *Journal of Environmental Quality* **42**, 726-736.

Arnold, J. G., Moriasi, D. N., Gassman, P. W., Abbaspour, K. C., White, M. J., Srinivasan, R., Santhi, C., Harmel, R. D., Van Griensven, A., and Van Liew, M. W. (2012). Swat: Model Use, Calibration, and Validation. *Transactions of the ASABE* **55**, 1491-1508.

Arnold, J. G., Srinivasan, R., Muttiah, R. S., and Williams, J. R. (1998). Large Area Hydrologic Modeling and Assessment - Part 1: Model Development. *Journal of the American Water Resources Association* **34**, 73-89.

Baffaut, C., Dabney, S. M., Smolen, M. D., Youssef, M. A., Bonta, J. V., Chu, M. L., Guzman, J. A., Shedekar, V. S., Jha, M. K., and Arnold, J. G. (2015). Hydrologic and Water Quality Modeling: Spatial and Temporal Considerations. *Transactions of the ASABE* **58**, 1661-1680.

Bari, F., Wood, M. K., and Murray, L. (1993). Livestock Grazing Impacts on Infiltration Rates in a Temperate Range of Pakistan. *Journal of Range Management* **46**, 367-372.

Barnett, T. P., Adam, J. C., and Lettenmaier, D. P. (2005). Potential Impacts of a Warming Climate on Water Availability in Snow-Dominated Regions. *Nature* **438**, 303-309.

Bekele, E., and Knapp, H. V. (2010). Watershed Modeling to Assessing Impacts of Potential Climate Change on Water Supply Availability. *Water Resources Management* **24**, 3299-3320.

Bennett, K. E., Werner, A. T., and Schnorbus, M. (2012). Uncertainties in Hydrologic and Climate Change Impact Analyses in Headwater Basins of British Columbia. *Journal of Climate* **25**, 5711-5730.

Beven, K., and Binley, A. (1992). The Future of Distributed Models: Model Calibration and Uncertainty Prediction. *Hydrological Processes* **6**, 279-298.

Bhattacharyya, R., Prakash, V., Kundu, S., and Gupta, H. S. (2006). Effect of Tillage and Crop Rotations on Pore Size Distribution and Soil Hydraulic Conductivity in Sandy Clay Loam Soil of the Indian Himalayas. *Soil and Tillage Research* **82**, 129-140.

Blöschl, G., and Sivapalan, M. (1995). Scale Issues in Hydrological Modelling: A Review. *Hydrological Processes* **9**, 251-290.

Borah, D., Xia, R., and Bera, M. (2002). Dwsm-a Dynamic Watershed Simulation Model. *Mathematical Model for Small Watershed Hydrology, WRP Edition*.

Clark, M. P., Bierkens, M. F. P., Samaniego, L., Woods, R. A., Uijenhoet, R., Bennet, K. E., Pauwels, V. R. N., Cai, X., Wood, A. W., and Peters-Lidard, C. D. (2017). The Evolution of Process-Based Hydrologic Models: Historical Challenges and the Collective Quest for Physical Realism. *Hydrology and Earth System Sciences* **2017**, 1-14.

Cubasch, U., D. Wuebbles, D. Chen, M.C. Facchini, D. Frame, N. Mahowald, and Winther, J. G. (2013). Introduction: The Physical Science Basis. Contribution of Working Group I to the Fifth Assessment Report of the Intergovernmental

Panel on Climate Change [Stocker, T.F., D. Qin, G.-K. Plattner, M. Tignor, S.K. Allen, J. Boschung, A. Nauels, Y. Xia, V. Bex and P.M. Midgley (Eds.)]. *Climate Change*.

Dabney, S. M. (1998). Cover Crop Impacts on Watershed Hydrology. *Journal of Soil and Water Conservation* **53**, 207-213.

Dabney, S. M., Delgado, J. A., and Reeves, D. W. (2001). Using Winter Cover Crops to Improve Soil and Water Quality. *Communications in Soil Science and Plant Analysis* **32**, 1221-1250.

De Wit, M., and Stankiewicz, J. (2006). Changes in Surface Water Supply across Africa with Predicted Climate Change. *Science* **311**, 1917-1921.

Falloon, P., Challinor, A., Dessai, S., Hoang, L., Johnson, J., and Koehler, A.-K. (2014). Ensembles and Uncertainty in Climate Change Impacts. *Frontiers in Environmental Science* **2**, 33.

FAO (2006). Crops and Cropping Systems. Accesed August 28, 2014 at http://www.fao.org/ag/ca/AfricaTrainingManualCD/PDF%20Files/06CROP1.PDF.

Ficklin, D., Stewart, I., and Maurer, E. (2013a). Effects of Projected Climate Change on the Hydrology in the Mono Lake Basin, California. *Climatic Change* **116**, 111-131.

Ficklin, D. L., Stewart, I. T., and Maurer, E. P. (2013b). Climate Change Impacts on Streamflow and Subbasin-Scale Hydrology in the Upper Colorado River Basin. *PLoS ONE* **8**, e71297.

Fowler, H., Blenkinsop, S., and Tebaldi, C. (2007). Linking Climate Change Modelling to Impacts Studies: Recent Advances in Downscaling Techniques for Hydrological Modelling. *International Journal of Climatology* **27**, 1547-1578.

Freeze, R. A., and Harlan, R. (1969). Blueprint for a Physically-Based, Digitally-Simulated Hydrologic Response Model. *Journal of Hydrology* **9**, 237-258.

Gassman, P. W., Williams, J. R., Wang, X., Saleh, A., Osei, E., Hauck, L. M., Izaurralde, R. C., and Flowers, J. D. (2010). The Agricultural Policy/Environmental Extender (APEX) Model: An Emerging Tool for Landscape and Watershed Environmental Analyses. *Transactions of the ASABE* **53**, 711-740.

Gautam, S., Mbonimpa, E., Kumar, S., Bonta, J., and Lal, R. (2015). Agricultural Policy Environmental Extender Model Simulation of Climate Change Impacts on Runoff from a Small No-Till Watershed. *Journal of Soil and Water Conservation* **70**, 101-109.

Gregory, R. D., Willis, S. G., Jiguet, F., Voříšek, P., Klvaňová, A., Strien, A. v., Huntley, B., Collingham, Y. C., Couvet, D., and Green, R. E. (2009). An Indicator of the Impact of Climatic Change on European Bird Populations. *PLoS ONE* **4**, e4678.

Gurtz, J., Lang, H., Verbunt, M., and Zappa, M. (2005). The Use of Hydrological Models for the Simulation of Climate Change Impacts on Mountain Hydrology. *In* "Global Change and Mountain Regions" (U. Huber, H. M. Bugmann and M. Reasoner, eds.), Vol. 23, pp. 343-354. Springer Netherlands.

Harman, W. L., Wang, E., and Williams, J. R. (2004). Reducing Atrazine Losses. *Journal of Environmental Quality* **33**, 7-12.

Hayhoe, K., Edmonds, J., Kopp, R., LeGrande, A., Sanderson, B., Wehner, M., and Wuebbles, D. (2017). Climate Models, Scenarios, and Projections.

Hirabayashi, Y., Kanae, S., Emori, S., Oki, T., and Kimoto, M. (2008). Global Projections of Changing Risks of Floods and Droughts in a Changing Climate. *Hydrological Sciences Journal* **53**, 754-772.

Hoorman, J. J. (2009). Using Cover Crops to Improve Soil and Water Quality. *In* "Fact Sheet Agriculture and Natural Resources". The Ohio State University.

Huang, S., Krysanova, V., and Hattermann, F. (2014). Projections of Climate Change Impacts on Floods and Droughts in Germany Using an Ensemble of Climate Change Scenarios. *Regional Environmental Change*, 1-13.

Huang, S., Krysanova, V., and Hattermann, F. (2015). Projections of Climate Change Impacts on Floods and Droughts in Germany Using an Ensemble of Climate Change Scenarios. *Regional Environmental Change* **15**, 461-473.

IPCC (2000). Special Report on Emissions Scenarios, in Emission Scenarios. Special Report of Working Group Iii of the Intergovernmental Panel on Climate Change. 1-599.

IPCC (2001). Climate Change 2001: The Scientific Basis. Contribution of Working Group 1 to the Third Assessment Report of the Intergovernmental Panel on Climate Change. *Cambridge University Press, Cambridge, UK.*

IPCC (2007). (Intergovermental Panal on Climate Change), Working Group I. Climate Change 2007: The Physical Science Basis. In : Solomon, S., D. Qin, M. Manning, Z. Chen, M. Marquis, K.B. Averyt, M. Tignor and H.L. Miller (Eds.), Contribution of Group I to the Fourth Assessment Report of the Intergovernental Panael on Climate Change.

IPCC (2014). "Climate Change 2014: Mitigation of Climate Change.," Cambridge University Press, Cambridge, United Kingdom and New York, NY, USA.

Jayakrishnan, R., Srinivasan, R., Santhi, C., and Arnold, J. G. (2005). Advances in the Application of the Swat Model for Water Resources Management. *Hydrological Processes* **19**, 749-762.

Jha, M., Gassman, P., and Panagopoulos, Y. (2015). Regional Changes in Nitrate Loadings in the Upper Mississippi River Basin under Predicted Mid-Century Climate. *Regional Environmental Change* **15**, 449-460.

Kiniry, J. R., Blanchet, R., Williams, J. R., Texier, V., Jones, C. A., and Cabelguenne, M. (1992). Sunflower Simulation Using Epic and Almanac Models. *Field Crops Research* **30**, 403-423.

Knisel, W. G. (1980). Creams: A field Scale Model for Chemical Runoff and Erosion from Agricultural Management Systems. pp. 640 pp. US Department of Agriculture, Washington, DC.

Krysanova, V., Wechsung, F., Arnold, J. G., Srinivasan, R., and Williams, J. R. (2000). Swim, User Manual. *PIK-Report, Potsdam Institut f̈ur Klimafolgenforschung*, H. 69.

Kumar, S., Udawatta, R. P., Anderson, S., and Mudgal, A. (2011). Apex Model Simulation of Runoff and Sediment Losses for Grazed Pasture Watersheds with Agroforestry Buffers. *Agroforestry Systems* **83**, 51-62.

Liang, X. (1994). A Two-Layer Variable Infiltration Capacity Land Surface Representation for General Circulation Models.

Liu, L., Hong, Y., Bednarczyk, C. N., Yong, B., Shafer, M. A., Riley, R., and Hocker, J. E. (2012). Hydro-Climatological Drought Analyses and Projections Using Meteorological and Hydrological Drought Indices: A Case Study in Blue River Basin, Oklahoma. *Water Resources Management* **26**, 2761-2779.

Maurer, E. (2007). Uncertainty in Hydrologic Impacts of Climate Change in the Sierra Nevada, California, under Two Emissions Scenarios. *Climatic Change* **82**, 309-325.

Moss, R. H., Edmonds, J. A., Hibbard, K. A., Manning, M. R., Rose, S. K., Van Vuuren, D. P., Carter, T. R., Emori, S., Kainuma, M., and Kram, T. (2010). The Next Generation of Scenarios for Climate Change Research and Assessment. *Nature* **463**, 747.

Ouyang, F., Zhu, Y., Fu, G., Lü, H., Zhang, A., Yu, Z., and Chen, X. (2015). Impacts of Climate Change under Cmip5 Rcp Scenarios on Streamflow in the Huangnizhuang Catchment. *Stochastic Environmental Research and Risk Assessment* **29**, 1781-1795.

Pachauri, R. K., Allen, M., Barros, V., Broome, J., Cramer, W., Christ, R., Church, J., Clarke, L., Dahe, Q., and Dasgupta, P. (2014). Climate Change 2014: Synthesis Report. Contribution of Working Groups I, Ii and Iii to the Fifth Assessment Report of the Intergovernmental Panel on Climate Change.

Panagopoulos, Y., Gassman, P., Arritt, R., Herzmann, D., Campbell, T., Jha, M., Kling, C., Srinivasan, R., White, M., and Arnold, J. (2014). Surface Water Quality and Cropping Systems Sustainability under a Changing Climate in the Upper Mississippi River Basin. *Journal of Soil and Water Conservation* **69**, 483-494.

Parajuli, P. B. (2010). Assessing Sensitivity of Hydrologic Responses to Climate Change from Forested Watershed in Mississippi. *Hydrological Processes* **24**, 3785-3797.

Peel, M. C., Srikanthan, R., McMahon, T. A., and Karoly, D. J. (2014). Uncertainty in Runoff Based on Global Climate Model Precipitation and Temperature Data &Ndash; Part 2: Estimation and Uncertainty of Annual Runoff and Reservoir Yield. *Hydrology and Earth System Sciences Discussions*, 4579-4638.

Perez, J., Menendez, M., Mendez, F., and Losada, I. (2014). Evaluating the Performance of Cmip3 and Cmip5 Global Climate Models over the North-East Atlantic Region. *Climate Dynamics* **43**, 2663-2680.

Pierce, D. W., Barnett, T. P., Santer, B. D., and Gleckler, P. J. (2009a). Selecting Global Climate Models for Regional Climate Change Studies. *Proceedings of the National Academy of Sciences* **106**, 8441-8446.

Pierce, D. W., Barnett, T. P., Santer, B. D., and Gleckler, P. J. (2009b). Selecting Global Climate Models for Rgional Climate Change Studies. *Proceedings of the National Academy of Sciences* **106**, 8441-8446.

Praskievicz, S., and Bartlein, P. (2014). Hydrologic Modeling Using Elevationally Adjusted Narr and Narccap Regional Climate-Model Simulations: Tucannon River, Washington. *Journal of Hydrology* **517**, 803-814.

Reeves, D. W. (1997). The Role of Soil Organic Matter in Maintaining Soil Quality in Continuous Cropping Systems. *Soil and Tillage Research* **43**, 131-167.

Romanowicz, R. J., and Wong, W. K. (2016). Trends in Projections of Standardized Precipitation Indices in a Future Climate in Poland. *Hydrology and Earth System Sciences* **20**, 1947.

Rosenzweig, C., Iglesias, A., Yang, X., Epstein, P. R., and Chivian, E. (2001). Climate Change and Extreme Weather Events; Implications for Food Production, Plant Diseases, and Pests. *Global Change and Human Health* **2**, 90-104.

Santhi, C., Arnold, J. G., Williams, J. R., Dugas, W. A., Srinivasan, R., and Hauck, L. M. (2001). Validation of the Swat Model on a Large Rwer Basin with Point

and Nonpoint Sources. *Journal of the American Water Resources Association* **37**, 1169-1188.

Sellami, H., Benabdallah, S., La Jeunesse, I., and Vanclooster, M. (2016). Climate Models and Hydrological Parameter Uncertainties in Climate Change Impacts on Monthly Runoff and Daily Flow Duration Curve of a Mediterranean Catchment. *Hydrological Sciences Journal* **61**, 1415-1429.

Sheffield, J., and Wood, E. F. (2008). Projected Changes in Drought Occurrence under Future Global Warming from Multi-Model, Multi-Scenario, Ipcc Ar4 Simulations. *Climate Dynamics* **31**, 79-105.

Suia, D. Z., and Maggiob, R. C. (1999). Integrating Gis with Hydrological Modeling: Practices, Problems, and Prospects. *Computers, Environment and Urban Systems* **23** 33-51.

Touma, D., Ashfaq, M., Nayak, M. A., Kao, S.-C., and Diffenbaugh, N. S. (2015). A Multi-Model and Multi-Index Evaluation of Drought Characteristics in the 21st Century. *Journal of Hydrology* **526**, 196-207.

van Vuuren, D., Edmonds, J., Kainuma, M., Riahi, K., Thomson, A., Hibbard, K., Hurtt, G., Kram, T., Krey, V., Lamarque, J.-F., Masui, T., Meinshausen, M., Nakicenovic, N., Smith, S., and Rose, S. (2011). The Representative Concentration Pathways: An Overview. *Climatic Change* **109**, 5-31.

Vu, M., Raghavan, V., and Liong, S.-Y. (2015). Ensemble Climate Projection for Hydro-Meteorological Drought over a River Basin in Central Highland, Vietnam. *KSCE Journal of Civil Engineering* **19**, 427-433.

Walther, G.-R., Post, E., Convey, P., Menzel, A., Parmesan, C., Beebee, T. J. C., Fromentin, J.-M., Hoegh-Guldberg, O., and Bairlein, F. (2002). Ecological Responses to Recent Climate Change. *Nature* **416**, 389-395.

Wang, D., Hejazi, M., Cai, X., and Valocchi, A. J. (2011). Climate Change Impact on Meteorological, Agricultural, and Hydrological Drought in Central Illinois. *Water Resources Research* **47**.

Wang, G. (2005). Agricultural Drought in a Future Climate: Results from 15 Global Climate Models Participating in the Ipcc 4th Assessment. *Climate Dynamics* **25**, 739-753.

Wang, G., Yang, H., Wang, L., Xu, Z., and Xue, B. (2014). Using the Swat Model to Assess Impacts of Land Use Changes on Runoff Generation in Headwaters. *Hydrological Processes* **28**, 1032-1042.

Wang, X., Saleh, A., McBroom, M. W., Williams, J. R., and Yin, L. (2007). Test of Apex for Nine Forested Watersheds in East Texas. *Journal of Environmental Quality* **36**, 983-995.

Williams, J. R., Arnold, J. G., and Srinivasan, R. (2000). The APEX Model. Texas Agricultural Experiment Station. 1-141.

Williams, J. R., and Izaurralde, R. C. (2005). The APEX Model.Brc Rep.2005-02.

Williams, J. R., Jones, C. A., and Dyke, P. T. (1984). A Modeling Approach to Determining the Relationship between Erosion and Soil Productivity. *Transactions of ASABE* **27**, 129-144.

Young, R. A., Onstad, C. A., Bosch, D. D., and Anderson, W. P. (1987). Agricultural Non-Point Source Pollution Model: A Large Watershed Analysis Tool. Agnps. *USDA, ARS Conservation Research Report #35*, 77 pp.

CHAPTER 3

ASSESSING LONG-TERM HYDROLOGIC IMPACT OF CLIMATE CHANGE USING ENSEMBLE APPROACH AND COMPARISON WITH GLOBAL GRIDDED MODEL-A CASE STUDY ON GOODWATER CREEK EXPERIMENTAL WATERSHED

ABSTRACT

Potential impacts of climate change on hydrologic components of Goodwater Creek Experimental Watershed were assessed using climate datasets from the Coupled Model Intercomparison Project Phase 5 and Soil and Water Assessment Tool (SWAT). Historical and future ensembles of downscaled precipitation and temperature, and modeled water yield, surface runoff, and evapotranspiration were compared. Ensemble SWAT results indicate increased springtime precipitation, water yield, surface runoff and a shift in evapotranspiration peak one month earlier in the future. To evaluate the performance of model spatial resolution, gridded surface runoff estimated by Lund–Potsdam–Jena managed Land (LPJmL) and Jena Diversity-Dynamic Global Vegetation model (JeDi-DGVM) were compared to SWAT. Long-term comparison shows 6-8% higher average annual runoff estimation for LPJmL and 5-30% lower estimation for JeDi-DGVM compared to SWAT simulated average annual runoff. Although simulated annual runoff showed little change for LPJmL, monthly runoff projection under estimated peak runoff and overestimated low runoff for LPJmL compared to simulated SWAT runoff. The reasons for these differences include difference in spatial resolution of model inputs and mathematical representation of physical processes. Results indicate benefits of impact assessments at small scales with heterogeneous sets of parameters to adequately represent extreme conditions that are muted in global gridded model studies by spatial averaging over large study domains.

Introduction

Climatic shift due to anthropogenic activities has been linked to water supply shortages (De Wit and Stankiewicz, 2006; Schewe et al., 2014), declining biodiversity (Bellard et al., 2012; Gregory et al., 2009; Moritz and Agudo, 2013), ecosystem damage (Walther et al., 2002), and economic impact (Schlenker et al., 2006). Increased greenhouse gas (GHG) concentrations alter the radiative balance of the Earth's atmosphere, causing an increase in average temperature (T) and changes in precipitation (P) patterns (Cubasch et al., 2013; Pachauri et al., 2014). The Intergovernmental Panel on Climate Change (IPCC) reports increases in mean surface temperature between 0.3 and 4.8°C by 2081-2100 relative to 1986-2005, and variable change in precipitation across the globe for the same period of comparison (IPCC, 2014) dependent upon GHG concentrations in the atmosphere. The atmospheric carbon dioxide (CO_2) concentration is estimated to increase from the present day concentration of approximately 400 ppm to approximately 850 ppm by year 2075 for the highest emission scenario (RCP 8.5) (IPCC, 2014). The projected changes in meteorological variables have been reported to impact hydrologic components and ultimately agroecosystem functioning (Kucharik and Serbin, 2008; Le et al., 2011; Piao et al., 2010). The majority of modeling exercises have been conducted at larger scales than this study, despite that in reality management decisions are taken at a local scale by individual farmers. . Therefore, it is important to develop approaches to increase the ability to predict how future climate changes could impact hydrologic components, and correspondingly, agricultural productivity through representation of localized systems.

Multiple Global Circulation Models (GCMs) have been developed to project future Earth climate given multiple plausible futures (IPCC, 2014). GCMs are three-dimensional numerical models that represent the physical dynamics of the atmosphere, ocean, cryosphere, and land surface, and are the best available methods for predicting how these systems behave given increasing GHG concentrations in the atmosphere (IPCC, 2013). In the Fifth Assessment Report, the climate projections are organized into four Representative Concentration Pathways (RCPs) (RCP 2.6, RCP 4.5, RCP 6.0, and RCP 8.5) based on radiative forcing levels associated with socioeconomic and technical assumptions by the end of the century (Taylor et al., 2012). Radiative forcing is defined as the difference between incoming solar radiation and outgoing infrared radiation caused by increased concentration of GHGs expressed in Watts per square meter (W/m^2) (Schneider, 1992).

Hydrologic models have been used to simulate the long-term impact of projected changes in climate to assist with the quantification of future risk and, if necessary, to assist with developing adaptive management strategies (Fowler et al., 2007; Haasnoot et al., 2014). Hydrologic simulation models have been applied to assess the impacts of climate change on nutrient loading (Jha et al., 2015), crop productivity (Panagopoulos et al., 2014), and streamflow (Ficklin et al., 2013a; Ouyang et al., 2015). The majority of climate impact assessment studies have been conducted at larger scales using gridded model structures matching with the resolution of Coupled Model Intercomparison Project (CMIP3 and CMIP5) (Ficklin et al., 2013a; Ficklin et al., 2013b; Mohammed et al., 2015; Panagopoulos et al., 2014). Studies in the Midwestern United States have focused on quantifying the impact of future climate on hydrologic processes at a regional scale using gridded climate data (50 × 50 km) (Jha et al., 2004; Qiao et al., 2014; Stone et al., 2003) and with some

studies conducted in mid-sized watersheds (Choi et al., 2017; Jha and Gassman, 2014; Tavakoli and De Smedt, 2011). There have been relatively few studies at smaller scales (Ahmadi et al., 2014; Al-Mukhtar et al., 2014; Ye and Grimm, 2013), in part due to lack of fine resolution climate model output and corresponding, data-intensive requirements to further downscale these data to a specific location to use in hydrological models for small scale applications (Fowler et al., 2007). Watershed sizes were defined using United States Geological Survey (USGS) classification scheme based on hydrologic unit code (HUC) which consists of six levels of classification (Seaber et al., 1987). Specifically, subwatershed to watershed (~100 km^2 to 585), subbasin to basin (>585 to 27,445 km^2), and sub region to region (>27,445 km^2 and above) were considered as small scale, mid-size and regional scale, respectively.

Hydrologic components can be simulated at various scales. The spatial and temporal scale of a hydrological model also defines the resolution of key output variables. For regional reservoir managers, a more coarse resolution of both space and time may be sufficient for anticipating and planning for predicting water levels. For example, the VIC model (Liang, 1994) operates at a 10-kmgrid cell size and a daily time-step, and is useful for large-scale water management planning and identification of general trends. In contrast, the APEX model (Williams and Izaurralde, 2006) operates at field scale (few to few hundreds hectare) and is useful for field-scale management planning. Thus, hydrologic models can produce distinct results, because of the model structure, parametrization and resolution of inputs (Clark et al., 2017; Freeze and Harlan, 1969). Comparison of model results at multiple scales can help to evaluate what resolution is necessary and appropriate for particular risk and adaptation questions. For example, early work on hydrologic impacts associated with

future climate change have focused on determining what regions of countries and even the globe may be at risk for changes in water availability, a question for which a coarse resolution may be adequate. However, in order to develop strategic responses in a specific location, and particularly the need to link hydrology to agricultural productivity, a finer resolution may be required in order to evaluate low probability, high-risk events (e.g., flooding, drought, etc.). Similarly, finer resolution for key parameters representing physical processes is likely to result in increased ability to predict responses to future climate conditions.

The geographic focus of this study is the Goodwater Creek Experimental Watershed (GCEW), which is part of a Long Term Agroecosystem Research (LTAR) site, has been a part of a broader USDA-ARS watershed network since 1971, and thus has ample high quality data (Sadler et al., 2015a). The Soil Water Assessment Tool (SWAT) (Arnold et al., 1998) has been used to model this watershed for many years in conjunction with this LTAR research program. The SWAT model (Arnold et al., 1998) is a widely used watershed-scale process-based distributed parameter hydrologic simulation model designed to simulate hydrologic components, and enables detailed representation of agricultural land cover and management practices (Neitsch et al., 2011; Santhi et al., 2001). SWAT includes algorithms for predicting how P, T, and CO_2 concentration affect plant growth and hydrologic components.

The GCEW is a headwater watershed in the Salt River Basin and the geophysical context of the study area represents the Central Claypan region, which includes Northeast Missouri, Southeast Iowa and Southern Illinois (Baffaut et al., 2015a; Sadler et al., 2015a). GCEW includes a restrictive clay layer in the subsurface soil (B-Horizon), which results in lower hydraulic conductivity, and, ultimately considerable surface water runoff despite shallow slopes (Jung et al., 2006; Udawatta et al., 2004).

The presence of this restrictive clay layer may result in more significant responses in hydrologic components as a result of future changes in T and P. For example, intense precipitation events could result in higher runoff and short-term dry periods may result in short-term drought, both of which can affect agricultural productivity. Hydrologic models with a coarse spatial resolution may not be able to capture hydrologic responses to climate adequately in areas with unique physical features such as the claypan in the GCEW.

The objectives of this study are to contribute to the body of knowledge developed in conjunction with the LTAR project in the GCEW, to characterize the potential hydrologic impacts in relation to climate change in the GCEW, and to compare hydrologic output from models of different spatial resolution as well as with and without localized downscaling of weather data. This is an important inquiry for developing modeling techniques to assess risks to hydrologic components and agricultural activity. To support these objectives, 12 climate model datasets obtained from CMIP5 were statistically downscaled using historic T and P data from GCEW (Sadler et al., 2015b) and modeled hydrologic responses were analyzed using an ensemble approach. To support the last objective, SWAT simulated runoff was compared with simulated runoff from the Lund–Potsdam–Jena managed Land (LPJmL) and Jena Diversity-Dynamic Global Vegetation (JeDi-DGVM)models forced with precipitation data bias corrected using a nonlinear regression with a spatial resolution of 0.5 degree (Hempel et al., 2013). These data were made available via the Inter-Sectoral Impact Model Intercomparison Project (ISI-MIP) (Warszawski et al., 2013). Runoff results were compared to evaluate the performance of these varying spatial resolutions to generate more insight on why there is a need for detailed simulation with higher spatial resolution in an agricultural setup.

Materials and Methods

Watershed Description and Data Sources

The study was conducted in the GCEW, located in Boone and Audrain counties, Missouri (Figure 3.1)with a drainage area of approximately 73 km^2 (Sadler et al., 2015a). The land uses in the watershed include row crops (72.8 % of total land area), pasture (14.3%), forest (6.0%), and urban land (6.9%) (Table 3.1). The study area received an average annual precipitation of 1027 mm between 1993 and 2010, with maximum and minimum annual precipitation of 1614 and 776 mm, respectively, for years 2008 and 2007 (Sadler et al., 2015b). The historical average annual snowfall for the study watershed is around 380 mm, given difficulty in snow measurement snow water equivalent is measured in the study area (Sadler et al., 2015b). The daily average maximum and minimum temperatures during this same period were 17.5°C and 6.5°C, respectively. The average annual discharge of the watershed (expressed as a depth over the drainage area) is 310 mm, proportioned of surface (80%) and base flow (20%) (Baffaut et al., 2015b).The watershed has flat topography, with 69% of the area having a slope of 0-2%, 15.2% having a slope of 2-3%, and the remaining 15.8% has a slope greater than 3%. The average elevation of the watershed is 256 m above sea level, ranging from 223 to 281 m.

Data required for the SWAT model included a Digital Elevation Model (DEM), soil database, Land Use/Land Cover (LULC), and weather datasets. The DEM (10-m resolution), soil (30-m resolution), and land use/land cover (30-m resolution) datasets were downloaded from Missouri Spatial Data Information Service (MSDIS) (http://msdis.missouri.edu/data/dem/), Soil Survey Geographic Data (SSURGO) (http://websoilsurvey.sc.egov.usda.gov/App/WebSoilSurvey.aspx) data set, and

National Agricultural Statistics Service (NASS) Cropland Data Layer (CDL)

(http://nassgeodata.gmu.edu/CropScape/) of the United States Department of

Agriculture (USDA), respectively. The historical weather datasets required for the

model, including daily P, daily maximum and minimum air T, wind speed, and solar

radiation were obtained from the weather station and rain gauge located in the

watershed (Figure 3.1). The precipitation datasets from 5 different rain gauges (Figure

3.1) were used to better represent the spatial variability of precipitation across the

watershed.

Description of SWAT model and model setup for GCEW

The SWAT 2012 version 635 was used by incorporating the changes included in an

earlier modeling effort to simulate the percolation through and saturation above the

claypan (Baffaut et al., 2015a) which controls the hydrologic components of Central

Claypan region. The watershed was delineated using Arc Hydro tools built in the Arc

SWAT interface using DEM data for the area (MSDIS). The watershed was

delineated using the threshold drainage area of 200 ha with delineation resulting in 7

sub-basins. The delineation scheme was consistent to previous modeling efforts for

GCEW (Baffaut et al., 2015a). LULC data were assumed to be constant throughout

the simulation. A two-year rotation of corn and soybean (conventional tillage corn

and no-till soybean rotation) was used to represent the dominant year-to-year

cropping patterns in the watershed. Pasture land was further divided into pasture1,

pasture2, hay and switchgrass to include more detail for SWAT simulation and to

represent proper stocking density by applying grazing in alternate pasture (Baffaut et

al., 2015a). The watershed was divided using five slope classes (<0.5 %, 0.5-1 %, 1-2

%, 2-3 %, and >3 %). The overlay of soil, land use layer, and slope resulted in 93

hydrologic response units (HRUs). Subbasin area thresholds were used to define

minor land uses, minor soils for each land use, and minor slope ranges for each land use/soil combination using values of 5% for land use, 20% for soils, and 25% for slopes. Minor land uses, soils, or slope ranges were not simulated and the corresponding area was redistributed among the simulated ones. The historic observed data values for all five weather variables (T, P, wind, relative humidity, and solar radiation) were input for historic model calibration and validation. The wind, relative humidity and solar radiation were generated using the SWAT weather generator for future simulations and T and P were based on statistically downscaled projections from CMIP5. The Natural Resources Conservation Service (NRCS) curve number (CN) method was used to calculate the surface runoff, and potential evapotranspiration (PET) was estimated using the Penman-Monteith (PM) method. Note that the PM method must be used for the climate change scenarios that account for CO_2 changes. This method accounts for the impact of CO_2 change on plant growth.

LPJmL and JeDi model overview

LPJmL and JeDi-DGVMare dynamic global vegetation models represent vegetation dynamics in addition to land surface processes with a spatial resolution of 0.5 degree (Bondeau et al., 2007; Pavlick et al., 2013). Runoff simulation for both models was conducted at a daily time step using daily meteorological variables including P, daily mean T, long wave net radiation and long wave downwelling radiation gridded at 0.5 degree. The change in leaf area index and stomatal conductance due to changes in CO_2 concentration was applied in the simulation to represent dynamic vegetation growth in both LPJmL and JeDi-DGVM. The saturation excess runoff scheme was used for simulation of runoff, i.e., excess water above field capacity was considered runoff and infiltration processes were not simulated. Evapotranspiration was

calculated using the Priestley-Taylor (PT) method. Soil data for the LPJmL model setup was taken from the Harmonized World Soil Database (HWSD). Soil data of HWSD is a 1-km-resolution raster database. HWSD soil data are available for two layers, top- and subsoil (Nachtergaele et al., 2008). The land use land cover database from gridded land use (HYDE 3.2) (Klein Goldewijk, 2016) with a horizontal resolution of 0.5-km was used for LPJmL, which means land use can't be subdivided at a resolution less than 0.25 km^2. The JeDi-DGVM model uses a parameter-based land surface model to simulate soil and land use. The parameters used in the JeDi-DGVM model include maximum plant available water storage in the root zone, transpiration rate, leaf area index, fractional vegetative cover, fractional forest cover, snow-free surface albedo, and canopy storage. Details about the parameter-based land surface model used in JeDi-DGVM can be found in Diimenil et al. (1996). The major differences between LPJmL and JeDi-DGVM include the definition of land use land cover, soil, and dynamic vegetation representation. Both models represent vegetation dynamics using semi-empirical plant functional types (PFTs). Vegetation in LPJmL is represented using only 12 PFTs compared to the large number of PFTs generated based on 15 trait parameters in JeDi-DGVM (Pavlick et al., 2013). LPJmL and JeDi-DGVM surface runoff output, generated based on weather data from the CMIP5 climate data, were retrieved via the ISI-MIP data repository [https://esg.pik-potsdam.de/search/isimip-ft/] for the grid cell overlapping the GCEW for comparison to SWAT output. The monthly average runoff projections for near and far future for LPJmL, JeDi-DGVM, and SWAT were compared using the paired-t test. Two Climate models, MIROC-ESM-CHEM and IPSL-CM5A-LR, were used for this study to represent both kinds of plausible futures (higher temperature and precipitation change and smaller temperature and precipitation change). Note that the runoff

simulation data are available using two impact models (LPJmL and JeDi-DGVM) in the ISI-MIP project.

SWAT Model Calibration, Validation and Evaluation Criteria

The model was calibrated for daily streamflow during the period 1993-2001 using data collected at the watershed outlet (Weir 1), and the model was validated using 2002-2010 streamflow data at Weir 1 and 1993-2001 streamflow data at Weir 11 (Baffaut et al., 2015b) (Figure 3.1). An initial three–year (1990–1992) warm-up period was used to initialize the SWAT model. The model sensitive parameters for streamflow were determined using the SWAT-CUP (SUFI-2) (Abbaspour et al., 2007), and calibration was conducted manually by adjusting a single parameter at a time to fit the observed and simulated streamflow. Manual calibration was preferred over auto-calibration as SWAT parameter ranges were well understood based on previous studies (Baffaut et al., 2015a). The model was calibrated to get the best fit value of the streamflow-sensitive parameters, and their values were changed within the range defined by Neitsch et al. (2002). Calibration was conducted through visual assessment of superposition of observed and simulated flow duration curves for whole range of flow, and further model performance statistics were calculated to confirm. The model performance was tested using coefficient of determination (r^2) and Nash Sutcliffe Efficiency (NSE). The r^2 value above 0.60 and NSE values above 0.50 and p-bias of ± 10% during the calibration and validation periods were set as a criterion for satisfactory model performance during the model simulation of daily streamflow as defined by Moriasi et al. (2015). The calibrated SWAT model was used for the future projection of hydrologic condition using the statistically downscaled temperature and precipitation data for the near (2016-2045) and far future (2046-2075) periods. Note that the parameter uncertainty can affect the simulated results as

there can be multiple set of hydrologic parameters that result in adequate model performance matrices (Ficklin and Barnhart, 2014). Studies indicate the uncertainty associated with GCMs and emission scenarios is higher compared to hydrologic parameter uncertainty (Bennett et al., 2012; Sellami et al., 2016), therefore one set of hydrologic parameters are used in this study and the uncertainty ranges of climate models are presented. The simplified flow chart shown in Figure 3.2 describes the steps followed in this study.

Climate data and bias correction methods

Climate projection data were obtained from the CMIP5 project (Maurer et al., 2007), which provides Bias Corrected Constructed Analog (BCCA) downscaled to one-eighth degree (12 km^2) from many GCM models (available at: http://gdo-dcp.ucllnl.org/downscaled_cmip_projections/). Data from twelve GCM models for four emission scenarios (RCP 2.6, RCP 4.5, RCP 6.0, and RCP 8.5) for a total of 48 unique datasets were selected for this study (Table 3.2 (Maurer et al., 2007) and Table S1). Daily P and air T (min and max) were extracted for the four grid cells spanning the GCEW. These data were further downscaled using observed P and T data over the years 1971-2010 from the weather station located in the watershed. The bias in temperature was corrected using the delta method and the bias in precipitation datasets was corrected using modified quantile mapping.

Statistical Downscaling: Temperature –Delta Method

The delta method aims to match the monthly mean of the corrected temperature values with observed temperature (Lenderink et al., 2007). The correction of the temperature involves linear shifting of future temperatures using a correction factor calculated based on the difference between the historic GCM simulated and historic

36

observed temperature data for each month (Choi et al., 2017). Temperature data extracted from CMIP5 were corrected to correspond to the study area using the delta method. The monthly correction factor was calculated by subtracting average monthly baseline CMIP5 simulated T data and baseline observed T data (1971-2010). Daily T over the analysis period was corrected with an additive term (b_j) computed for each month as Eq. (1):

$$b_j = \frac{\sum_{C=1}^{C_i} T_{ij} - \sum_{C=1}^{C_i} \hat{T}_{ij}}{C_{ij}} \qquad (1)$$

Where, C_i= is the total number of days for month j over the entire baseline historic period, T_{ij} is the daily observed T in °C (maximum or minimum), and $\hat{T}_{ij}$ is the daily model temperature (maximum or minimum) on day i in month j. Finally, the additive factor for each respective month was added to raw data for bias correction (Eq. (2)).

$$T_{ij} = \hat{T}_{ij} + b_j \qquad (2)$$

Statistical Downscaling: Precipitation-Quantile mapping

Quantile mapping adjusts the daily CMIP5 precipitation values to match the statistical distribution of the observed precipitation. This method is known by many other names, for example as 'distribution mapping' (Boé et al., 2007; Johnson and Sharma, 2011) and 'probability mapping' (Block et al., 2009; Ines and Hansen, 2006). One major assumption of quantile mapping is that the precipitation distribution doesn't change over time, and variance and skewness of the distribution remain the same with only a change in mean (Li et al., 2010). Cumulative Distribution Functions (CDFs) were constructed for both CMIP5 and observed daily P (1970-2010) on a monthly

basis. A transfer function was constructed to transform CMIP5 data values to probabilities based on the CDF of the model distribution, and these values were transformed back to data values using the inverse CDF or quantile function of the observed distribution. This procedure is expressed mathematically as (Eq. (3)):

$$P_{i,j}^{corr\ gcm} = CDF_{obs,j}^{-1} \left[CDF_{gcm,j}^{his} \left(P_{i,j}^{raw} \right) \right] \quad (P_{i,j}^{raw} \le P_{max,j}^{his\ gcm}) \tag{3}$$

Where, $P_{i,j}^{raw}$, $P_{i,j}^{corr\ gcm}$ and $P_{max,j}^{his\ gcm}$ are the projection's raw CMIP5, corrected CMIP5, and maximum historical CMIP5 precipitation for i[th] day of jth month, respectively. The $CDF_{obs,j}^{-1}$ is the quantile function of the observed precipitation and $CDF_{gcm,j}^{his}$ is the CDF of an individual GCM.

Quantile mapping was modified to correct two major limitations in CMIP5 P data: 1) the P frequency or dry bias, i.e., the data contain a large number of very low P days, i.e., "drizzle days," (Hidalgo et al., 2008) and 2) an underestimation of extreme P compared to historical observation. The number of P days was more than 300 days/year for projected gridded data compared to 94 days/year in the observed dataset (1971-2010). To correct for these excess "drizzle days," a P threshold was determined and the P values below the threshold were removed (Equation 4). A P threshold for each month was determined for each GCM model to ensure the same number of P days for GCM baseline and observed as was done by Grillakis et al. (2013). Monthly thresholds ranged from 0.60 to 4.5 mm/day; similar to ranges of P thresholds reported by Themeßl et al. (2011). Quantile mapping was performed after removing "drizzle day" corrections.

$$P_{i,j}^{raw}(d) = \begin{cases} 0, if\ P_{i,j}^{raw} <\ P_{threshold,j} \\ P_{i,j}^{raw}, otherwise \end{cases} \tag{4}$$

The second limitation of quantile mapping is that the method limits the upper value of future daily precipitation to the highest value observed in the past. Given that climate projections indicate that precipitation events are likely to increase in magnitude and this sort of extreme event poses potential risks a second adjustment was made to the CMIP5 P data to allow a daily P to exceed the historic maximum using Eqns. (5) and (6). P was scaled on a monthly basis to represent the monthly extreme. A separate scaling factor was calculated for each month. Where S_j is the scaling factor for a given month and $P_{i,j}^{his\ gcm}$ is the CMIP5 daily P data for month j during the historic period. This approach retained the relationship between the historic period and future periods within a CMIP5 P dataset for a given model without constraining future P data to the maximum historical observation.

$$P_{i,j}^{corr\ gcm} = S_j * P_{i,j}^{raw} \quad (P_{i,j}^{raw} > P_{i,j}^{his\ gcm}) \tag{5}$$

$$S_j = \frac{Max\left(P_{i,j}^{obs}\right)}{Max\left(P_{i,j}^{his\ gcm}\right)} \tag{6}$$

Simulation Scenarios. Impacts of climate change on water yield, evapotranspiration, and surface runoff

The validated SWAT model was run at a daily time step starting in 1981 and continuing until 2075. For analysis, the baseline represents 1981-2010, the near future is defined as 2016-2045, and the far future is defined as 2046-2075. Different atmospheric CO_2 concentrations were applied within SWAT for each RCP for different time periods; these values were calculated by averaging the projected CO_2 concentrations over each 30-year period. The details of CO_2 concentration used for each model for each time frame and RCP are presented in Table 3.3. The CO_2

concentration of 330 ppm was used for all the historic simulations. The ensemble median and quartile values (Q1 and Q3) of monthly water yield, evapotranspiration, and surface runoff were calculated for the three analyses periods. Reporting results as ensembles allows for greater confidence in simulated hydrologic outputs (Perez et al., 2014). Pierce et al. (2009) found that the average of a multi-model ensemble is a better predictor than any individual GCM for global studies examining the mean climate, as the ensemble of results cancels out the bias and errors.

The modified PM method was used to calculate ET. This equation allows for the incorporation of variability in radiation-use efficiency, plant growth, and transpiration induced by change in atmospheric CO_2 concentration (Neitsch et al., 2011). Note that the future projections of solar radiation are based on weather generator, which uses monthly statistics of historic daily solar radiation data to project the future weather. Sensitivity analysis was conducted by elevating daily solar radiation. Increase in daily solar radiation by 1 MJ/m^2 resulted in ~2% (650 to 663 mm) increase in ET. Results indicate less sensitivity of SWAT model to change in solar radiation. Therefore, majority of climate change impact assessment studies using SWAT use weather generator for future projection for solar radiation. SWAT simulates the impact of change in CO_2 concentration on stomatal conductance by linear interpolation between current conditions and a 40% decrease of stomatal conductance for doubling of CO_2 up to 660 ppm (Neitsch et al., 2011). However, SWAT does not simulate effects of CO_2 on leaf area index; thus, this study does not incorporate the impact of increased CO_2 concentration on leaf area and other feedbacks associated with it.

Results and Discussion

Model calibration and validation

The default and adjusted model parameter values are presented in Table 3.4. The model parameters controlling surface runoff, groundwater, and snowmelt were important parameters considered during calibration. The calibrated model parameters are similar to those reported by previous researchers for GCEW (Baffaut et al., 2015a). Daily streamflow simulation at weir1 (watershed outlet) resulted in r^2 of 0.66, NSE of 0.66, and p-bias of 5.6% during calibration (1993-2001), and r^2 of 0.60, NSE of 0.59, and p-bias of -6.9% during the validation. The model was further validated using the streamflow data at weir11 resulting in r^2 of 0.73, NSE of 0.68, and p-bias of 18%. SWAT simulated dry (2007) and wet (2008) years accurately, indicating that the model was suitable for evaluating climate change impacts. The flow duration curve is a description of the frequency at which a given discharge is reached or exceeded over the simulation period. The flow duration curves for observed and simulated flow for calibration and validation periods are presented in Figure 3.3. The calibration objective was to superimpose observed and simulated flow duration curves to match low, intermediate and high flow.

Downscaled GCM projection

Temperature

Minimum temperatures were under-predicted and maximum temperatures, particularly in the summer months, were over-predicted in CMIP5 output compared to historical observations. The scaling factors used for correction of the maximum and minimum daily T are presented in supplement Tables 3.S2 and 3.S3. The maximum bias was for the month of March for both the maximum and minimum T. Average

monthly T (observed, CMIP5, bias-corrected) for the period 1981-2010 for one of the

GCM models included in the study is presented in Figure 3.4 as an example. These

results are consistent with previous reports of over-prediction of annual mean T for

CMIP5 GCMs for Northern Eurasia (Chiyuan et al., 2014; Terink et al., 2010),

Northern hemisphere (Zhao et al., 2013), and globally (Kim et al., 2012).

Figure 3.5 shows GCM projected changes in average annual T, between the

baseline (1981–2010) and near (2016–2045) (Figure 3.5a) and far future (2046-2075)

(Figure 3.5b) for the 12 sets of downscaled T data from CMIP5 for four RCP

scenarios. Ensemble average T change in the near future period shows minimum T

change for RCP 6.0 (1.13 °C) and maximum T change for RCP 8.5 (1.63 °C). The far

future period shows minimum T change for RCP 2.6 (0.33 °C) and maximum T

change for RCP 8.5 (1.92 °C). The most significant increase in T occurred for models

under RCP 8.5 scenarios for both near and far future (Figure 3.5a and Figure 3.5b).

This is consistent with the assumptions associated with technological and

socioeconomic conditions leading to the concentrations of GHGs associated with each

RCP. That is, RCP 2.6 includes a decrease in the concentration of GHGs in the

atmosphere to below currently observed levels, while RCP 8.5 represents the largest

increases of GHG concentrations in the atmosphere. For RCP 4.5, atmospheric CO_2

peaks around 2040, then declines compared to RCP 6.0, where CO_2 peaks in 2080 and

declines (Meinshausen et al., 2011) . Therefore, in the near future, RCP 6.0 has the

lowest CO_2 concentration compared to RCP 4.5 scenarios resulting in the least T

change (Figure 3.5a). The spread of predicted changes in T for models in RCP 4.5

(0.7 °C - 2.2 °C) and RCP 8.5 (0.9 °C - 2.5 °C) demonstrates the value of a multiple

model ensemble approach for future climate change impact assessment studies.

Figure 3.5 also shows GCM projected percentage changes in average annual P, for baseline (1981–2010), near future (2016–2045), and far future (2046-2075) respectively, for the 12 different GCMs used in this study. An ensemble P change for the far future scenario was the least for the RCP 6.0 scenario (1.0% increase) and most for RCP 8.5 (6.9% increase). The highest simulated increase in average annual precipitation was for RCP 8.5 with a change in P ranging from -7 to 16% across 12 GCMs in the near future and -10 to 28% in the far future, followed by the RCP 4.5. Note that in near future (2016-2045), RCP 4.5 had a higher CO_2 concentration than RCP 6.0 (van Vuuren et al., 2011), which may explain the elevated T and P for RCP 4.5 compared to RCP 6.0 over this period. Use of variable monthly thresholds for daily precipitation enabled exact matching of wet days between historic modeled P to observed P, which is critical for quantile mapping. The monthly P thresholds and scaling factors used to correct these biases are presented in supplement Table 3.S4 and Table 3.S5. Quantile mapping of the CMIP5 data to the historical data for one model under the RCP 8.5 scenario (micro-esm.1) is presented in Figure 3.7.

Monthly ensemble median P results indicate increased spring P compared to the baseline for both near and far future for all the emission scenarios (Figure 3.6). A previous study also reported an increase in precipitation during the spring months based on historic data for Central US (Feng et al., 2016). Decrease in ensemble monthly P compared to the baseline was simulated for near-future for the months from July-November for RCP 2.6 (Figure 3.6). For RCP 4.5, the decrease in P for July was 7 and 14%, and August was 6 and 14%, respectively, for near and far future. The decrease in precipitation for July and August was 12% and 14%, and 9% and 21%, respectively, for far future of RCP 6.0 and RCP 8.5. There was minimal change in the

monthly precipitation during the winter months. Occurrence of more P during spring may delay agricultural operations, and dry summers with very low P may result in short-term drought and possible crop losses. Previous regional modeling efforts using the Regional Climate Models (RCM) to assess the climate change impact on hydrology of the Mississippi River Basin indicated increased future P, as high as 21% on a mean annual basis (Jha et al., 2004). Downscaling of P based on point scale (weather station) data is more relevant at the small watershed scale and may help to better understand how changes in P and T impact the hydrologic components in the watershed.

Climate change impact on hydrologic output

<u>Water yield</u>

The ensemble median annual water yield was predicted to increase in both the near and far future compared to the baseline for RCP 2.6, RCP 4.5, and RCP 8.5 climate scenarios. Climate scenario RCP 6.0 showed 1% reduction in median water yield for far future scenario, due to minimum P change projected for far future for models under these climate scenarios. The highest change of 29% was observed for the far future scenario of RCP 8.5, which also resulted in the greatest increase for the near future (19%). The changes in water yield for RCP 2.6 and 4.5 were similar for near future, with the water yield increasing by around 10%. The water yield for RCP 2.6 and RCP 4.5 increased by 12% and 6%, respectively for the far future (Table 3.5). The models in RCP 6.0 showed very small changes in P (2% for near and 1% for far future). The increase in water yield was due to increased P; the model with the highest increase in P resulted in the highest increase in water yield. For example, the greatest

increase in water yield occurred for the month of May where the P was maximum for RCP 8.5 (Figures 3.6 and 3.8).

The first and third quartiles for water yield in Figure 3.8 show the variation in predicted water yield, which reflects the differences in GCM projections for each RCP. Despite this variation across GCM outputs, in all cases the ensemble median for near and far future was above the baseline median (Figure 3.8, Table 3.5).

For all the RCPs, the GCM ensemble range indicated a projected increase in the 3rd quartile of water yield. Monthly peak water yield occurs in June except for the far future of RCP 6.0 and RCP 8.5 scenario where it occurs in May (Figure 3.8). Elevated water yield during the spring months (March, April, and May) is due to an increase in spring P projected by all four emission pathways. Such change in distribution of water yield compared to baseline may cause increase risk of extreme (flood and drought) events in the watershed. Similar trends were simulated for the region, as shown by elevated future spring and mean annual water yield for the Missouri River Basin simulated using the GCM output and the SWAT model (Stone et al., 2003). These results, as well as previous studies (Risbey and Entekhabi, 1996), document that the runoff processes can be amplified due to fluctuations in P, resulting in significant impacts on streamflow. Our study shows similar results; the highest increase of water yield (83%) (270.5 to 494.9 mm) was simulated using the microc-esm.1 model under RCP 8.5 with 28% (from 969.2 to 1239 mm) increase in precipitation compared to baseline.

Surface Runoff

Ensemble mean annual surface runoff is predicted to increase compared to the historic period in all scenarios with the exception of RCP 6.0 in the far future (Figure 3.9).

RCP 8.5 resulted in the greatest increase compared to the historic period in surface runoff for both near future (20.9%) and far future (29.9%) (Table 3.5). The first and the third quartile ranges for surface runoff in Figure 3.9 show the range in predicted runoff associated with individual climate models. These variations reflect the difference in GCM projections among RCPs (Figure 3.9 and Table 3.5). The largest increases are shown in the spring months as a direct result of increased precipitation. The monthly peak runoff occurred in June except for in the far future of RCP 8.5 where it occurred in May (Figure 3.9). The magnitude of the peaks is larger than those observed in the historical dataset for all the RCPs except RCP 6.0 which shows small change in ensemble water yield (Table 3.5). Decreased surface runoff in August was simulated for RCP 4.5, RCP 6.0, and RCP 8.5 compared to historic baseline (Figure 3.9).

The relationship between increased P and surface runoff is a function of physical characteristics of the location, e.g., soil type, land cover, and in a mathematical model is also a function of the spatial and temporal resolution of the model inputs and response. Hydrologic models use geomorphologic and topographic parameters to characterize land forms to represent hydrologic process (Yang et al., 2001). The parameters used to represent the scale lead to differences in the simulated results. For example, SWAT uses detailed parameters to represent small sub-areas within a watershed, in this case 93 HRUs to represent the heterogeneity in GCEW, compared to single, spatially-averaged parameters applied in JeDi and LPJml to represent the grid that encompasses GCEW.

In this analysis, the GCM model microc-esm.1 under RCP 8.5 results in the largest increase in P with an average annual increase of 28% (969.2 to 1239 mm) which resulted in an increase in runoff of 88% (230.6 to 434.9 mm). Jha et al. (2004)

found that an increased runoff up to 51% in the Upper Mississippi River Basin (UMRB) for a 21% increase in P, using regional climate model output and SWAT. The SWAT model version used by Jha et al. (2004) was not modified to represent percolation through claypan soil. In contrast, a modified version of SWAT was used in our study to represent claypan hydrology (Baffaut et al., 2015a). The GCEW's relatively larger modeled surface runoff response is likely due to increased heavy precipitation events, differences in the model spatial resolution, and accounting for the claypan condition in the watershed (Baffaut et al., 2015a). Lower saturated hydraulic conductivity of the claypan layer results in lower infiltration and higher runoff response. The representation of small-scale details (e.g. claypan) conditions is often overlooked in large-scale simulations as these models are constructed to simulate average conditions. Model correction to represent each unique local situation is not feasible in a model with a large spatial resolution. The small watershed-scale studies are important as they help to better represent heterogeneity within the watershed, which ultimately can help local-scale decision making.

Monthly surface runoff estimated using SWAT in GCEW was compared to the surface runoff output from the LPJmL and JeDi-DGVM models forced using two sets of CMIP5 data (miroc-esm-chem and ipsl-cm5a-lr) and obtained from ISI-MIP, Figure 3.10 (Warszawski et al., 2014). For peak runoff, the flow duration curve comparison showed good agreement between SWAT and observed data (Figure 3.10). A lower peak value by the gridded models indicates an under-estimation of peak flow. The comparison indicates that the gridded models were unable to simulate the monthly peaks predicted by the SWAT simulations (Figure 3.10). Average annual surface runoff during 2016-2075 was over-estimated by 6-8% using LPJmL and under-estimated by 5-30% using JeDi-DGVM compared to the SWAT simulated

results. Paired t-test results indicate significantly lower prediction of average monthly runoff by JeDi-DVGM compared to SWAT simulated results and greater prediction by LPJmL. The results for paired t-tests are presented in Table 3.6.

The causes for these differences include model assumptions, model parameterization, input spatial resolution, and model structure in the respective models. Evapotranspiration was calculated using the PT method in LPJmL compared to the PM approach in SWAT. Suleiman and Hoogenboom (2007) report that the accuracy of the PM method for ET estimation is superior for predicting ET in the U.S. and that the PT method tends to overestimate ET for U.S. conditions. The difference in runoff prediction between the LPJmL and JeDi-DGVM models is also due to differences in approaches for representing dynamic vegetation in the model as presented in section 2.3. The lower peak monthly runoff and greater low runoff values in the gridded model output may also be due to simulation at a coarse resolution with a homogenous set of parameters compared to the fine resolution input data of SWAT model as described in section 2.1 and 2.3, as well as differences in accounting for local weather (i.e., statistical downscaling) and local hydrologic conditions (e.g. claypan). The comparison shows the importance of impact assessment at the smaller scale to predict hydrologic change through representing soil and land use with greater detail. Recommending simulation at small scale for every single point on the globe can be resource intensive and even not possible. However, simulation of small watersheds that represent major characteristics of regions can be useful for anticipating risks and corresponding decision-making, especially within the agriculture sector, which can experience quick response to change in precipitation and temperature. Likewise, global gridded models, which are generally better at simulating average conditions, may be sufficient for other applications. For a global

resource analyst, general trends noted by a global gridded model may be sufficient. Although LPJmL was able to represent the long-term average monthly conditions, it failed to represent extremes (peak and minimum runoff), which are important from an agricultural perspective.

Evapotranspiration

Median annual ET in the near and far future had little change, -1 to 3% compared to historical observations on an annual basis (Table 3.5). There was minimal change in annual ET in the near future for RCP 2.6 and RCP 6.0 (Table 3.5). However, there was an increase in ET in spring months and a decrease in summer months for both the near and far future for all four RCPs (Figure 3.11). The decrease in summer ET was maximum for RCP 8.5 and minimum for RCP 2.6.

Results indicated shifts in the peak monthly ET from July (baseline) to June for RCP 4.5, RCP 6.0, and RCP 8.5 in the far future (Figure 3.11). Land use and land cover were fixed during the entire simulation period. Therefore, variation of the simulated ET from the watershed was mostly controlled by meteorological variables and corresponding plant growth responses. For each crop, a base T must be reached for plant growth to begin in SWAT. With increased T, base T values were reached sooner than they have been reached historically, resulting in a shift in the plant growth cycle to earlier in the calendar year. This earlier emergence of biomass resulted in a corresponding shift in evapotranspiration to earlier in the season, with an earlier peak for all far future RCPs except for 2.6. The impact of elevated T on the hydrologic cycle due to shift of the crop growth cycle has been documented previously by Ficklin et al. (2009). However, it remains unclear whether farmers would actually plant crops

earlier. In addition, for this study region, increased spring precipitation may preclude early planting.

Conclusions

A calibrated and validated SWAT model for the GCEW was used to simulate the effect of climate change using downscaled T and P data from 12 GCMs under four emission scenarios. Downscaled climate model projections suggested an increase in spring precipitation and increased temperatures in the future for the study region, with the magnitude varying with the GCM model and emission scenarios. The change in precipitation for the extreme scenario (RCP 8.5) ranged from -7 to 16% for near future and from -10 to 28% for far future scenarios. The majority of CMIP5 data showed a reduction of summer precipitation and increase in spring precipitation. SWAT simulated hydrologic results indicated a range of possible futures due to increased temperature, precipitation changes, and elevated CO_2. Results show increased water yield, surface runoff during spring months, and a shift in ET for all the RCPs except RCP 2.6 in the far future. The greatest increase in the median water yield and surface runoff (29% and 30%) compared to the baseline was for the far future of the most extreme future climate scenario, i.e., RCP 8.5. Small changes in precipitation amounts can impact the runoff and water yield response, which is especially apparent at the small watershed scale. The shift in the peak ET from July to June for RCP 4.5, RCP 6.0, and RCP 8.5 indicated the probable impact of increased CO_2 concentration and temperature on the planting dates and seasonality, which may ultimately impact future crop yields. The particular concern for this watershed is the increase in precipitation, and the potential for more frequent occurrence of high-intensity rainfall events, in the springtime. This could negate potential for earlier planting, noted by some researchers as a potential benefit of increasing temperatures

50

due to climate change. Further, this study has found that cumulative precipitation is likely to decrease in the late summer, combined with higher temperatures could lead to drought conditions in July and August. Depending on planting date this could overlap with the tasseling stage of corn development. Modeling at this scale allows for a finer understanding of the patterns and processes of the hydrologic response, as well as potential implications with regard to agricultural activity, to changes in temperature and precipitation.

The comparison with gridded model output indicated that hydrological modeling at larger scales fails to capture peak and minimum runoff, which may be very important for adaptation responses at small scales. Average annual surface runoff during 2016-2075 was over-estimated by 6-8% using LPJmL and under-estimated by 5-30% using JeDi-DGVM compared to the SWAT simulated runoff. Global gridded data with coarse spatial resolution does not capture small-scale details that are necessary for agricultural management decisions. Simulation using higher spatial resolution as well as additional downscaling of weather data provided by CMIP5 helps to adequately represent the hydrologic components of small watersheds. This may be particularly important in a watershed with problematic soils, such as claypan soils found in GCEW and the surrounding region that have a very thin top soil layer above claypan to hold and supply water to plants.

Supplementary Materials: The following are available online at www.mdpi.com/link, Table 3.S1. List of the model used for impact assessment, Table 3.S2. Monthly additive factor used for the bias correction of maximum temperature using delta method for all the models, Table 3.S3. Monthly additive factor used for the bias correction of

minimum temperature using delta method for all the models, Table 3.S4. Monthly

scaling factor used for the bias correction of precipitation using quantile mapping for

gage25 datasets for all the models and Table 3.S5. Monthly precipitation threshold

(mm) used for the bias correction of precipitation using quantile mapping for gage25

datasets for all models.

Author Contributions: In this article, Sagar Gautam and Christine Costello designed

the study and wrote the initial draft of the manuscript and facilitated integration of team

comments and revisions; Claire Baffaut contributed in hydrologic model setup and

execution; Bohumil M. Svoma and Quang A. Phung contributed in statistical

downscaling; Claire Baffaut, Allen Thompson and Edward J. Sadler contributed with

discussions and scientific advice pertaining to hydrologic processes and the functioning

of the Goodwater Creek Experimental Watershed.

Conflicts of Interest: The authors declare no conflict of interest

References

Abbaspour, K., Vejdani, M., and Haghighat, S. (2007). Swat-Cup Calibration and Uncertainty Programs for Swat. *In* "MODSIM 2007 International Congress on Modelling and Simulation, Modelling and Simulation Society of Australia and New Zealand".

Ahmadi, M., Records, R., and Arabi, M. (2014). Impact of Climate Change on Diffuse Pollutant Fluxes at the Watershed Scale. *Hydrological Processes* **28**, 1962-1972.

Al-Mukhtar, M., Dunger, V., and Merkel, B. (2014). Assessing the Impacts of Climate Change on Hydrology of the Upper Reach of the Spree River: Germany. *Water Resources Management* **28**, 2731-2749.

Arnold, J. G., Srinivasan, R., Muttiah, R. S., and Williams, J. R. (1998). Large Area Hydrologic Modeling and Assessment Part I: Model Development. Wiley Online Library.

Baffaut, C., John Sadler, E., Ghidey, F., and Anderson, S. H. (2015a). Long-Term Agroecosystem Research in the Central Mississippi River Basin: SWAT Simulation of Flow and Water Quality in the Goodwater Creek Experimental Watershed. *Journal of Environmental Quality* **44**, 84-96.

Baffaut, C., Sadler, E. J., and Ghidey, F. (2015b). Long-Term Agroecosystem Research in the Central Mississippi River Basin: Goodwater Creek Experimental Watershed Flow Data. *Journal of Environmental Quality* **44**, 18-27.

Bellard, C., Bertelsmeier, C., Leadley, P., Thuiller, W., and Courchamp, F. (2012). Impacts of Climate Change on the Future of Biodiversity. *Ecology Letters* **15**, 365-377.

Bennett, K. E., Werner, A. T., and Schnorbus, M. (2012). Uncertainties in Hydrologic and Climate Change Impact Analyses in Headwater Basins of British Columbia. *Journal of Climate* **25**, 5711-5730.

Bentsen, M., Bethke, I., Debernard, J., Iversen, T., Kirkevåg, A., Seland, Ø., Drange, H., Roelandt, C., Seierstad, I., and Hoose, C. (2012). The Norwegian Earth System Model, Noresm1-M-Part 1: Description and Basic Evaluation. *Geoscientific Model Development Discussions* **5**, 2843-2931.

Block, P. J., Souza Filho, F. A., Sun, L., and Kwon, H. H. (2009). A Streamflow Forecasting Framework Using Multiple Climate and Hydrological Models. Wiley Online Library.

Boé, J., Terray, L., Habets, F., and Martin, E. (2007). Statistical and Dynamical Downscaling of the Seine Basin Climate for Hydro-Meteorological Studies. *International Journal of Climatology* **27**, 1643-1655.

Bondeau, A., Smith, P. C., Zaehle, S., Schaphoff, S., Lucht, W., Cramer, W., Gerten, D., LOTZE-CAMPEN, H., Müller, C., and Reichstein, M. (2007). Modelling

the Role of Agriculture for the 20th Century Global Terrestrial Carbon Balance. *Global Change Biology* **13**, 679-706.

Chiyuan, M., Qingyun, D., Qiaohong, S., Yong, H., Dongxian, K., Tiantian, Y., Aizhong, Y., Zhenhua, D., and Wei, G. (2014). Assessment of Cmip5 Climate Models and Projected Temperature Changes over Northern Eurasia. *Environmental Research Letters* **9**, 055007.

Choi, W., Pan, F., and Wu, C. (2017). Impacts of Climate Change and Urban Growth on the Streamflow of the Milwaukee River (Wisconsin, USA). *Regional Environmental Change* **17**, 889-899.

Clark, M. P., Bierkens, M. F. P., Samaniego, L., Woods, R. A., Uijenhoet, R., Bennet, K. E., Pauwels, V. R. N., Cai, X., Wood, A. W., and Peters-Lidard, C. D. (2017). The Evolution of Process-Based Hydrologic Models: Historical Challenges and the Collective Quest for Physical Realism. *Hydrology and Earth System Sciences* **2017**, 1-14.

Cubasch, U., D. Wuebbles, D. Chen, M.C. Facchini, D. Frame, N. Mahowald, and Winther, J. G. (2013). Introduction: The Physical Science Basis. Contribution of Working Group I to the Fifth Assessment Report of the Intergovernmental Panel on Climate Change [Stocker, T.F., D. Qin, G.-K. Plattner, M. Tignor, S.K. Allen, J. Boschung, A. Nauels, Y. Xia, V. Bex and P.M. Midgley (Eds.)]. *Climate Change*.

De Wit, M., and Stankiewicz, J. (2006). Changes in Surface Water Supply across Africa with Predicted Climate Change. *Science* **311**, 1917-1921.

Diimenil, M. E., Giorgetta, M., Schlese, U., and Schullzweida, U. (1996). The Atmospheric General Circulation Model Echam-4: Model Description and Simulation of Present-Day Climate. *Max Planck Institute for Meteorology, Hamburg, Germany* **MPI Rep. 218**, 90.

Dunne, J. P., John, J. G., Adcroft, A. J., Griffies, S. M., Hallberg, R. W., Shevliakova, E., Stouffer, R. J., Cooke, W., Dunne, K. A., and Harrison, M. J. (2012). Gfdl's Esm2 Global Coupled Climate-Carbon Earth System Models. Part I: Physical Formulation and Baseline Simulation Characteristics. *Journal of Climate* **25**, 6646-6665.

Dunne, J. P., John, J. G., Shevliakova, E., Stouffer, R. J., Krasting, J. P., Malyshev, S. L., Milly, P., Sentman, L. T., Adcroft, A. J., and Cooke, W. (2013). Gfdl's Esm2 Global Coupled Climate–Carbon Earth System Models. Part Ii: Carbon System Formulation and Baseline Simulation Characteristics. *Journal of Climate* **26**, 2247-2267.

Feng, Z., Leung, L. R., Hagos, S., Houze, R. A., Burleyson, C. D., and Balaguru, K. (2016). More Frequent Intense and Long-Lived Storms Dominate the Springtime Trend in Central Us Rainfall. *Nature Communications* **7**, 13429.

Ficklin, D., Stewart, I., and Maurer, E. (2013a). Effects of Projected Climate Change on the Hydrology in the Mono Lake Basin, California. *Climatic Change* **116**, 111-131.

Ficklin, D. L., and Barnhart, B. L. (2014). Swat Hydrologic Model Parameter Uncertainty and Its Implications for Hydroclimatic Projections in Snowmelt-Dependent Watersheds. *Journal of Hydrology* **519**, 2081-2090.

Ficklin, D. L., Luo, Y., Luedeling, E., and Zhang, M. (2009). Climate Change Sensitivity Assessment of a Highly Agricultural Watershed Using Swat. *Journal of Hydrology* **374**, 16-29.

Ficklin, D. L., Stewart, I. T., and Maurer, E. P. (2013b). Climate Change Impacts on Streamflow and Subbasin-Scale Hydrology in the Upper Colorado River Basin. *PLoS ONE* **8**, e71297.

Fowler, H., Blenkinsop, S., and Tebaldi, C. (2007). Linking Climate Change Modelling to Impacts Studies: Recent Advances in Downscaling Techniques for Hydrological Modelling. *International Journal of Climatology* **27**, 1547-1578.

Freeze, R. A., and Harlan, R. (1969). Blueprint for a Physically-Based, Digitally-Simulated Hydrologic Response Model. *Journal of Hydrology* **9**, 237-258.

Gent, P. R., Danabasoglu, G., Donner, L. J., Holland, M. M., Hunke, E. C., Jayne, S. R., Lawrence, D. M., Neale, R. B., Rasch, P. J., and Vertenstein, M. (2011). The Community Climate System Model Version 4. *Journal of Climate* **24**, 4973-4991.

Gregory, R. D., Willis, S. G., Jiguet, F., Voříšek, P., Klvaňová, A., Strien, A. v., Huntley, B., Collingham, Y. C., Couvet, D., and Green, R. E. (2009). An Indicator of the Impact of Climatic Change on European Bird Populations. *PLoS ONE* **4**, e4678.

Grillakis, M. G., Koutroulis, A. G., and Tsanis, I. K. (2013). Multisegment Statistical Bias Correction of Daily Gcm Precipitation Output. *Journal of Geophysical Research: Atmospheres* **118**, 3150-3162.

Haasnoot, M., van Deursen, W. P. A., Guillaume, J. H. A., Kwakkel, J. H., van Beek, E., and Middelkoop, H. (2014). Fit for Purpose? Building and Evaluating a Fast, Integrated Model for Exploring Water Policy Pathways. *Environmental Modelling & Software* **60**, 99-120.

Hempel, S., Frieler, K., Warszawski, L., Schewe, J., and Piontek, F. (2013). A Trend-Preserving Bias Correction–the ISI-MIP Approach. *Earth System Dynamics* **4**, 219-236.

Hidalgo, H. G., Dettinger, M. D., and Cayan, D. R. (2008). "Downscaling with Constructed Analogues: Daily Precipitation and Temperature Fields over the United States."

Ines, A. V., and Hansen, J. W. (2006). Bias Correction of Daily Gcm Rainfall for Crop Simulation Studies. *Agricultural and Forest Meteorology* **138**, 44-53.

IPCC (2013). What Is a GCM? *In* "Guidance on the use of data". Data Distribution Centre.

IPCC (2014). "Climate Change 2014: Mitigation of Climate Change.," Cambridge University Press, Cambridge, United Kingdom and New York, NY, USA.

Jha, M., Pan, Z., Takle, E. S., and Gu, R. (2004). Impacts of Climate Change on Streamflow in the Upper Mississippi River Basin: A Regional Climate Model Perspective. *Journal of Geophysical Research: Atmospheres* **109**, 1-12.

Jha, M., Gassman, P., and Panagopoulos, Y. (2015). Regional Changes in Nitrate Loadings in the Upper Mississippi River Basin under Predicted Mid-Century Climate. *Regional Environmental Change* **15**, 449-460.

Jha, M. K., and Gassman, P. W. (2014). Changes in Hydrology and Streamflow as Predicted by a Modelling Experiment Forced with Climate Models. *Hydrological Processes* **28**, 2772-2781.

Johnson, F., and Sharma, A. (2011). Accounting for Interannual Variability: A Comparison of Options for Water Resources Climate Change Impact Assessments. *Water Resources Research* **47**, 1-20.

Jung, W., Kitchen, N., Sudduth, K., and Anderson, S. (2006). Spatial Characteristics of Claypan Soil Properties in an Agricultural Field. *Soil Science Society of America Journal* **70**, 1387-1397.

Kim, H. M., Webster, P. J., and Curry, J. A. (2012). Evaluation of Short-Term Climate Change Prediction in Multi-Model Cmip5 Decadal Hindcasts. *Geophysical Research Letters* **39**.

Klein Goldewijk, K. (2016). A Historical Land Use Data Set for the Holocene; Hyde 3.2. *In* "EGU General Assembly Conference Abstracts", Vol. 18, pp. 1574.

Kucharik, C. J., and Serbin, S. P. (2008). Impacts of Recent Climate Change on Wisconsin Corn and Soybean Yield Trends. *Environmental Research Letters* **3**, 034003.

Le, P. V., Kumar, P., and Drewry, D. T. (2011). Implications for the Hydrologic Cycle under Climate Change Due to the Expansion of Bioenergy Crops in the Midwestern United States. *Proceedings of the National Academy of Sciences* **108**, 15085-15090.

Lenderink, G., Buishand, A., and Deursen, W. v. (2007). Estimates of Future Discharges of the River Rhine Using Two Scenario Methodologies: Direct Versus Delta Approach. *Hydrology and Earth System Sciences* **11**, 1145-1159.

Li, H., Sheffield, J., and Wood, E. F. (2010). Bias Correction of Monthly Precipitation and Temperature Fields from Intergovernmental Panel on Climate Change Ar4 Models Using Equidistant Quantile Matching. *Journal of Geophysical Research: Atmospheres* **115**, 1984-2012.

Liang, X. (1994). A Two-Layer Variable Infiltration Capacity Land Surface Representation for General Circulation Models. Water Resources Series Tech Rep 140, Seattle, Washington.

Maurer, E. P., Brekke, L., Pruitt, T., and Duffy, P. B. (2007). Fine-Resolution Climate Projections Enhance Regional Climate Change Impact Studies. *Eos, Transactions American Geophysical Union* **88**, 504-504.

Meinshausen, M., Smith, S. J., Calvin, K., Daniel, J. S., Kainuma, M., Lamarque, J.-F., Matsumoto, K., Montzka, S., Raper, S., and Riahi, K. (2011). The Rcp Greenhouse Gas Concentrations and Their Extensions from 1765 to 2300. *Climatic Change* **109**, 213.

Mohammed, I. N., Bomblies, A., and Wemple, B. C. (2015). The Use of Cmip5 Data to Simulate Climate Change Impacts on Flow Regime within the Lake Champlain Basin. *Journal of Hydrology: Regional Studies* **3**, 160-186.

Moriasi, D. N., Gitau, M. W., Pai, N., and Daggupati, P. (2015). Hydrologic and Water Quality Models: Performance Measures and Evaluation Criteria. *Transactions of the ASABE* **58**, 1763-1785.

Moritz, C., and Agudo, R. (2013). The Future of Species under Climate Change: Resilience or Decline? *Science* **341**, 504-508.

Nachtergaele, F., van Velthuizen, H., Verelst, L., Batjes, N., Dijkshoorn, J., van Engelen, V., Fischer, G., Jones, A., Montanarella, L., and Petri, M. (2008). "Harmonized World Soil Database (Version 1.0)." Food and Agric Organization of the UN (FAO); International Inst. for Applied Systems Analysis (IIASA); ISRIC-World Soil Information; Inst of Soil Science-Chinese Acad of Sciences (ISS-CAS); EC-Joint Research Centre (JRC).

Neitsch, S., Arnold, J., Kiniry, J. e. a., Srinivasan, R., and Williams, J. (2002). Soil and Water Assessment Tool User's Manual Version 2000. *GSWRL report* **202**.

Neitsch, S. L., Arnold, J. G., Kiniry, J. R., and Williams, J. R. (2011). Soil and Water Assessment Tool Theoretical Documentation: Version 2009. USDA Agricultural Research Service and Texas A&M Blackland Research Center, Temple, Texas.

Ouyang, F., Zhu, Y., Fu, G., Lü, H., Zhang, A., Yu, Z., and Chen, X. (2015). Impacts of Climate Change under Cmip5 Rcp Scenarios on Streamflow in the Huangnizhuang Catchment. *Stochastic Environmental Research and Risk Assessment* **29**, 1781-1795.

Pachauri, R. K., Allen, M., Barros, V., Broome, J., Cramer, W., Christ, R., Church, J., Clarke, L., Dahe, Q., and Dasgupta, P. (2014). Climate Change 2014: Synthesis Report. Contribution of Working Groups I, II and III to the Fifth Assessment Report of the Intergovernmental Panel on Climate Change.

Panagopoulos, Y., Gassman, P., Arritt, R., Herzmann, D., Campbell, T., Jha, M., Kling, C., Srinivasan, R., White, M., and Arnold, J. (2014). Surface Water Quality and Cropping Systems Sustainability under a Changing Climate in the Upper Mississippi River Basin. *Journal of Soil and Water Conservation* **69**, 483-494.

Pavlick, R., Drewry, D. T., Bohn, K., Reu, B., and Kleidon, A. (2013). The Jena Diversity-Dynamic Global Vegetation Model (Jedi-Dgvm): A Diverse

Approach to Representing Terrestrial Biogeography and Biogeochemistry Based on Plant Functional Trade-Offs. *Biogeosciences* **10**, 4137-4177.

Perez, J., Menendez, M., Mendez, F., and Losada, I. (2014). Evaluating the Performance of Cmip3 and Cmip5 Global Climate Models over the North-East Atlantic Region. *Climate Dynamics* **43**, 2663-2680.

Peters, G. P., Andrew, R. M., Boden, T., Canadell, J. G., Ciais, P., Le Quéré, C., Marland, G., Raupach, M. R., and Wilson, C. (2013). The Challenge to Keep Global Warming Below 2° C. *Nature Climate Change* **3**, 4.

Piao, S., Ciais, P., Huang, Y., Shen, Z., Peng, S., Li, J., Zhou, L., Liu, H., Ma, Y., and Ding, Y. (2010). The Impacts of Climate Change on Water Resources and Agriculture in China. *Nature* **467**, 43-51.

Pierce, D. W., Barnett, T. P., Santer, B. D., and Gleckler, P. J. (2009). Selecting Global Climate Models for Rgional Climate Change Studies. *Proceedings of the National Academy of Sciences* **106**, 8441-8446.

Qiao, L., Pan, Z., Herrmann, R. B., and Hong, Y. (2014). Hydrological Variability and Uncertainty of Lower Missouri River Basin under Changing Climate. *JAWRA Journal of the American Water Resources Association* **50**, 246-260.

Risbey, J. S., and Entekhabi, D. (1996). Observed Sacramento Basin Streamflow Response to Precipitation and Temperature Changes and Its Relevance to Climate Impact Studies. *Journal of Hydrology* **184**, 209-223.

Sadler, E. J., Lerch, R. N., Kitchen, N. R., Anderson, S. H., Baffaut, C., Sudduth, K. A., Prato, A. A., Kremer, R. J., Vories, E. D., and Myers, D. B. (2015a). Long-Term Agroecosystem Research in the Central Mississippi River Basin: Introduction, Establishment, and Overview. *Journal of Environmental Quality* **44**, 3-12.

Sadler, E. J., Sudduth, K. A., Drummond, S. T., Vories, E. D., and Guinan, P. E. (2015b). Long-Term Agroecosystem Research in the Central Mississippi River Basin: Goodwater Creek Experimental Watershed Weather Data. *Journal of Environmental Quality* **44**, 13-17.

Santhi, C., Arnold, J. G., Williams, J. R., Dugas, W. A., Srinivasan, R., and Hauck, L. M. (2001). Validation of the Swat Model on a Large Rwer Basin with Point and Nonpoint Sources. *Journal of the American Water Resources Association* **37**, 1169-1188.

Schewe, J., Heinke, J., Gerten, D., Haddeland, I., Arnell, N. W., Clark, D. B., Dankers, R., Eisner, S., Fekete, B. M., and Colón-González, F. J. (2014). Multimodel Assessment of Water Scarcity under Climate Change. *Proceedings of the National Academy of Sciences* **111**, 3245-3250.

Schlenker, W., Hanemann, W. M., and Fisher, A. C. (2006). The Impact of Global Warming on Us Agriculture: An Econometric Analysis of Optimal Growing Conditions. *The Review of Economics and Statistics* **88**, 113-125.

Schneider, S. H. (1992). Introduction to Climate Modeling. *SMR* **648**, 6.

Seaber, P. R., Kapinos, F. P., and Knapp, G. L. (1987). "Hydrologic Unit Maps." USGPO.

Sellami, H., Benabdallah, S., La Jeunesse, I., and Vanclooster, M. (2016). Climate Models and Hydrological Parameter Uncertainties in Climate Change Impacts on Monthly Runoff and Daily Flow Duration Curve of a Mediterranean Catchment. *Hydrological Sciences Journal* **61**, 1415-1429.

Stone, M. C., Hotchkiss, R. H., and Mearns, L. O. (2003). Water Yield Responses to High and Low Spatial Resolution Climate Change Scenarios in the Missouri River Basin. *Geophysical Research Letters* **30**.

Suleiman, A. A., and Hoogenboom, G. (2007). Comparison of Priestley-Taylor and Fao-56 Penman-Monteith for Daily Reference Evapotranspiration Estimation in Georgia. *Journal of Irrigation and Drainage Engineering* **133**, 175-182.

Tavakoli, M., and De Smedt, F. (2011). Impact of Climate Change on Streamflow and Soil Moisture in the Vermilion Basin, Illinois. *Journal of Hydrologic Engineering* **17**, 1059-1070.

Taylor, K. E., Stouffer, R. J., and Meehl, G. A. (2012). An Overview of Cmip5 and the Experiment Design. *Bulletin of the American Meteorological Society* **93**, 485-498.

Terink, W., Hurkmans, R. T. W. L., Torfs, P. J. J. F., and Uijlenhoet, R. (2010). Evaluation of a Bias Correction Method Applied to Downscaled Precipitation and Temperature Reanalysis Data for the Rhine Basin. *Hydrology and Earth System Sciences* **14**, 687-703.

Themeßl, M. J., Gobiet, A., and Leuprecht, A. (2011). Empirical-Statistical Downscaling and Error Correction of Daily Precipitation from Regional Climate Models. *International Journal of Climatology* **31**, 1530-1544.

Udawatta, R. P., Motavalli, P. P., and Garrett, H. E. (2004). Phosphorus Loss and Runoff Characteristics in Three Adjacent Agricultural Watersheds with Claypan Soils. *Journal of Environmental Quality* **33**, 1709-1719.

Van Vuuren, D., Edmonds, J., Kainuma, M., Riahi, K., Thomson, A., Hibbard, K., Hurtt, G., Kram, T., Krey, V., Lamarque, J.-F., Masui, T., Meinshausen, M., Nakicenovic, N., Smith, S., and Rose, S. (2011). The Representative Concentration Pathways: An Overview. *Climatic Change* **109**, 5-31.

Walther, G.-R., Post, E., Convey, P., Menzel, A., Parmesan, C., Beebee, T. J. C., Fromentin, J.-M., Hoegh-Guldberg, O., and Bairlein, F. (2002). Ecological Responses to Recent Climate Change. *Nature* **416**, 389-395.

Warszawski, L., Frieler, K., Huber, V., Piontek, F., Serdeczny, O., and Schewe, J. (2014). The Inter-Sectoral Impact Model Intercomparison Project (ISI–MIP): Project Framework. *Proceedings of the National Academy of Sciences* **111**, 3228-3232.

Warszawski, L., Frieler, K., Piontek, F., Schewe, J., Serdeczny, O., and Huber, V. (2013). Research Design of the Intersectoral Impact Model Intercomparison Project (ISI-MIP). *PNAS, accepted*.

Watanabe, M., Suzuki, T., O'ishi, R., Komuro, Y., Watanabe, S., Emori, S., Takemura, T., Chikira, M., Ogura, T., and Sekiguchi, M. (2010). Improved Climate Simulation by MIROC5: Mean States, Variability, and Climate Sensitivity. *Journal of Climate* **23**, 6312-6335.

Watanabe, S., Hajima, T., Sudo, K., Nagashima, T., Takcmura, T., Okajima, H., Nozawa, T., Kawase, H., Abe, M., and Yokohata, T. (2011). Miroc-Esm 2010: Model Description and Basic Results of Cmip5-20c3m Experiments. *Geoscientific Model Development* **4**, 845-872.

Williams, J. R., and Izaurralde, R. (2006). The APEX Model. *Watershed Models*, 437-482.

Wu, T., Song, L., Li, W., Wang, Z., Zhang, H., Xin, X., Zhang, Y., Zhang, L., Li, J., Wu, F., Liu, Y., Zhang, F., Shi, X., Chu, M., Zhang, J., Fang, Y., Wang, F., Lu, Y., Liu, X., Wei, M., Liu, Q., Zhou, W., Dong, M., Zhao, Q., Ji, J., Li, L., and Zhou, M. (2014). An Overview of Bcc Climate System Model Development and Application for Climate Change Studies. *Journal of Meteorological Research* **28**, 34-56.

Yang, D., Herath, S., and Musiake, K. (2001). Spatial Resolution Sensitivity of Catchment Geomorphologic Properties and the Effect on Hydrological Simulation. *Hydrological Processes* **15**, 2085-2099.

Ye, L., and Grimm, N. (2013). Modelling Potential Impacts of Climate Change on Water and Nitrate Export from a Mid-Sized, Semiarid Watershed in the Us Southwest. *Climatic Change* **120**, 419-431.

Yukimoto, S., Adachi, Y., Hosaka, M., Sakami, T., Yoshimura, H., Hirabara, M., Tanaka, T. Y., Shindo, E., Tsujino, H., and Deushi, M. (2012). A New Global Climate Model of the Meteorological Research Institute: Mri-Cgcm3-Model Description and Basic Performance. *Journal of the Meteorological Society of Japan* **90**, 23-64.

Zhao, L., Xu, J., and Powell Jr, A. (2013). Discrepancies of Surface Temperature Trends in the Cmip5 Simulations and Observations on the Global and Regional Scales. *Climate of the Past Discussions* **9**, 6161-6178.

Table 3.1. Land use land cover for the Goodwater Creek Experimental Watershed based on NASS 2010

Land use	Area (ha)	%Watershed area
Corn	1702.6	23.1
Forest	444.5	6.0
Hay	540.7	7.3
Pasture	1049.5	14.3
Soybean	3052.1	41.4
Switchgrass	73.5	1.0
Urban	501.5	6.9

Table 3.2. List of the General Circulation Models used in this study

Model	CMIP5 Climate Modeling Group	Model ID	Reference
1	Beijing Climate Center, China Meteorological Administration	bcc-csm1-1	(Wu et al., 2014)
2	National Center for Atmospheric Research	ccsm4.1	(Gent et al., 2011)
3	National Center for Atmospheric Research	ccsm4.2	(Gent et al., 2011)
4	NOAA Geophysical Fluid Dynamics Laboratory	gfdl-esm2g	(Dunne et al., 2012)
5	NOAA Geophysical Fluid Dynamics Laboratory	gfdl-esm2m	(Dunne et al., 2013)
6	Institut Pierre-Simon Laplace	ipsl-cm5a-lr	(Dunne et al., 2013)
7	Institut Pierre-Simon Laplace	ipsl-cm5a-mr	(Dunne et al., 2013)
8	Japan Agency for Marine-Earth Science and Technology, Atmosphere and Ocean Research Institute (The University of Tokyo), and National Institute for Environmental Studies	miroc-esm	(Watanabe et al., 2011)
9	Japan Agency for Marine-Earth Science and Technology, Atmosphere and Ocean Research Institute (The University of Tokyo), and National Institute for Environmental Studies	miroc-esm-chem	(Watanabe et al., 2011)
10	Atmosphere and Ocean Research Institute (The University of Tokyo), National Institute for Environmental Studies, and Japan Agency for Marine-Earth Science and Technology	miroc5	(Watanabe et al., 2010)
11	Meteorological Research Institute	mri-cgcm3	(Yukimoto et al., 2012)
12	Norwegian Climate centre	noresm1-m	(Bentsen et al., 2012)

Table 3.3. Variable initial carbon dioxide concentration used for SWAT simulation under different emission scenarios (Peters et al., 2013)

Scenarios	2016-2045	2046-2075
	CO_2 concentration in part per million (ppm)	
RCP 2.6	428	440
RCP 4.5	437	507
RCP 6.0	431	515
RCP 8.5	454	611

Table 3.4. Sensitivity results of key SWAT parameters for stream discharge in the Goodwater Creek Experimental Watershed including the default values

Parameter	Definition	Default Value	Adjusted Value
ESCO	Soil evaporation compensation factor	0.95	0.88
GWQMN	Shallow aquifer depth of water required for return flow to occur (mm)	0	55
GW_DELAY	Groundwater delay time (days)	31	55
SOL_AWC	Available water capacity of the soil layer (mm H_2O/mm soil)	-	0.04†
CH_N	Manning's "n" value for the main channel	0.014	0.019
CH_K	Effective hydraulic conductivity in main channel	0	0.08
	Alluvium (mm/hr.)		
SMTMP	Snow melt temperature (°C)	0.5	-2.5
SMFMN	Snow melt min rate (mm H_20/°C-day)	4.5	1.5
EVRCH	Reach evaporation adjustment factor	1	0.5
MSK_X	Weighting factor that controls the relative importance of inflow and outflow in determining the storage in the reach	0.2	0.1
MSK_CO_2	Calibration coefficient used to control impact of the storage time constant for low flow upon the time constant value calculated for the reach	0.25	3.5
ALPHA_BF	Baseflow alpha factor (1/days)	0.0048	0.1
SHALLST	Initial depth of water in the shallow aquifer (mm)	1000	600

Note: † denote the relative change in the parameter value

Table 3.5. Ensemble median and quartiles of annual simulated water yield, surface runoff and ET changes (in percent) for the Goodwater Creek Experimental Watershed

Water Yield (% change over the baseline)

	RCP 2.6		RCP 4.5		RCP 6.0		RCP 8.5	
	Near future	Far future	Near future	Far future	Near future	Far future	Near future	Far future
Median	9.9	12.0	10.4	6.2	5.4	-1.0	19.0	29.4
1st Quartile	5.6	8.4	2.4	0.1	-2.9	-2.7	7.7	19.9
3rd Quartile	11.1	19.2	11.6	28.3	8.9	16.3	23.1	31.4
Surface Runoff								
Median	10.1	12.2	9.7	7.2	5.9	-0.9	20.9	29.9
1st Quartile	6.6	10.0	3.6	1.6	-3.0	-3.0	7.8	20.0
3rd Quartile	12.4	20.0	11.3	28.1	8.2	17.6	24.4	31.0
Evapotranspiration								
Median	0.1	3.1	1.6	0.1	0.8	-0.3	2.1	-2.1
1st Quartile	-1.1	1.9	1.8	-0.8	-0.7	-2.5	0.4	-1.4
3rd Quartile	1.0	2.2	0.1	1.3	0.5	0.7	0.4	-2.4

Table 3.6. Comparison of average monthly runoff predicted by the hydrologic models SWAT, JeDi-DVGM, and LPjmL forced with two different global climate model (GCM) datasets

GCM/Period	Runoff (mm)-SWAT		Runoff (mm)-LPJmL		Runoff (mm)-JeDi-DVGM	
	NF	FF	NF	FF	NF	FF
ipsl-cm5a-lr	24.4^{aA}	20^{cC}	23.9^{a}	23.3^{d}	26.5^{A}	15.5^{D}
miroc-esm-chem	20.7^{aA}	26.4^{cC}	24^{a}	26.8^{c}	18.4^{B}	14.8^{D}

Note: Means followed by different letters between the columns for each of the time periods (Near Future (NF) and Far Future (FF)) are significant at $p \leq 0.05$. Small letter shows difference in runoff between SWAT vs LPJmL and capital letter shows difference between SWAT vs JEDI-DVGM
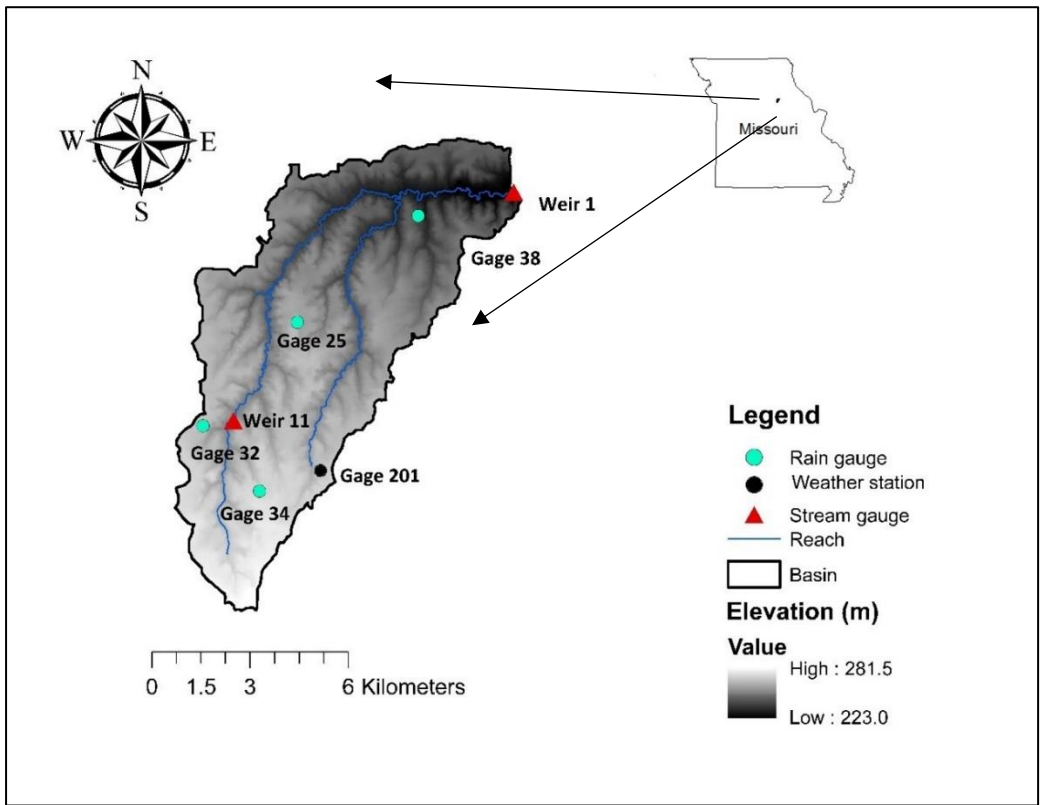
Figure 3.1. Goodwater Creek Experimental Watershed showing rain gauges and weir outlets
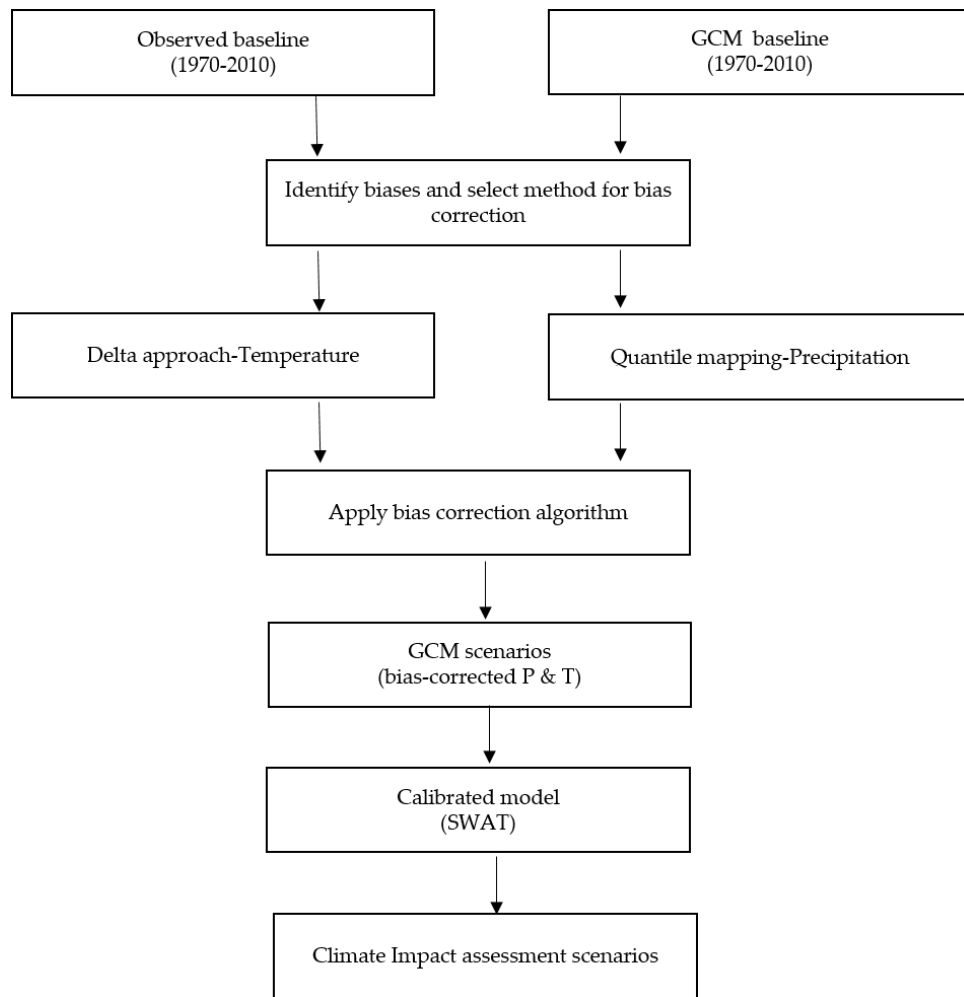
Figure 3.2. A flow chart describing the analysis completed to assess climate change impact on the Goodwater Creek Experimental Watershed using historical weather observations, CMIP5 climate data, and SWAT.
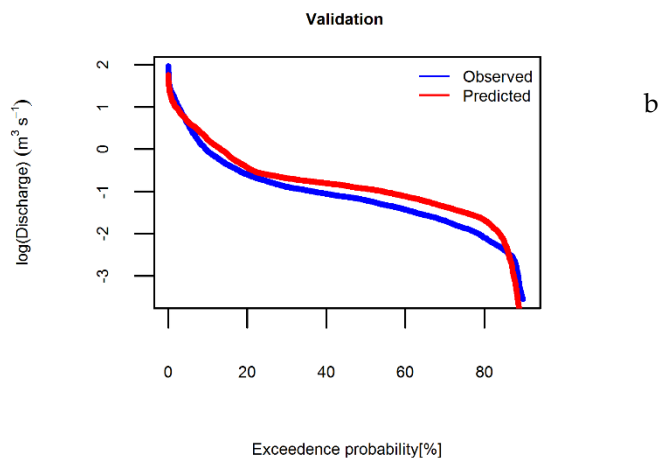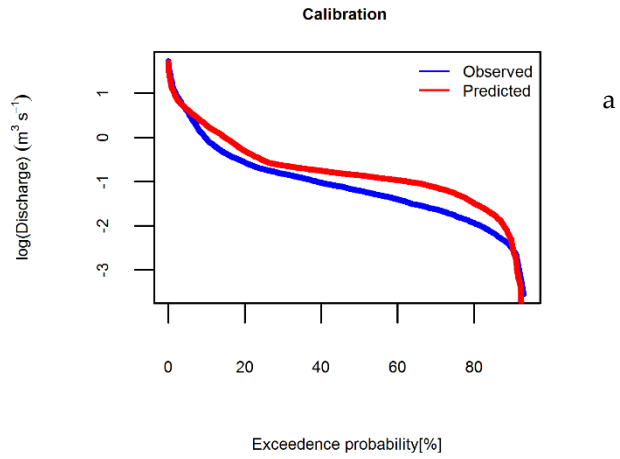
Figure 3.3. Flow duration curve for calibration (a) and validation (b) of SWAT model for Goodwater Creek Experimental Watershed at weir 1
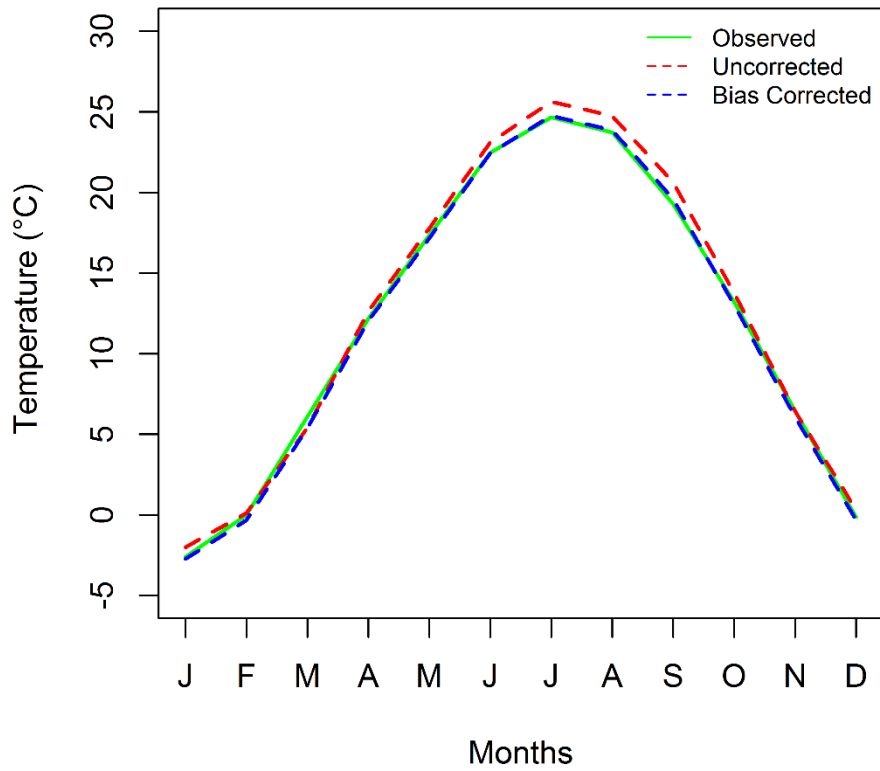
Figure 3.4. Monthly temperature (°C) over Goodwater Creek Experimental Watershed for the period of 1971–2010. Results are shown for the observations, uncorrected, and bias-corrected RCP4.5 microesm.1
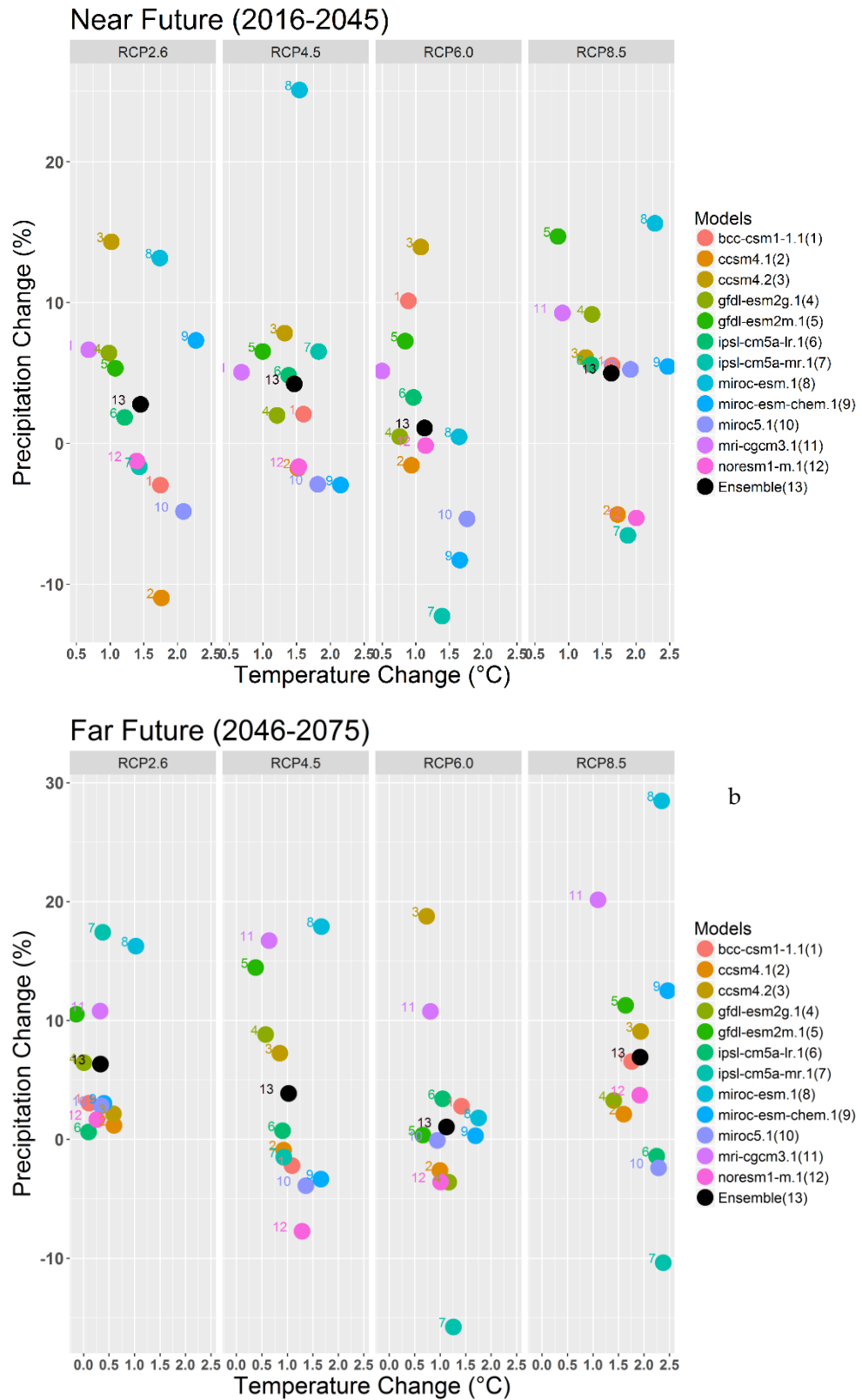
Figure 3.5. Change in average yearly temperature and total precipitation relative to the baseline (1981-2010) for the periods a) Near Future (2016–2045) and b) Far Future (2046–2075) for all the GCMs.
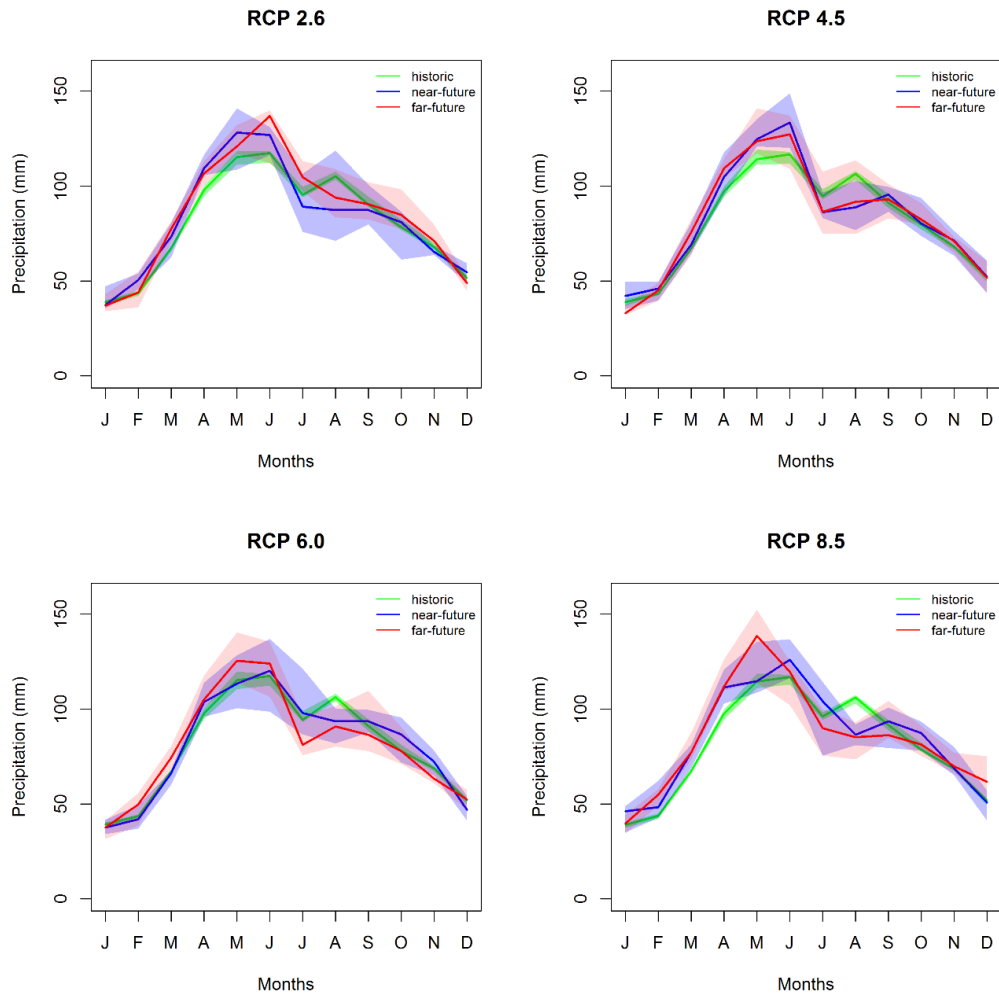
Figure 3.6. Monthly ensemble median and quartile of downscaled monthly precipitation for historic and future projections in Goodwater Creek Experimental Watershed. The median is represented by the solid line with Q1 represented by the lower bound of the shaded region and Q3 represented by the upper bound of the shaded region.
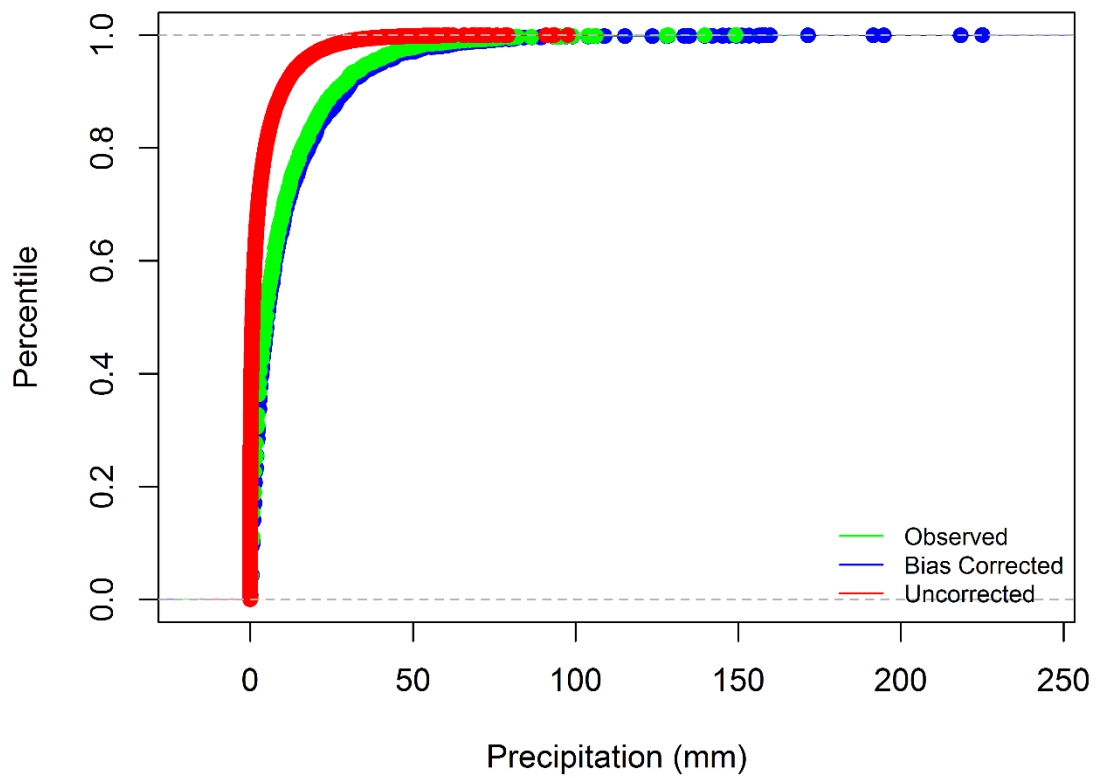
Figure 3.7. Quantile mapping approach for the correction of dry bias and representation of future extreme events (Plotted data: RCP 8.5 microesm.1)
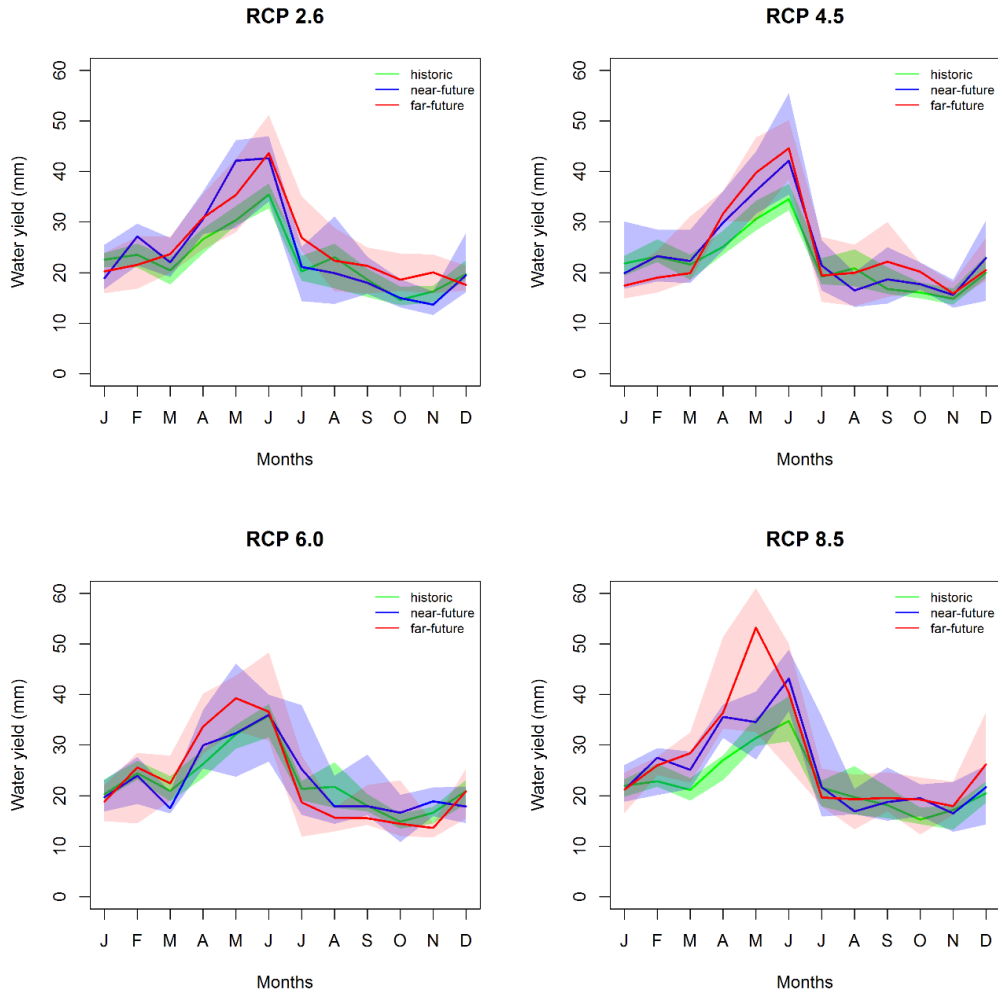
Figure 3.8. Monthly ensemble median and quartile of downscaled monthly water yield for historic and future projections in Goodwater Creek Experimental Watershed. The median is represented by the solid line with Q1 represented by the lower bound of the shaded region and Q3 represented by the upper bound of the shaded region.
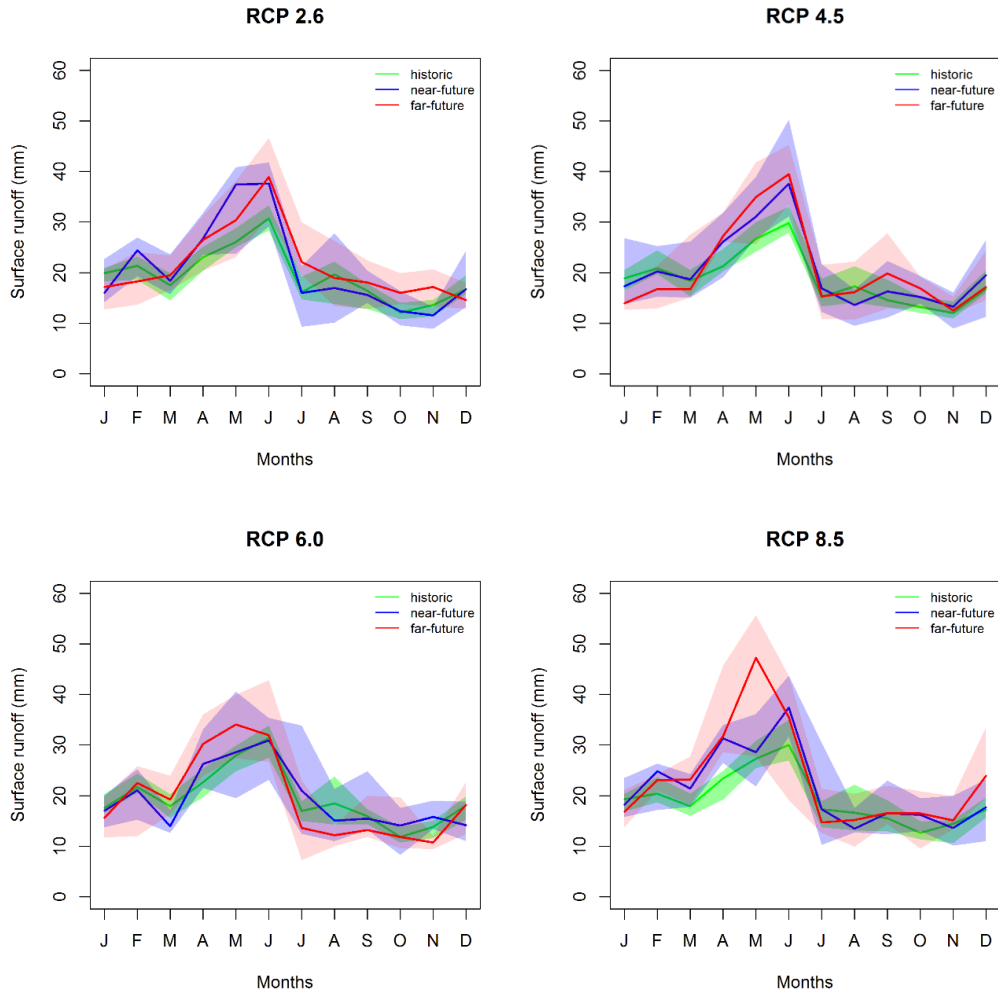
Figure 3.9. Monthly ensemble median and quartile of downscaled monthly surface runoff for historic and future projections in Goodwater Creek Experimental Watershed. The median is represented by the solid line with Q1 represented by the lower bound of the shaded region and Q3 represented by the upper bound of the shaded region
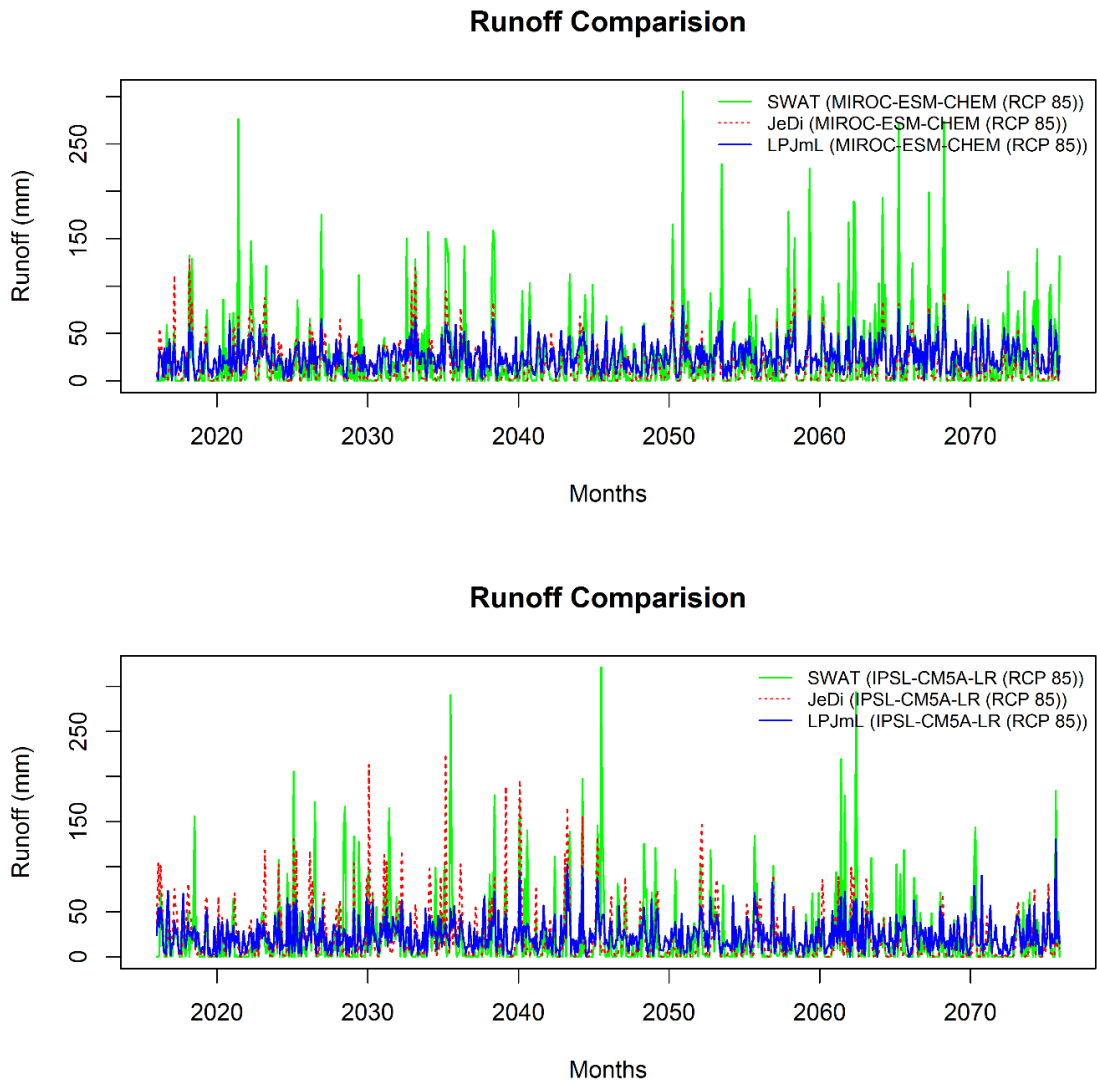
Figure 3.10. Runoff comparison of simulated monthly runoff from simulation forced with MIROC-ESM-CHEM (a) and IPSL-CM5A-LR (b) for RCP 8.5 climate scenarios for the SWAT, LPJmL and JeDi-DGVM model.
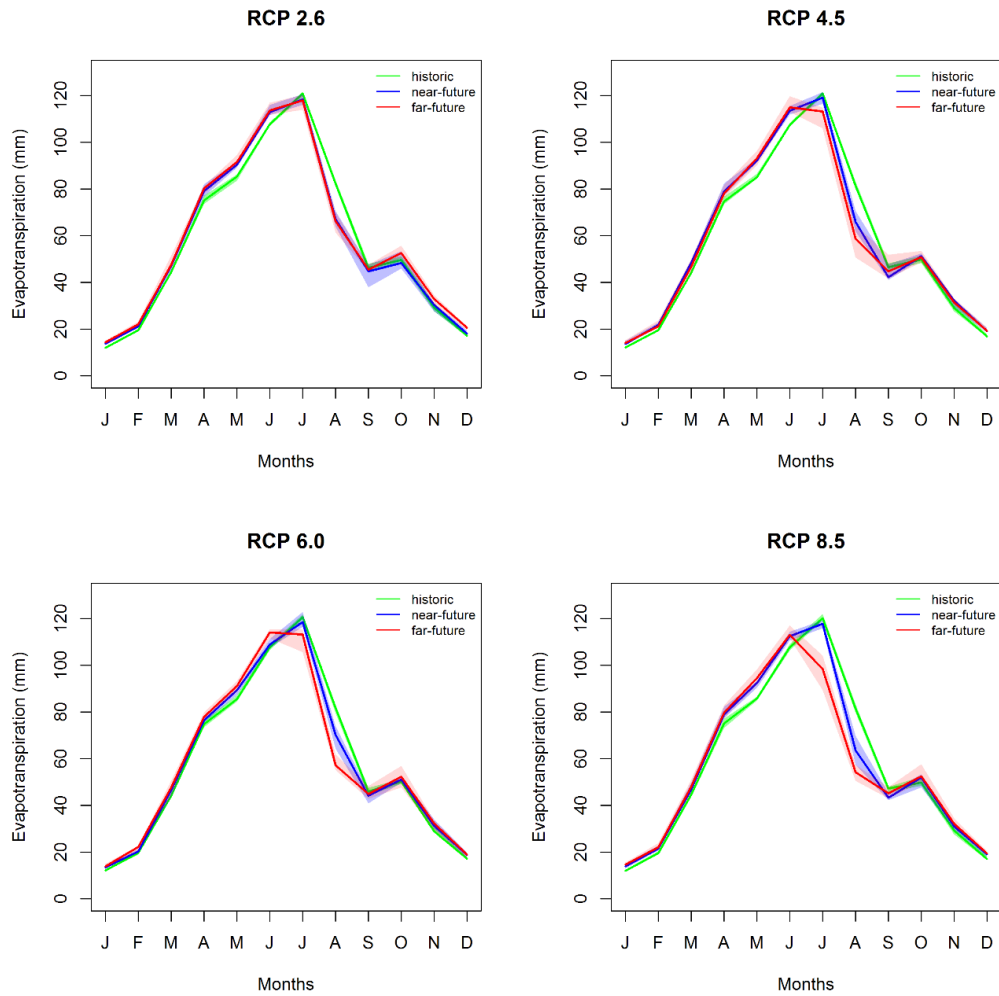
Figure 3.11. Monthly ensemble median and quartile of downscaled monthly evapotranspiration for historic and future projections in Goodwater Creek Experimental Watershed. The median is represented by the solid line with Q1 represented by the lower bound of the shaded region and Q3 represented by the upper bound of the shaded region

CHAPTER 4

MULTI-INDEX EVALUATION OF FUTURE DROUGHT AND CLIMATE EXTREME OCCURRENCE IN AN AGRICULTURAL WATERSHED

ABSTRACT

Understanding and projecting the frequency and occurrence of drought and extreme events under future climate is essential for managing natural resources, agricultural decision-making, and setting policy. This study identifies future (2016-2075) occurrence of meteorological, hydrological, agricultural droughts, and extreme events based on projections of future climate in the Goodwater Creek Experimental Watershed, which is dominated by agriculture and located in central Missouri, USA. Daily precipitation and temperature projections until 2075 were taken from the Couple Model Intercomparison Project phase 5 (CMIP5) and statistically downscaled using historical observations. Twelve different general circulation models were selected for two Representative Concentration Pathways (RCPs) (RCP 4.5 and RCP 8.5). These data were used as input to the Soil and Water Assessment Tool (SWAT) hydrological model to simulate streamflow and soil moisture content. Standardized Precipitation Index, Standardized Streamflow Index, and Soil Moisture Index were used to represent the three types of drought. Historical drought events were calculated based on observed precipitation and observed streamflow and SWAT soil moisture datasets for the period of 1980-2015. The physical values corresponding to the indices used to identify drought in the past were used to characterize drought in the future. The analysis of multiple drought types provides multiple perspective for evaluating drought under future climate. All three-drought indices indicated increased drought occurrence for the future in this region for both RCP 4.5 and RCP 8.5 emission pathways. Seven different indices developed by the Expert Team on Climate Change Detection Monitoring Indices were calculated on an annual scale for extreme analysis.

The results based on extreme indices indicate increased warm spell duration along with projected decline in summer precipitation favoring summer drought for study region.

KEYWORDS: Climate; Climate Adaptation; Drought; Extreme Events; Index; Model; SWAT; Agriculture

Introduction

Global climate change due to anthropogenic activities has a significant impact on atmospheric circulation and ultimately hydrologic cycling (IPCC, 2007; Kramer and Soden, 2016). Of the many potential impacts associated with these changes, drought and extreme precipitation events pose considerable risks to agricultural and energy systems, as well as the built environment. Increased temperatures lead to greater evaporation leading to surface drying, thereby increasing the frequency of drought. On the other hand, a temperature increase of 1°C was found to lead to a 7% increase in the water holding capacity of air resulting in increased probability of more intense precipitation (Trenberth, 2011). While hydrologic impacts due to climate change are often reported in terms of long-term annual averages, there is increasing attention to the impacts of increasing frequency and intensity of extreme events, e.g., heavy rainfall over a short duration, consecutive warm days and prolonged consecutive days without rain. Extreme occurrences can alter terrestrial water cycling, which can result in both excess water traveling over the land surface causing flooding, and prolonged absence of water causing drought. The Intergovernmental Panel on Climate Change (IPCC) points out the increased risk of drought and extreme events during the 21st century across the globe (IPCC, 2007, 2014). Some studies have analyzed the potential changes in drought using the future climate scenarios at the global scale (Hirabayashi et al., 2008; Sheffield and Wood, 2008; Touma et al., 2015; Wang,

2005), regional scale (Huang et al., 2015; Romanowicz and Wong, 2016), and watershed scale (Liu et al., 2012; Vu et al., 2015; Wang et al., 2011). Drought is projected to vary considerably across the globe and little work has been done at the small watershed-scale (~100 km^2 to 585 km^2) using both drought indices and extreme indices.

Drought is one of the most costly natural disasters, averaging annual damages of $6-$8 billion globally and affecting around 2 billion people since 1990 (Organization, 2013; Wilhite, 2012). Researchers have identified links between droughts in 20th century and a changing climate. Significant droughts over this time period include long-term events in the western United States, northeast China, southeast Australia and recent severe short-term drought events in central United States and Russia (Sheffield et al., 2012). The occurrence of drought is likely to increase given projected future climate with increased temperature, more frequent weather extremes and variability in precipitation (Sheffield et al., 2012). Past drought events have significantly impacted crop yields across the globe. The 2012 drought event in the United States resulted in approximately $17.3 billion damage to crop production (O'Connor, 2013). In comparison, the historic flood of 2011 along the Mississippi and Missouri Rivers inundated large acreage, resulting in loss of around 5.2 billion dollar (NOAA, 2013). In addition, an analysis of long-term historic data suggests climatic extremes are increasing globally with changing climate (Frich et al., 2002; Tigchelaar et al., 2018). Characterizing and anticipating climate change-induced risk of drought and extreme events at the local or regional scale is an important query for planning adaptive measures.

Drought is a natural feature of climate that occurs over most parts of the world and is defined as a dry spell relative to conditions in the location (Dai, 2011;

Redmond, 2002). Droughts are often defined based on disciplinary perspectives. Specifically, meteorological drought is defined using precipitation data, hydrological drought is defined using streamflow data and agricultural drought is defined using soil moisture, each of which are of interest from environmental and agriculture perspectives (Wilhite and Glantz, 1985). Drought has most often been evaluated using precipitation and temperature data due to data availability and the relative simplicity (Touma et al., 2015). Thus, earlier work has primarily focused on meteorological drought (Panu and Sharma, 2002). A more sophisticated approach is to use temperature and precipitation data and outputs from climate models to force hydrological models and use model output, i.e., streamflow and soil water, to evaluate drought conditions. Such an approach benefits from process-based simulations of land surface processes including those affecting vegetation and soils and their impact on water balance, which is not considered in precipitation based indices.

Drought development is complex and depends on a variety of factors, e.g. soil, plant species, and topography (Wilhite, 2012). Previous studies on drought modeling suggest use of multiple drought indices, defined using different critical variables, is necessary to comprehensively evaluate drought conditions (Tian et al., 2018) and its associated impacts. The time scale for drought analysis varies from the frequently used annual time step to the monthly and seasonal time steps (Panu and Sharma, 2002). Annual time scale analysis can help to understand the regional behavior of drought and monthly time scale is more appropriate for evaluating the effect of drought on agriculture, groundwater abstraction, and water supply (Panu and Sharma, 2002).

In addition to drought indices, the calculation of extreme indices based on climate variables (temperature and precipitation) can inform the future risk to

agriculture. Occurrence of climatic extremes during critical growing periods can significantly impact crop production (Gourdji et al., 2013). The Expert Team on Climate Change Detection (ETTCCDI) defined a set of indices to analyze extreme weather events (Sillmann et al., 2013b). These indices have been widely used for analyzing changes in extremes in observed records and under projected future climates (Alexander et al., 2006; N'Tcha M'Po et al., 2017; Sillmann et al., 2013a; Sillmann et al., 2013b). Drought characterization and extreme analysis can help provide early warning and drought risk analysis, which can help in drought and extreme preparedness (Zargar et al., 2011).

The study area is the Goodwater Creek Experimental Watershed (GCEW) located at the headwater of the Salt River Basin. The geophysical context of the study area represents most of the Central Claypan region, which includes Northeast Missouri, Southeast Iowa, and Southern Illinois (Baffaut et al., 2015; Sadler et al., 2015). Historically, major droughts occurred in 1901, the Dust Bowl years of the 1930's and early 1940's, the drought years of the 1950's, particularly 1953-1957, and the summer of 1988 (Center, 2010). The recent drought of 2012 was the worst drought experienced in nearly 60 years for the state of Missouri, with 93% of the state under "extreme" drought conditions based on the U.S. Drought Monitor (Fuchs et al., 2015). In the study watershed, a restrictive clay layer in the subsurface soil (B-Horizon) and low hydraulic conductivity limit vertical infiltration, which results in a lower water holding capacity of soil profile above the restrictive layer (Jiang et al., 2007; Mudgal et al., 2012; Udawatta et al., 2004). The lower water holding capacity makes the watershed vulnerable under projected future with more extreme dry and wet conditions. The thin layer of topsoil leads to short-term drought whenever there is shortage of precipitation even for short periods. The objective of this study was to

project change in frequency of short term drought and climate extremes in the future relative to historic trends using output (soil water, streamflow) from the Soil and Water Assessment Tool (SWAT) forced with downscaled climate data from 12 General Circulation Models under two Representative Concentration Pathways (RCP 4.5 and RCP 8.5) using multiple drought and climate extreme indices. Analysis of future short-term drought frequency can help to make appropriate adaptation decisions. This work is important for effectively projecting the potential future drought occurrence for the region with limiting subsurface soil, which is often poorly represented using global projections due to coarse resolution.

Materials and Methods

Watershed, model description, and climate data

The study is conducted in the GCEW, located in Boone and Audrain counties, Missouri (Fig. 4.1) with a drainage area of approximately 73 km^2. Land use in the watershed includes row crops (72.8 %), pasture (14.3%), forest (6.0%), and urban land (6.8%). The majority of soils in the watershed are claypan with lower available water for plants. For this study a previously calibrated SWAT model output was used (Gautam et al., 2018) in which the watershed was divided into 93 homogenous units with unique soil, land use and slope combination known as hydrologic response units (HRU). Climate data (T and P) from 12 GCMs (Table 4.1) with two RCPs for each GCM were obtained from CMIP5 for the near future (2016-2045) and far future (2046-2075) scenarios. These projected T and P data were downscaled to GCEW using observed historic data (1980-2015) and were used to force SWAT to analyze changes in hydrologic components given future climate data (Gautam et al., 2018).

Three different drought indices were used to quantify different types of drought, all used on monthly basis. The indices, variables used, and the distribution fitting approach for calculation of different indices are described in Table 4.2. Note that the drought indices are used for calculation of drought frequency in historic period using observed precipitation, observed streamflow and SWAT simulated soil water data. For future projection, threshold physical values of precipitation, streamflow and soil water corresponding to drought class based on historic calculation were used. The approach used for calculation of the indices for historic period and future projection is presented in Fig. 4.2. These indices were also used to characterize normal and wet periods. Additional indices were used to characterize events that were considered to be extreme due to prolonged dryness, wetness, coldness or hotness. These indices were calculated on an annual basis using historical and projected daily temperature and precipitation. The next few sections describe all the indices applied to define drought and extreme events in this study.

Standardized Index for calculation of meteorological and hydrologic drought
Meteorological drought was quantified based on Standardized Precipitation Index (SPI) (McKee et al., 1993) and hydrologic drought was quantified using the Standardized Streamflow Index (SSFI) (Modarres, 2007). The SPI calculations are based on the long-term precipitation record, with the data series fitted to a probability distribution. The two-parameter gamma distribution is recommended for general use for calculating SPI (Stagge et al., 2015). This index gives the relative measure of both the dryness and wetness for the location based on the historical precipitation data in the study region. Both precipitation and streamflow empirical distributions tend to have positive skewness, and therefore gamma distribution has often been a natural choice for statistically describing these data (Stagge et al., 2015). The gamma

distribution is fitted through a process of maximum likelihood estimation of the gamma distribution parameters, α and β (Thom, 1958), eq. (1). The inverse normal function is then applied to the cumulative probability to calculate the SPI (Guttman, 1999), eq. (2).

$$g(x) = \frac{1}{\beta^\alpha \Gamma(\alpha)} x^{\alpha-1} e^{\frac{-x}{\beta}}, \qquad\qquad for\ x > 0 \qquad (1)$$

$$\Gamma(\alpha) = \int_0^\infty x^{\alpha-1} e^{-x} dx \qquad\qquad (2)$$

where x is the monthly precipitation and $\Gamma(\alpha)$ is the Gamma function. In eqs. (3) and (4), α and β are the shape and scale parameters, which are estimated by the maximum likelihood method as follows:

$$\alpha = \frac{1}{4A}\left(1 + \sqrt{1 + \frac{4A}{3}}\right),$$

$$\beta = \frac{\bar{x}}{\alpha} \qquad\qquad (3)$$

$$A = ln(\bar{x}) - \frac{\sum ln(x)}{n} \qquad\qquad (4)$$

where n is the number of months. The resulting parameters are then used to find the cumulative probability of precipitation for the given month as follows:

$$G(X) = \int_0^x g(x)dx = \frac{1}{\beta^\alpha \Gamma(x)} = \int_0^x x^{\alpha-1} e^{\frac{-x}{\beta}} dx \qquad (5)$$

The cumulative probability G(X) is transformed to standard normal random variable z with mean of zero and variance of one, which is termed as SPI. Same methodology was applied for calculation of SSFI using monthly simulated streamflow data. The criteria to define the SPI/SSFI threshold values are presented in Table 4.3.

Index for calculation of agricultural drought

The monitoring and projection of agricultural drought can provide the means for taking appropriate relief measures for the reduction of economic loss by farmers. Agricultural drought is computed using soil water available for the entire soil profile (1.5 m to 2 m based on soil series). Spatial coverage of soil water observation is limited across most of the United States, soil water is estimated by the SWAT model for the GCEW. Soil water is a good indicator of available water reflecting the impact of recent precipitation and antecedent soil moisture content on plant growth. The available root zone soil moisture is a major factor in biomass accumulation (vegetative growth) through the availability of water for transpiration (Keyantash and Dracup, 2002). This study used soil water from the entire profile to make comparisons between the soils in the watershed, even though the ability of a crop to extract soil water from different depths varies based on crop, crop growth stage, and soil.

The response to drought may differ based on soil type, as the water retention capacity differs based on soil properties (physical, chemical and biological). Major soil series in the watershed included: Adco, Armstrong, Belknap, Leonard, Mexico, and Putnam. All these soil series except Belknap were characterized by a claypan underlying a top soil layer, which restricted the storage of plant-available water holding capacity, thus leaving soil dry more frequently and causing short-term drought. Drought projection using Soil Moisture Index (SMI) was made for each soil series present in GCEW. A one-month index was calculated to account for short-term drought. Dry and wet spells were defined in term of deviation from the average soil water value determined using the historical dataset. Monthly soil moisture values for each soil were computed by aggregating the soil moisture value of each HRU with the same soil.

$$Z_{i,k} = \frac{\theta_{i,k} - \bar{\theta}_i}{\sigma_i} \qquad (6)$$

Where, $\theta_{i,k}$ is the monthly average soil moisture for ith month at kth year, $\bar{\theta}_i$ and σ_i are long-term average and standard deviation of the soil moisture for ith month. Agricultural drought is characterized into four categories by the European Drought Observatory (EDO) based on z-score, eq. (6): severely dry ($z \leq -2$), moderately dry ($-2 < z < -1$), Normal ($-1 \geq z \geq 1$) moderately wet ($1 < z < 2$) and severely wet ($z \geq 2$). A previous study conducted in South-central United States suggested the superiority of the z-score compared to precipitation-based indices as it accounts for the influence of land surface processes for drought calculation (Tian et al., 2018). Droughts defined using these Z-scores showed higher correlation with crop yield changes (Tian et al., 2018).

Future projection of drought

The major concern in the GCEW watershed includes projected decreases in summer precipitation and higher temperatures, which could lead to more frequent short term drought (Gautam et al., 2018). The standardized indices used in this study are designed to express drought conditions relative to normal conditions at a given site for a given period. Independent calculations and comparison of drought indices for two different periods are not applicable. The ranges of values for precipitation, streamflow, and soil moisture that corresponded to a particular index during the historic period were used to evaluate future drought. This ensured a consistent definition of droughts during the historic and future periods. Use of a physical value of variable (i.e., mm of precipitation, streamflow and soil water) to define drought for the future period based on historic drought ensures robustness of future drought projection. These indices were calculated each month using 36 years of historic

observed (precipitation and stream flow) and simulated (soil moisture) data (1980-2015). The ranges of physical values corresponding to the drought categories for each index were then used for defining drought in near (2016-2045) and far future (2046-2075). This calculation was made for all 12 models under RCP 4.5 and 8.5. The results are presented as ensemble and compared with historic projection.

Extreme precipitation and temperature indices

Multiple indicators have been established by the Expert Team on Climate Change Detection Monitoring Indices (ETCCDMI) for understanding climate extremes and trends. The ETCCDI community supports the need of multi-parameters indices, that describe high impact phenomena, such as drought indices that are based on temperature and precipitation (Zhang et al., 2011). Seven extreme indices, proposed by ETCCDMI and based on temperature and precipitation, were analyzed (Table 4.4). While ETCCDI defines 20 mm precipitation days as very heavy precipitation days, the threshold for very heavy precipitation days was modified to 50 mm to represent the study area. Rabinowitz (2016) used a similar value (50.8 mm) to define the heavy precipitation threshold, based on regional precipitation behavior (Rabinowitz, 2016). These extreme event indices were calculated for the historic, near and far future periods. The results are presented as ensemble of 12 GCM models using histograms.

Results and Discussion

Historic and Projected Drought for GCEW

Meteorological and Hydrological Drought

The threshold monthly ranges of precipitation that define drought classes based on SPI calculated over the historic period are presented on Table 4.5. Analysis of future precipitation indicated an increased risk of wet periods during the spring, and

increased risk of drought during summer. The number of meteorological drought months, i.e., with SPI< -1, during the historic period were 27, 28, 23 and 23 months for winter, spring, summer and, fall, respectively (Fig. 4.3). These results indicated more meteorological drought months for the winter and spring seasons compared to other seasons during historic period. The same was observed recently with 2017/2018 being the driest winter among the last four decades with Missouri receiving an average precipitation of 211 mm during the winter months (September through January) compared to the historic average of 404 mm (Colville, 2018). Historic SPI projection was able to match the historic drought severity during growing season for major drought years (e.g 1992, 2005 and 2012) during the historic simulation period used in this study. The results for the near and far future indicated increased frequency of dry months for both RCPs for the winter, summer, and fall seasons (Fig. 4.3 and Fig 4.4). Further, the count of months rated as extremely dry months almost doubled for winter, summer and fall suggesting more extreme dry spells in the future. No change in meteorological drought frequency was projected for the spring months the results are similar to Ahmadalipour et al. (2017). The spring precipitation is projected to increase in the region for future resulting no drought in spring. A previous modeling study on drought projection in the contiguous USA indicated a tendency toward more frequent and intense summer droughts for Missouri (Ahmadalipour et al., 2017).

Ensemble results indicated a decrease of wet months during the winter and an increase of wet months during the spring for both RCPs for near and far future (Fig. 4.3 and Fig. 4.4). The increased instances of meteorological drought during summer were due to projected increases in temperature and decreases in summer precipitation. Previous modeling studies are also consistent in predicting global summer dryness for

future (Wang, 2005). Studies have reported increased drying trends during summer months in Europe (Pal et al., 2004), U.S. (Cayan et al., 2010), and Asia (Kim and Byun, 2009). Previous study indicates impact of prolonged drought in agricultural yield, water supply and hydropower in the US (Feng et al., 2010).

Threshold monthly values of streamflow that define the different drought classes based on SSFI calculation using historic observed streamflow data are presented in Table 4.6. Historical comparison of the number of hydrologic drought months based on SSFI indicated that months with SSFI< -1 were 29, 31, 34 and 43 for winter, spring, summer and fall, respectively (Fig. 4.5), which indicates more hydrologic drought months for summer and fall seasons during the historic period compared to other seasons. Historic SSFI projection was able to predict the historic drought severity during the growing season for major drought years (e.g. 1992, 1997, 2002, 2005, and 2012) of the historic simulation period used in this study. Results indicate SSFI is a better predictor of historic drought events than SPI. SPI being solely based on precipitation, requires stationary of other variable e.g., temperature and evapotranspiration. The result for near and far future indicated an increase in the frequency of dry months and a decrease in the number of wet months for both RCPs for all four seasons compared to historic (Fig. 4.5 and Fig. 4.6). The ensemble results for hydrologic drought also indicated an increase in the frequency of extremely dry months by nearly three times for summer and spring months for both near and far future (Fig. 4.5 and Fig. 4.6), indicating more dry surface water bodies in future. The simulated streamflow for future July and August are very small, resulting in more extremely dry months. Results based on SSFI indicate the increase in the frequency of hydrologic drought months during the crop-growing season (spring and summer).

Studies conducted in Midwest region also report increased hydrologic drought based on long term historic streamflow data (Lu et al., 2015).

Agricultural Drought

The threshold monthly values of soil moisture (mm), based on simulated historic soil moisture, were used to define agricultural drought and are presented in Supplement Table 4.1 through Supplement Table 4.6. The ranges of soil moisture values to define drought class differed based on depth of soil profile. The ranges were highest for Belknap soil with 2 m soil profile depth and lowest for Adco soil with 1.5 m soil profile depth. Note that the SMI indicated drought on floodplain soil of the watershed (Belknap) as the dryness in SMI is defined based on moisture distribution within the soil series, which is one of the limitation of SMI based drought calculation. The comparison of agricultural drought indices for spring and summer months for RCP 4.5 and RCP 8.5 are presented in Fig. 4.7 and Fig. 4.8 indicating more wet or dry months in the future. Different soil types across the watershed exhibited different frequencies of the dry, normal, and wet months for the historic period (Fig. 4.7). However, a few consistent patterns appeared clearly across all soil types. In all cases, the number of months in which the soil moisture was in the "normal" historical range decreased in the future while counts in both the dry and wet SMI categories increased.

Mexico silt loam soil, covering around 80% of the watershed area, showed more drought months during summer (6 months) compared to spring months (3 months) over the historic period (Fig. 4.7). Increased chance of drought was greater in summer compared to spring for the Mexico soils for both RCPs for the future then for the historic period (Fig. 4.7 and Fig. 4.8). This result confirms earlier studies based on multi model-simulated soil moisture, which indicated decreased soil moisture globally with a corresponding doubling of the spatial extent of severe soil moisture deficits and

frequency of short-term drought in the future (Sheffield and Wood, 2008). Our results at local scale were similar to earlier continental-scale results, which showed increased summer time drought across US based on soil moisture as proxy for drought estimation (Wang, 2005). Similarly, a study conducted in Southwest U.S. reported more severe future drought due to increased temperature, which leads to reduced spring snowpack, late spring and summer soil moisture resulting in more drought. In Missouri, short-term droughts are projected to increase similar to our results, however long-duration droughts (two years or more) are likely to decline due to projected increase in precipitation (UCS, 2009). From an agriculture prospective, short-term drought assessments are important as these events directly impact crop phenology and ultimately biomass production. The study region could face greater risk of short-term drought, with temperature rise, the evaporative demand increases, requiring more precipitation to maintain the same soil moisture level. In addition, projected decrease in summer precipitation and soil with low water holding capacity leads to increase drought during summer.

Annual Historic and Future Climate Indices Trends for GCEW

The major concerns about the potential impacts of climate change include increased frequency of extreme events; a study using observed data indicated amplified tails for total precipitation and increased temperature extreme (Easterling et al., 2000). Ensemble comparison of consecutive dry day (CDD) in a year indicated no change in median number of CDD in a year for both near and far future compared to historic for both RCP 4.5 and RCP 8.5 (Supplement Fig. 4.1a). Ensemble comparison of consecutive wet days (CWD) indicated an increase in median number of CWD in a year for both near and far future both RCPs compared to the historic period (Supplement Fig. 4.1b). The range for the CWD indicated comparatively greater

variability in the future for the occurrence of consecutive wet days compared to CWD (Supplement Fig. 4.1a and Fig. 4.1b).

Ensemble comparison of annual total precipitation greater than 1 mm indicated an increase in median precipitation for both RCPs (RCP 4.5 and RCP 8.5) compared to historic period for both near and far future (Supplement Fig. 4.2a). Seasonal comparison of total precipitation indicated an increase in total precipitation for spring and decrease in total precipitation for summer for all the RCPs for both near and far future. However, there was not much change for winter and fall season. This result indicates future wetter springs and dryer summers, which may bring some challenges to agricultural land management. The ensemble comparison of annual count of days with >50 mm precipitation (R50) indicated no change in the median number of R50 for near future and far future for all the ensemble of the RCPs (Supplement Fig. 4.2b). Historical data also showed the similar trend, despite the increase of total precipitation since the mid-1950, the distribution of precipitation event 50.8 mm or greater has remained the same (Rabinowitz, 2016).

Ensemble comparison of annual total very wet days (R95p) and extremely wet days (R99p) precipitation indicated an increase in median R95p and R99p for both RCPs for near future with greatest increase in median R95p and R99p for extreme scenario (RCP 8.5) (Fig. 4.9a and Fig. 4.9b). Seasonal comparison of R95p indicates increased R95p for spring and decreases R95p for summer for all the RCPs for both near and far future; however, there was little change for winter and fall season. The increase in heavy precipitation days and amount during spring as indicated by R95p and R99p may lead to more frequent wet field conditions during planting time hindering agricultural operations. The increased extreme precipitation for future have been reported in various studies for global (Min et al., 2011), Scandinavian

93

(Irannezhad et al., 2017) and Central/Eastern Europe (Bartholy et al., 2015). Ensemble comparison of warm spell duration indicator (WSDI) indicated significant increases in WSDI days for all RCPs for both near future and far future (Fig. 4.10). The occurrence of WSDI is expected to increase significantly for RCP 8.5 in far future compared to the near future (Fig. 4.10). These results support the finding of increased instances of summer droughts under dryer summers with warmer temperatures. Previous studies also projected increases in heatwave and warm spell duration over the next century over both the Northern Hemisphere and Southern Hemisphere (Alexander and Arblaster, 2009; Meehl and Tebaldi, 2004). Although GCM projected a wetter future, summers are expected to be drier due to decreased summer precipitation.

Conclusions

In this study, a modeling approach of projecting future climate change impact on drought events in the Goodwater Creek Experimental Water (GCEW) was presented. The modeling approach included using the SWAT hydrological model forced with climate outputs from multiple models under two RCP scenarios for streamflow and soil water prediction. Frequency analysis of monthly occurrence of three major drought types was conducted. Use of physical values to define droughts for future period based on historic drought can be a robust option for future drought projection. The meteorological drought indicated increased frequency of dry months; especially extremely dry months for both RCPs for winter, summer, and fall season for both near and far future. Hydrologic drought results indicated an increase in the frequency of hydrologic drought, especially extremely dry months throughout the all four season. The agricultural drought results indicated increased frequency of dry months for all RCPs for both spring and summer for future. The overall analysis of drought

frequency using multiple indices indicated the increase frequency of overall drought condition for both near and far future. The results from the precipitation-based indices indicate an increase in heavy precipitation days and amount for the spring season and decrease in heavy precipitation days and amount for summer season. The results based on the warm spell duration indicator indicate significant increase in WSDI days for future for all the RCPs. The results based on both drought and extreme indices indicate extreme summer with dry and hot condition. In addition, projected increase in heavy precipitation days and amount during spring may lead to frequent wet field conditions during planting time hindering agricultural management. Future studies should focus on building mitigation scenarios to combat the impact of these changes.

Disclosure statement

No potential conflict of interest was reported by the authors

Funding

References

Ahmadalipour, A., Moradkhani, H., and Svoboda, M. (2017). Centennial Drought Outlook over the Conus Using Nasa-Nex Downscaled Climate Ensemble. *International Journal of Climatology* **37**, 2477-2491.

Alexander, L., Zhang, X., Peterson, T., Caesar, J., Gleason, B., Klein Tank, A., Haylock, M., Collins, D., Trewin, B., and Rahimzadeh, F. (2006). Global Observed Changes in Daily Climate Extremes of Temperature and Precipitation. *Journal of Geophysical Research: Atmospheres* **111**.

Alexander, L. V., and Arblaster, J. M. (2009). Assessing Trends in Observed and Modelled Climate Extremes over Australia in Relation to Future Projections. *International Journal of Climatology* **29**, 417-435.

Baffaut, C., John Sadler, E., Ghidey, F., and Anderson, S. H. (2015). Long-Term Agroecosystem Research in the Central Mississippi River Basin: Swat Simulation of Flow and Water Quality in the Goodwater Creek Experimental Watershed. *Journal of Environmental Quality* **44**, 84-96.

Bartholy, J., Pongrácz, R., and Kis, A. (2015). Projected Changes of Extreme Precipitation Using Multi-Model Approach. *Quarterly Journal of the Hungarian Meterological Service* **119**, 129-142.

Cayan, D. R., Das, T., Pierce, D. W., Barnett, T. P., Tyree, M., and Gershunov, A. (2010). Future Dryness in the Southwest Us and the Hydrology of the Early 21st Century Drought. *Proceedings of the National Academy of Sciences* **107**, 21271-21276.

Center, M. C. (2010). Significant Weather Events of the Century for Missouri.

Colville, W. (2018). Driest Winter in 40 Years Exacerbates Missouri Drought. *Columbia Daily Tribune*, 12 February 2018, Columbia, MO.

Dai, A. (2011). Drought under Global Warming: A Review. *Wiley Interdisciplinary Reviews: Climate Change* **2**, 45-65.

Easterling, D. R., Meehl, G. A., Parmesan, C., Changnon, S. A., Karl, T. R., and Mearns, L. O. (2000). Climate Extremes: Observations, Modeling, and Impacts. *Science* **289**, 2068-2074.

Feng, S., Krueger, A. B., and Oppenheimer, M. (2010). Linkages among Climate Change, Crop Yields and Mexico–Us Cross-Border Migration. *Proceedings of the National Academy of Sciences* **107**, 14257-14262.

Frich, P., Alexander, L. V., Della-Marta, P., Gleason, B., Haylock, M., Tank, A. K., and Peterson, T. (2002). Observed Coherent Changes in Climatic Extremes During the Second Half of the Twentieth Century. *Climate Research* **19**, 193-212.

Fuchs, B., Wood, D., and Ebbeka, D. (2015). From Too Much to Too Little: How the Central Us Drought of 2012 Evolved out of One of the Most Devastating Floods on Record in 2011. *Drought Mitigation Center Faculty Publications* **118**.

Gautam, S., Baffaut, C., Thompson, A., Svoma, B., Phung, Q., and Sadler, E. (2018). Assessing Long-Term Hydrological Impact of Climate Change Using an Ensemble Approach and Comparison with Global Gridded Model-a Case Study on Goodwater Creek Experimental Watershed. *Water* **10**, 564.

Gourdji, S. M., Sibley, A. M., and Lobell, D. B. (2013). Global Crop Exposure to Critical High Temperatures in the Reproductive Period: Historical Trends and Future Projections. *Environmental Research Letters* **8**, 024041.

Guttman, N. B. (1999). Accepting the Standardized Precipitation Index: A Calculation Algorithm. Wiley Online Library. *Journal of the American Water Resources Association* **35**, 311-322.

Hirabayashi, Y., Kanae, S., Emori, S., Oki, T., and Kimoto, M. (2008). Global Projections of Changing Risks of Floods and Droughts in a Changing Climate. *Hydrological Sciences Journal* **53**, 754-772.

Huang, S., Krysanova, V., and Hattermann, F. (2015). Projections of Climate Change Impacts on Floods and Droughts in Germany Using an Ensemble of Climate Change Scenarios. *Regional Environmental Change* **15**, 461-473.

IPCC (2007). (Intergovermental Panal on Climate Change), Working Group I. Climate Change 2007: The Physical Science Basis. In : Solomon, S., D. Qin, M. Manning, Z. Chen, M. Marquis, K.B. Averyt, M. Tignor and H.L. Miller (Eds.), Contribution of Group I to the Fourth Assessment Report of the Intergovernental Panael on Climate Change.

IPCC (2014). Climate Change 2014: Mitigation of Climate Change., Cambridge University Press, Cambridge, United Kingdom and New York, NY, USA.

Irannezhad, M., Chen, D., Kløve, B., and Moradkhani, H. (2017). Analysing the Variability and Trends of Precipitation Extremes in Finland and Their Connection to Atmospheric Circulation Patterns. *International Journal of Climatology* **37**, 1053-1066.

Jiang, P., Anderson, S. H., Kitchen, N. R., Sadler, E. J., and Sudduth, K. A. (2007). Landscape and Conservation Management Effects on Hydraulic Properties of a Claypan-Soil Toposequence. *Soil Science Society of America Journal* **71**, 803-811.

Keyantash, J., and Dracup, J. A. (2002). The Quantification of Drought: An Evaluation of Drought Indices. *Bulletin of the American Meteorological Society* **83**, 1167-1180.

Kim, D.-W., and Byun, H.-R. (2009). Future Pattern of Asian Drought under Global Warming Scenario. *Theoretical and Applied Climatology* **98**, 137-150.

Kramer, R. J., and Soden, B. J. (2016). The Sensitivity of the Hydrological Cycle to Internal Climate Variability Versus Anthropogenic Climate Change. *Journal of Climate* **29**, 3661-3673.

Liu, L., Hong, Y., Bednarczyk, C. N., Yong, B., Shafer, M. A., Riley, R., and Hocker, J. E. (2012). Hydro-Climatological Drought Analyses and Projections Using Meteorological and Hydrological Drought Indices: A Case Study in Blue River Basin, Oklahoma. *Water Resources Management* **26**, 2761-2779.

Lu, H., Bryant, R. B., Buda, A. R., Collick, A. S., Folmar, G. J., and Kleinman, P. J. (2015). Long-Term Trends in Climate and Hydrology in an Agricultural, Headwater Watershed of Central Pennsylvania, USA. *Journal of Hydrology: Regional Studies* **4**, 713-731.

McKee, T. B., Doesken, N. J., and Kleist, J. (1993). The Relationship of Drought Frequency and Duration to Time Scales. *In* "Proceedings of the 8th Conference on Applied Climatology", Vol. 17, pp. 179-183. American Meteorological Society Boston, MA.

Meehl, G. A., and Tebaldi, C. (2004). More Intense, More Frequent, and Longer Lasting Heat Waves in the 21st Century. *Science* **305**, 994-997.

Min, S.-K., Zhang, X., Zwiers, F. W., and Hegerl, G. C. (2011). Human Contribution to More-Intense Precipitation Extremes. *Nature* **470**, 378.

Modarres, R. (2007). Streamflow Drought Time Series Forecasting. *Stochastic Environmental Research and Risk Assessment* **21**, 223-233.

Mudgal, A., Baffaut, C., Anderson, S. H., Sadler, E.J., Kitchen, N., Sudduth, K. A., and Lerch, R. N. (2012). Using the Agricultural Policy/Environmental Extender to Develop and Validate Physically Based Indices for the Delineation of Critical Management Areas. *Journal of Soil and Water Conservation* **67**, 284-299.

N'Tcha M'Po, Y., Lawin, E. A., Yao, B. K., Oyerinde, G. T., Attogouinon, A., and Afouda, A. A. (2017). Decreasing Past and Mid-Century Rainfall Indices over the Ouémé River Basin, Benin (West Africa). *Climate* **5**, 74.

NOAA (2013). Billion-Dollar Weather and Climate Disasters: Overview. Vol. 2018.

O'Connor, C. (2013). Soil Matters: How the Federal Crop Insurance Program Should Be Reformed to Encourage Low-Risk Farming Methods with High-Reward Environmental Outcomes. *Agricultural & Applied Economics Association's 2013 Crop Insurance and the Farm Bill Symposium, Louisville, Kentucky*.

Organization, UN. FAO. (2013). UN Lays Foundations for More Drought Resilient Societies Vol. 2018.

Pal, J. S., Giorgi, F., and Bi, X. (2004). Consistency of Recent European Summer Precipitation Trends and Extremes with Future Regional Climate Projections. *Geophysical Research Letters* **31**.

Panu, U., and Sharma, T. (2002). Challenges in Drought Research: Some Perspectives and Future Directions. *Hydrological Sciences Journal* **47**, S19-S30.

Rabinowitz, J. (2016). The Relationship between Mid-West Precipitation Rates, Teleconnections and Blocking in the Eastern and Central Pacific, University of Missouri-Columbia (MS thesis).

Redmond, K. T. (2002). The Depiction of Drought: A Commentary. *Bulletin of the American Meteorological Society* **83**, 1143-1147.

Romanowicz, R. J., and Wong, W. K. (2016). Trends in Projections of Standardized Precipitation Indices in a Future Climate in Poland. *Hydrology and Earth System Sciences* **20**, 1947.

Sadler, E. J., Lerch, R. N., Kitchen, N. R., Anderson, S. H., Baffaut, C., Sudduth, K. A., Prato, A. A., Kremer, R. J., Vories, E. D., and Myers, D. B. (2015). Long-Term Agroecosystem Research in the Central Mississippi River Basin: Introduction, Establishment, and Overview. *Journal of Environmental Quality* **44**, 3-12.

Sheffield, J., and Wood, E. F. (2008). Projected Changes in Drought Occurrence under Future Global Warming from Multi-Model, Multi-Scenario, Ipcc Ar4 Simulations. *Climate Dynamics* **31**, 79-105.

Sheffield, J., Wood, E. F., and Roderick, M. L. (2012). Little Change in Global Drought over the Past 60 Years. *Nature* **491**, 435.

Sillmann, J., Kharin, V., Zhang, X., Zwiers, F., and Bronaugh, D. (2013a). Climate Extremes Indices in the Cmip5 Multimodel Ensemble: Part 1. Model Evaluation in the Present Climate. *Journal of Geophysical Research: Atmospheres* **118**, 1716-1733.

Sillmann, J., Kharin, V., Zwiers, F., Zhang, X., and Bronaugh, D. (2013b). Climate Extremes Indices in the Cmip5 Multimodel Ensemble: Part 2. Future Climate Projections. *Journal of Geophysical Research: Atmospheres* **118**, 2473-2493.

Stagge, J. H., Tallaksen, L. M., Gudmundsson, L., Van Loon, A. F., and Stahl, K. (2015). Candidate Distributions for Climatological Drought Indices (Spi and Spei). *International Journal of Climatology* **35**, 4027-4040.

Thom, H. C. (1958). A Note on the Gamma Distribution. *Monthly Weather Review* **86**, 117-122.

Tian, L., Yuan, S., and Quiring, S. M. (2018). Evaluation of Six Indices for Monitoring Agricultural Drought in the South-Central United States. *Agricultural and Forest Meteorology* **249**, 107-119.

Tigchelaar, M., Battisti, D. S., Naylor, R. L., and Ray, D. K. (2018). Future Warming Increases Probability of Globally Synchronized Maize Production Shocks. *Proceedings of the National Academy of Sciences* **115**, 6644-6649.

Touma, D., Ashfaq, M., Nayak, M. A., Kao, S.-C., and Diffenbaugh, N. S. (2015). A Multi-Model and Multi-Index Evaluation of Drought Characteristics in the 21st Century. *Journal of Hydrology* **526**, 196-207.

Trenberth, K. E. (2011). Changes in Precipitation with Climate Change. *Climate Research* **47**, 123-138.

UCS (2009). Confronting Climate Change in the U.S. Midwest-Missouri. Union of Concerneed Scientists.

Udawatta, R. P., Motavalli, P. P., and Garrett, H. E. (2004). Phosphorus Loss and Runoff Characteristics in Three Adjacent Agricultural Watersheds with Claypan Soils. *Journal of Environmental Quality* **33**, 1709-1719.

Vu, M., Raghavan, V., and Liong, S.-Y. (2015). Ensemble Climate Projection for Hydro-Meteorological Drought over a River Basin in Central Highland, Vietnam. *KSCE Journal of Civil Engineering* **19**, 427-433.

Wang, D., Hejazi, M., Cai, X., and Valocchi, A. J. (2011). Climate Change Impact on Meteorological, Agricultural, and Hydrological Drought in Central Illinois. *Water Resources Research* **47**, 1-13.

Wang, G. (2005). Agricultural Drought in a Future Climate: Results from 15 Global Climate Models Participating in the IPCC 4th Assessment. *Climate Dynamics* **25**, 739-753.

Wilhite, D. A. (2012). Drought Assessment, Management, and Planning: Theory and Case Studies: Theory and Case Studies, Springer Science & Business Media.

Wilhite, D. A., and Glantz, M. H. (1985). Understanding: The Drought Phenomenon: The Role of Definitions. *Water International* **10**, 111-120.

Zargar, A., Sadiq, R., Naser, B., and Khan, F. I. (2011). A Review of Drought Indices. *Environmental Reviews* **19**, 333-349.

Zhang, X., Alexander, L., Hegerl, G. C., Jones, P., Tank, A. K., Peterson, T. C., Trewin, B., and Zwiers, F. W. (2011). Indices for Monitoring Changes in Extremes Based on Daily Temperature and Precipitation Data. *Wiley Interdisciplinary Reviews: Climate Change* **2**, 851-870.

Table 4.1. List of the models used in the study

Model	CMIP5 Climate Modeling Group	CMIP5 Climate Model ID	Reference
1	Beijing Climate Center, China Meteorological Administration	BCC-CSM1-1	(Wu et al., 2014)
2	National Center for Atmospheric Research	CCSM4.1	(Gent et al., 2011)
3	National Center for Atmospheric Research	CCSM4.2	(Gent et al., 2011)
4	NOAA Geophysical Fluid Dynamics Laboratory	GFDL-ESM2G	(Dunne et al., 2012)
5	NOAA Geophysical Fluid Dynamics Laboratory	GFDL-ESM2M	(Dunne et al., 2013)
6	Institut Pierre-Simon Laplace	IPSL-CM5A-LR	(Dufresne et al., 2013)
7	Institut Pierre-Simon Laplace	IPSL-CM5A-MR	(Dufresne et al., 2013)
8	Japan Agency for Marine-Earth Science and Technology, Atmosphere and Ocean Research Institute (The University of Tokyo), and National Institute for Environmental Studies	MIROC-ESM	(Watanabe et al., 2011)
9	Japan Agency for Marine-Earth Science and Technology, Atmosphere and Ocean Research Institute (The University of Tokyo), and National Institute for Environmental Studies	MIROC-ESM-CHEM	(Watanabe et al., 2011)
10	Atmosphere and Ocean Research Institute (The University of Tokyo), National Institute for Environmental Studies, and Japan Agency for Marine-Earth Science and Technology	MIROC5	(Watanabe et al., 2010)
11	Meteorological Research Institute	MRI-CGCM3	(Yukimoto et al., 2012)
12	Norwegian Climate Centre	NorESM1-M	(Bentsen et al., 2012)

Table 4.2. Drought indices used, variables used in their calculation, and methods with which the time series of the variables are standardized

Drought Index †	Variable used	Distribution Fitted	Standardization
SPI	Precipitation	Gamma Distribution	CDF standardized to Gaussian values
SSFI	Streamflow	Gamma Distribution	CDF standardized to Gaussian values
Z-score based SMI	Soil Moisture	Empirical Cumulative Probability	Z-score

† SPI, Standardized Precipitation Index; SSFI, Standardized Stream Flow Index; SMI, Soil Moisture Index.

Table 4.3. Drought index class definition for standardized precipitation and standardized streamflow index

SPI or SSFI†	Classification
2.0 >	Extremely wet
1.5-1.99	Very wet
1.0-1.49	Moderately wet
-0.99 to 0.99	Near normal
-1 to -1.49	Moderately dry
-1.5 to -1.99	Severely dry
-2 <	Extremely dry

† SPI, Standardized Precipitation Index; SSFI, Standardized Stream Flow Index

Table 4.4. List of the extreme precipitation indices used in this study

ID	Indicator	Definitions†	Units
WSDI	Warm spell duration indicator	Annual count of days with at least 6 consecutive days when TX>90th percentile	Days
CDD	Consecutive dry days	Maximum number of consecutive days with RR<1mm	Days
CWD	Consecutive wet days	Maximum number of consecutive days with RR>=1mm	Days
R95p	Very wet days	Annual total PRCP when RR>95th percentile	Mm
R99p	Extremely wet days	Annual total PRCP when RR>99th percentile	Mm
PRCPTOT	Annual total wet-day precipitation	Annual total PRCP in wet days (RR>=1mm)	Mm
R50	Number of very heavy precipitation days	Annual count of days when PRCP>=50mm	Days

† TX, daily max temperature; PRCP, Precipitation.

Table 4.5. Threshold monthly precipitation (mm) value to define different drought classes based on Standardized Precipitation Index (SPI) calculation using historical precipitation datasets

Month	EW	VW	MW	NN	MD	SD	ED
Jan	101.1	82.8	64.3	17.5	11.9	9.9	<9.9
Feb	105.2	88.7	79.8	25.9	19	16.3	<16.3
Mar	122.7	106.7	94.2	48.2	42.2	38.6	<38.6
Apr	184.7	162.8	135.9	65.5	56.1	42.9	<42.9
May	216.2	192.8	173.2	82.8	68.6	56.9	<56.9
Jun	308.9	208.8	171.7	76.7	65.3	51.6	<51.6
Jul	253	182.1	151.6	50.8	35.6	23.6	<23.6
Aug	206	168.2	143	62.2	50.3	38.1	<38.1
Sep	196.4	156.7	140	47.5	35.3	32.8	<32.8
Oct	218.9	139.7	116.6	49	38.1	38.1	<38.1
Nov	173.5	126.5	107.7	45	35.3	35.3	<35.3
Dec	137.4	110.5	78.5	34	25.1	20.6	<20.6

EW=Extremely Wet; VW=Very wet; MW=Moderately Wet; NN=Normal; MD=Moderately Dry; SD= Severely Dry; ED=Extremely Dry

Precipitation values greater than or equal to the value presented in the EW column are considered extremely wet; values smaller than the value presented in the EW column and greater than or equal to the value presented in the VW column is considered very wet and so on; values lower than SD are considered extremely dry

Table 4.6. Threshold monthly streamflow (mm) value to define different drought classes based on Standardized Streamflow Index (SSFI) calculation using historical streamflow datasets

Month	EW	VW	MW	NN	MD	SD	ED
Jan	77.9	56.8	44.1	5	2.1	1.1	<1.1
Feb	101.8	88.8	52.2	10.2	5.2	3.4	<3.4
Mar	91.5	68.8	60	12.6	7.7	4.8	<4.8
Apr	139.6	100	74	12.6	6.6	3.1	<3.1
May	176.8	95.9	80.9	15.9	8.8	4.2	<4.2
Jun	113.7	103	60.1	9.6	5	2.9	<2.9
Jul	151.1	117.5	62.2	4.7	1.3	0.3	<0.3
Aug	59.3	46.9	27.2	1.4	0.4	0.1	<0.1
Sep	175.4	66.1	51.5	1.5	0.2	0.1	<0.1
Oct	96.4	44.6	44.6	1	0.4	0.1	<0.1
Nov	119.7	56.8	39.2	6.4	1.1	0.4	<0.4
Dec	134.6	74.6	44.2	4.1	2.5	0.6	<0.6

EW=Extremely Wet; VW=Very wet; MW=Moderately Wet; NN=Normal; MD=Moderately Dry; SD= Severely Dry; ED=Extremely Dry

Precipitation values greater than or equal to the value presented in the EW column are considered extremely wet; values smaller than the value presented in the EW column and greater than or equal to the value presented in the VW column is considered very wet and so on; values lower than SD are considered extremely dry
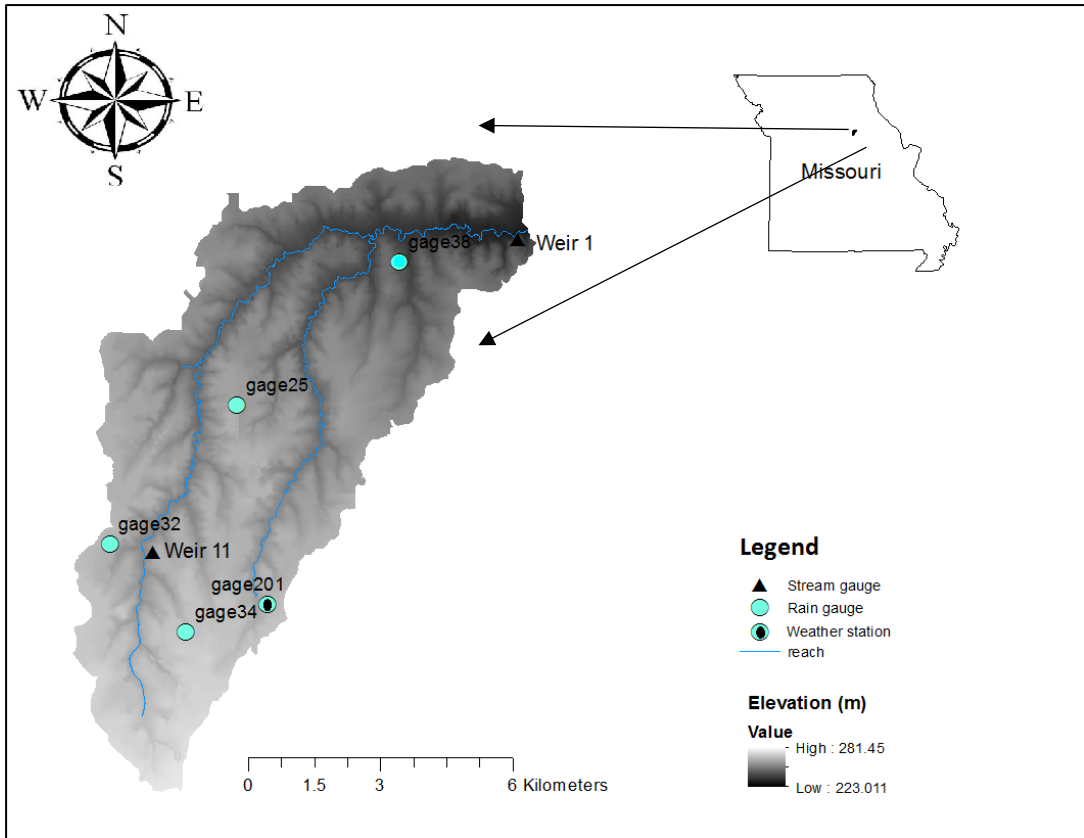
Figure 4.1. Goodwater Creek Experimental Watershed showing rain gauge and weir outlets
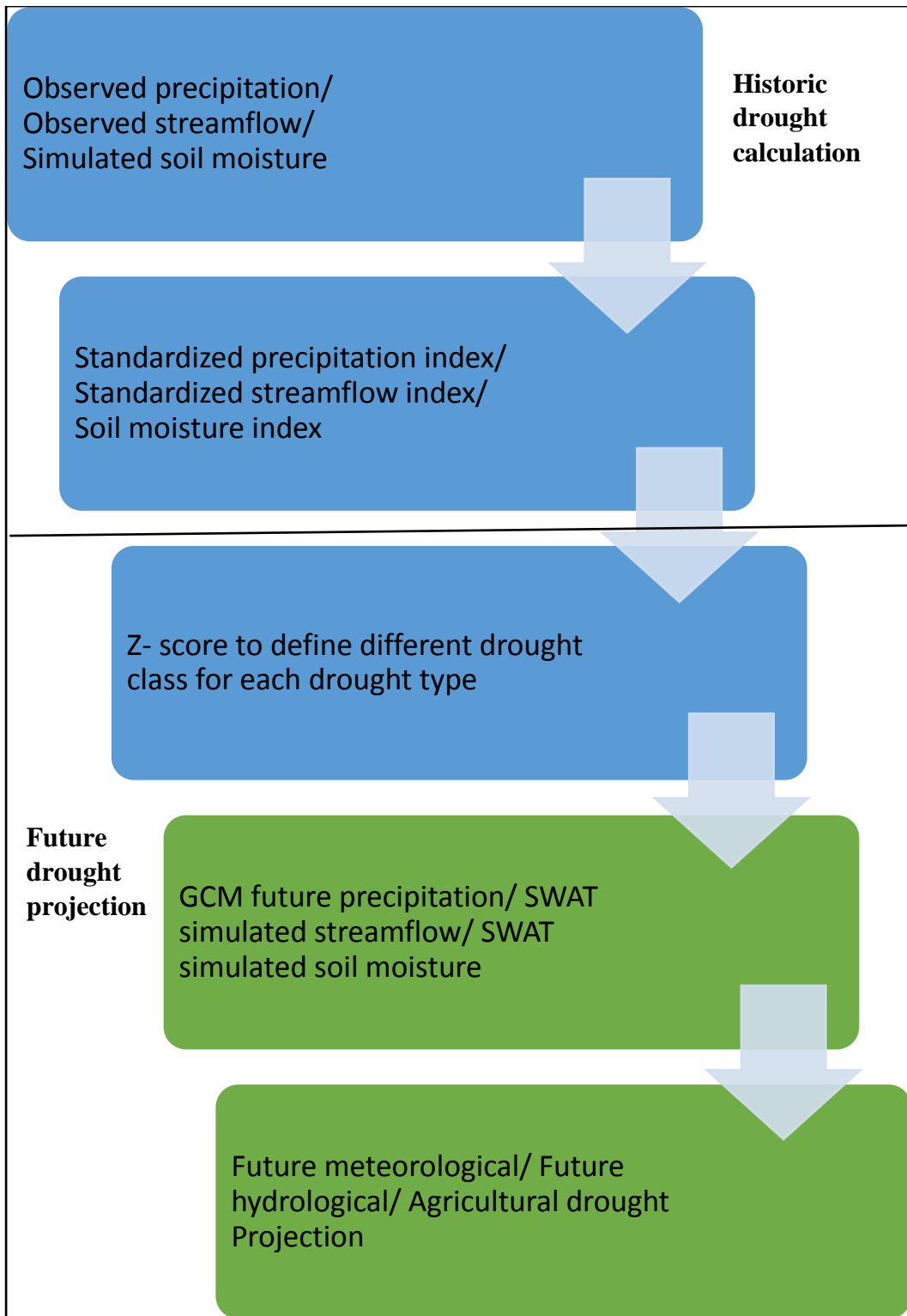
Figure 4.2. A flow chart describing the drought analysis for the historic period and future projection of drought based on GCM projected precipitation, simulated stream flow and simulated soil moisture
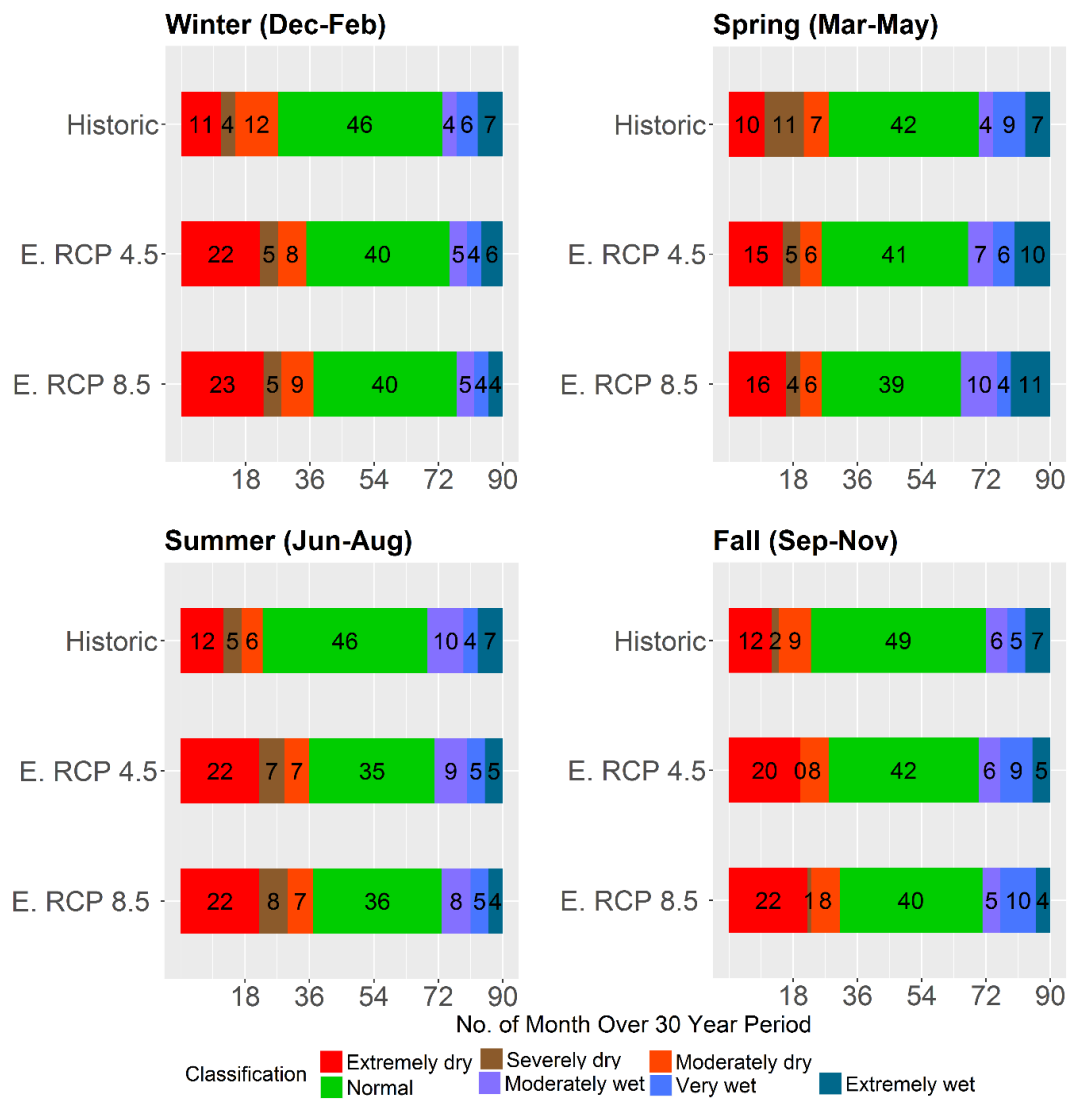
Figure 4.3. Projected seasonal count of month over 30 years for seven classifications of standardized precipitation index for near future (2016-2045) for ensemble of each of two RCPs scenarios
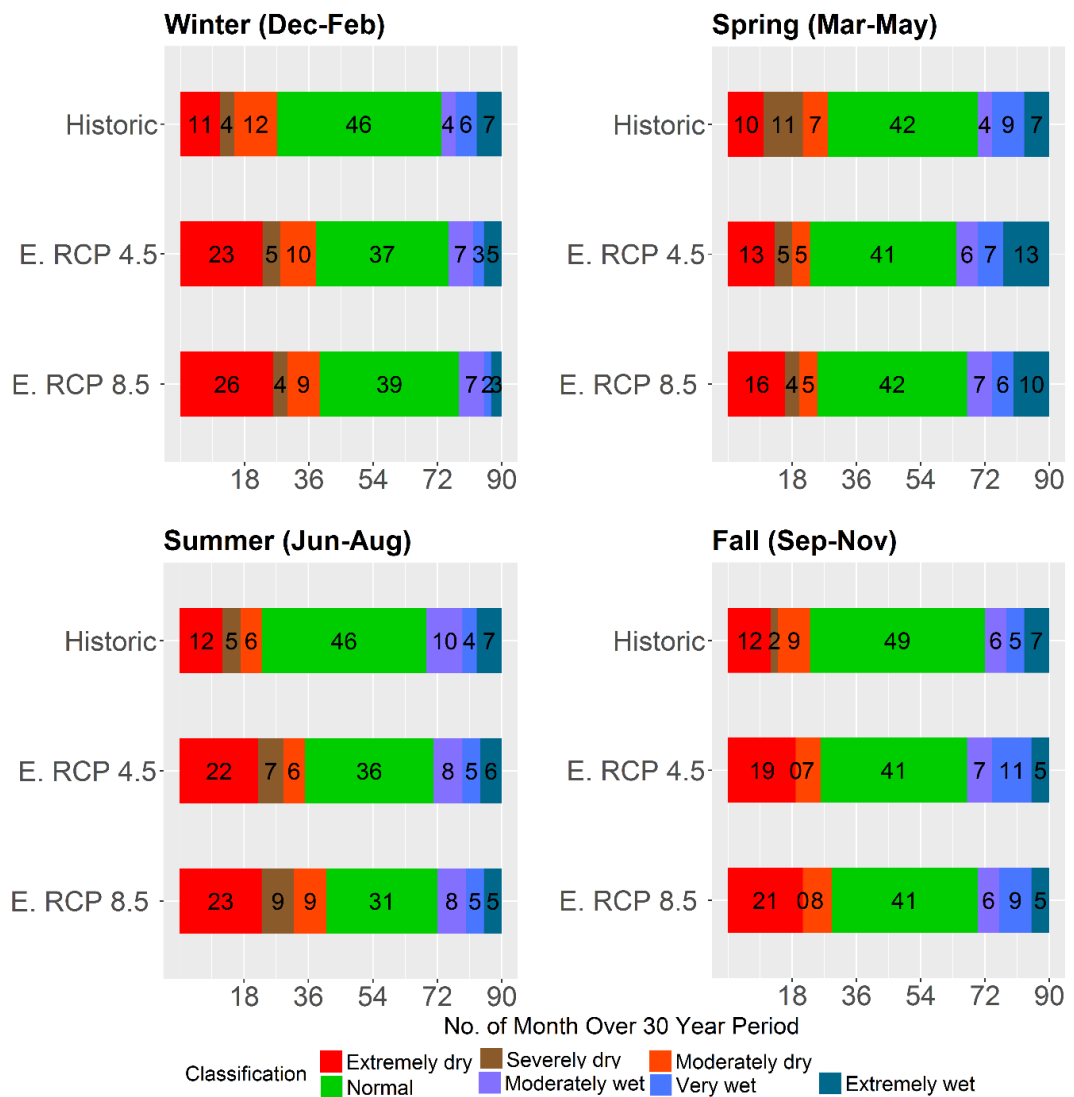
Figure 4.4. Projected seasonal count of month over 30 years for seven classifications of standardized precipitation index for far future (2046-2075) for ensemble of each of two RCPs scenarios
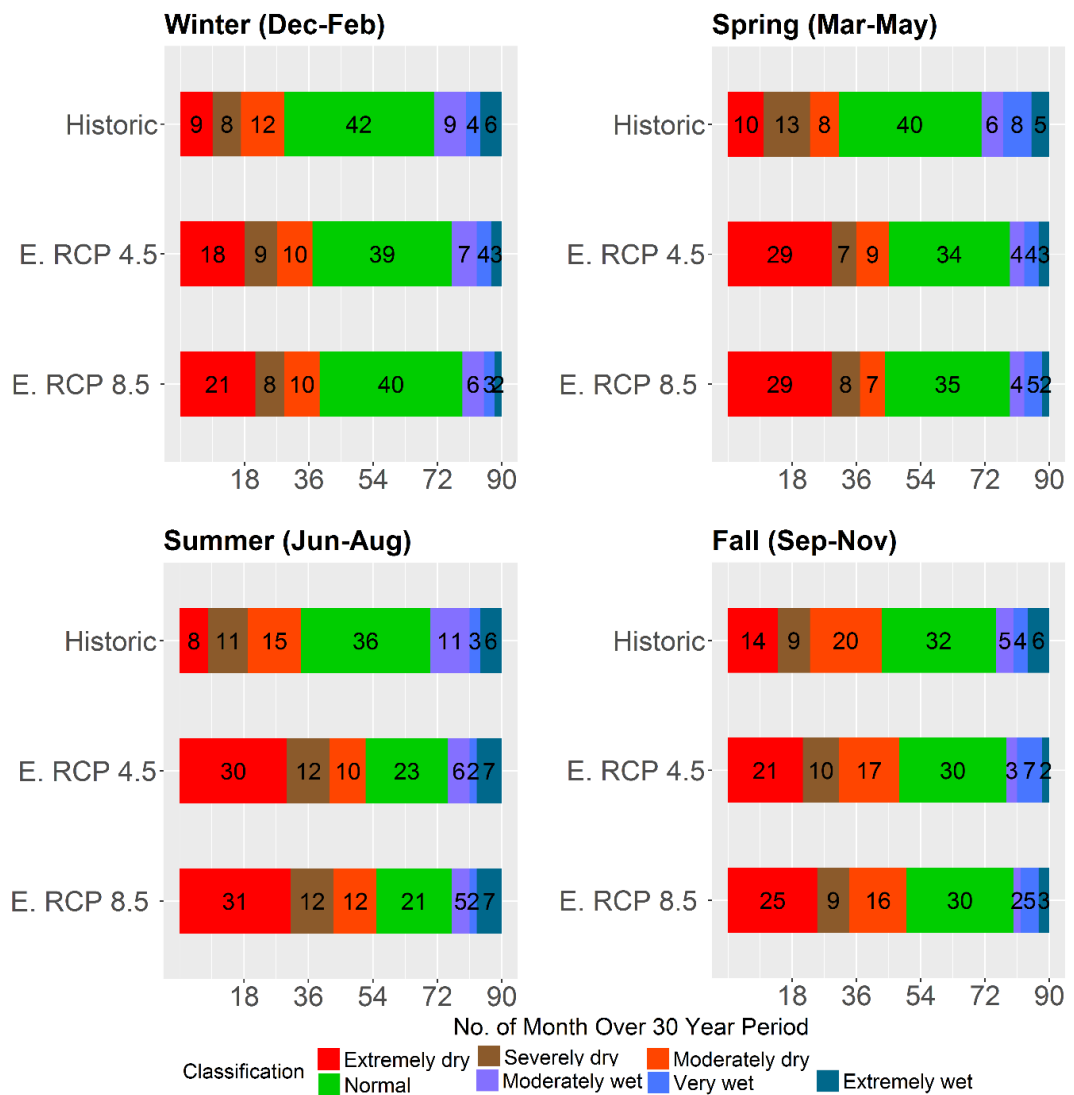
Figure 4.5. Projected seasonal count of months over 30 years for seven classifications of standardized streamflow index for near future (2016-2045) for ensemble of each of two RCPs scenarios
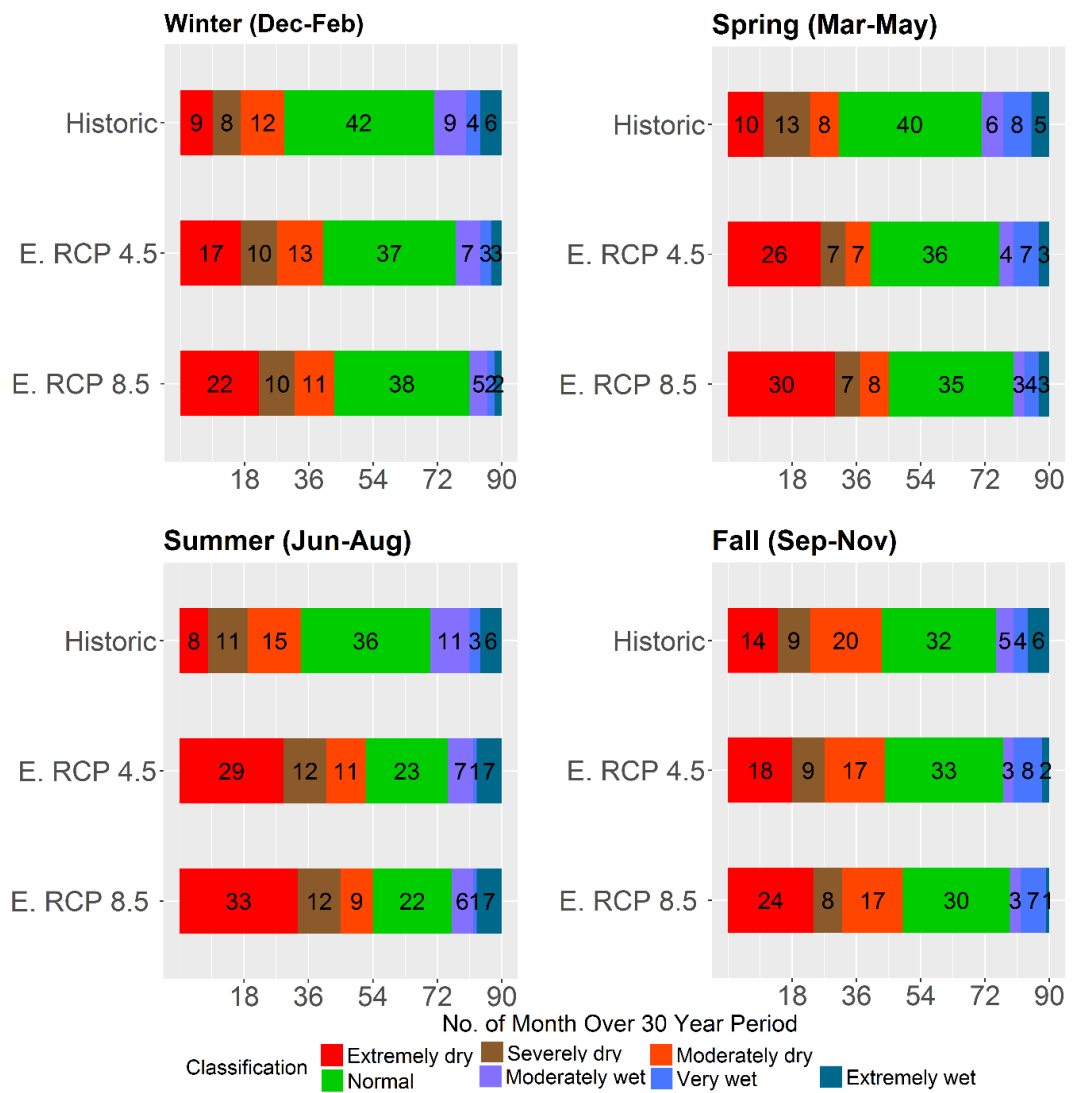
Figure 4.6. Projected seasonal count of months over 30 years for seven classifications of standardized streamflow index for far future (2046-2075) for ensemble of each of four RCPs scenarios
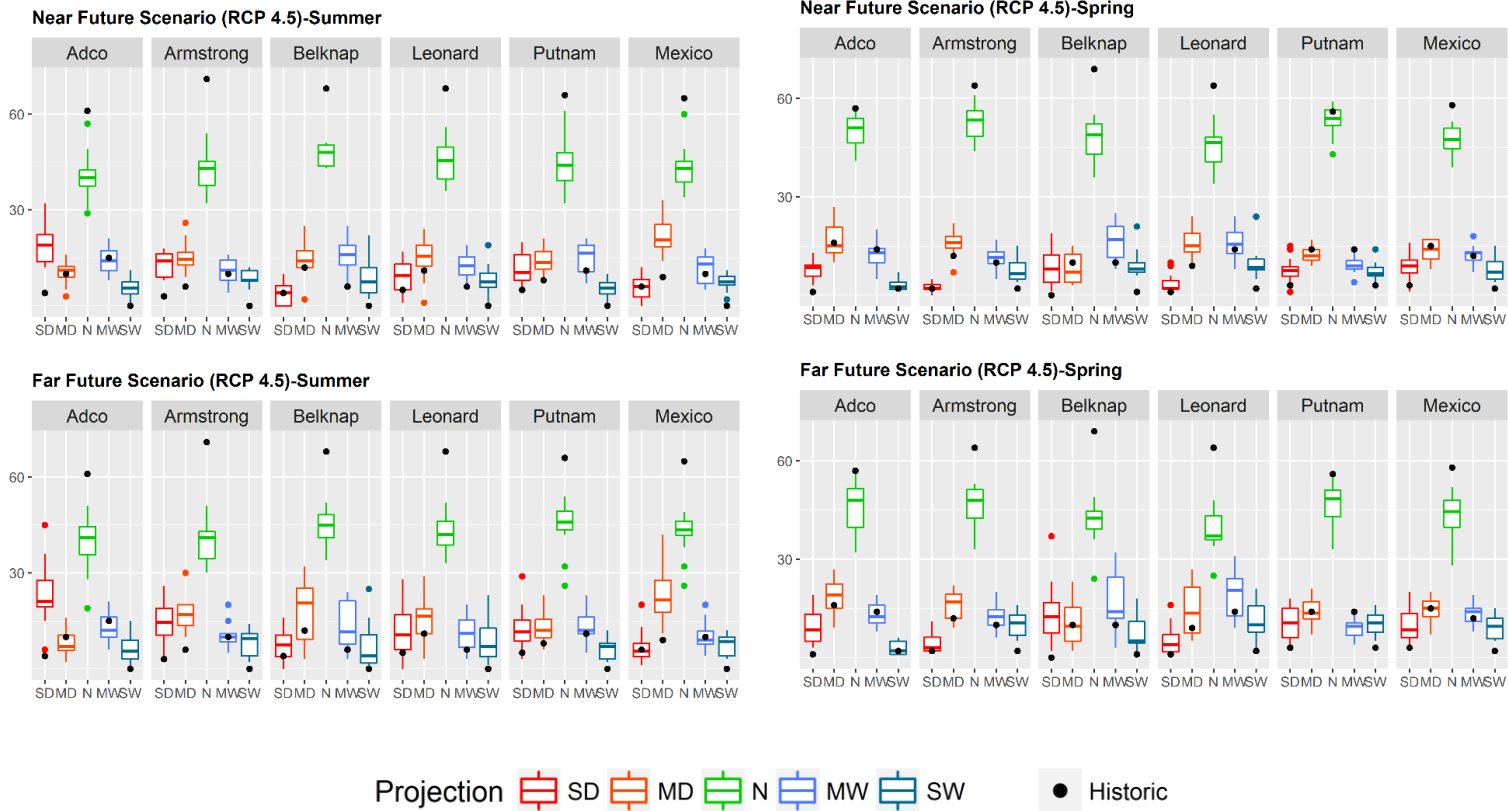
Figure 4.7. Projected count of months for five classifications of drought (MD: Moderately Dry, MW: Moderately Wet, N: Normal, SD: Severely Dry, and SW: Severely Wet) for near (2016-2045) and far (2046-2075) future scenarios for soils across the watershed under RCP 4.5 scenarios. Color dots represent outliers, defined by more than 1.5 times the interquartile range above the third quartile or below the first quartile
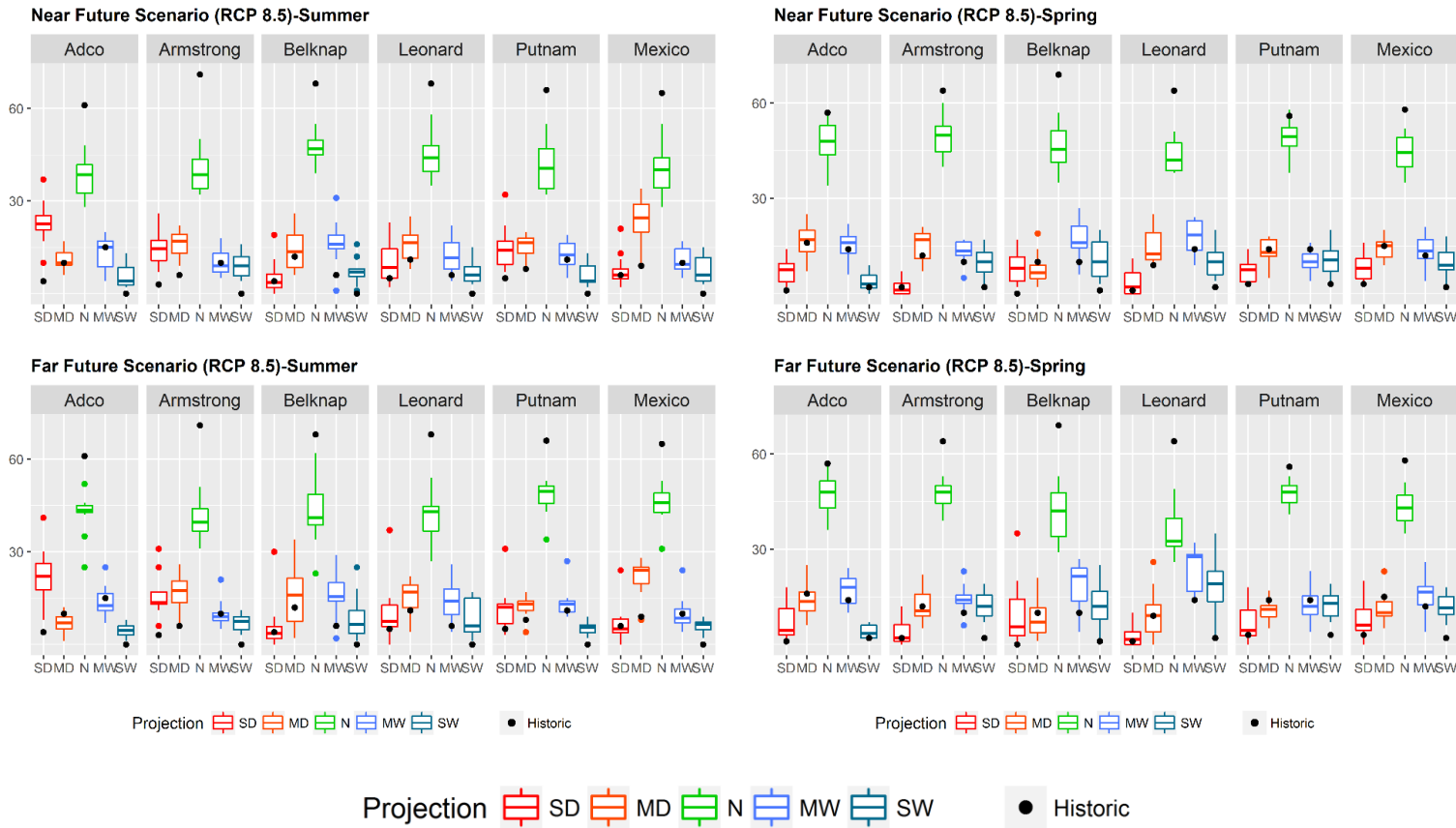
Figure 4.8. Projected count of month for five classifications of drought (MD: Moderately Dry, MW: Moderately Wet, N: Normal, SD: Severely Dry, and SW: Severely Wet) for near (2016-2045) and far (2046-2075) future scenarios for soils across the watershed under RCP 8.5 scenarios. Color dots represent outliers, defined as more than 1.5 times the interquartile range above the third quartile or below the first quartile
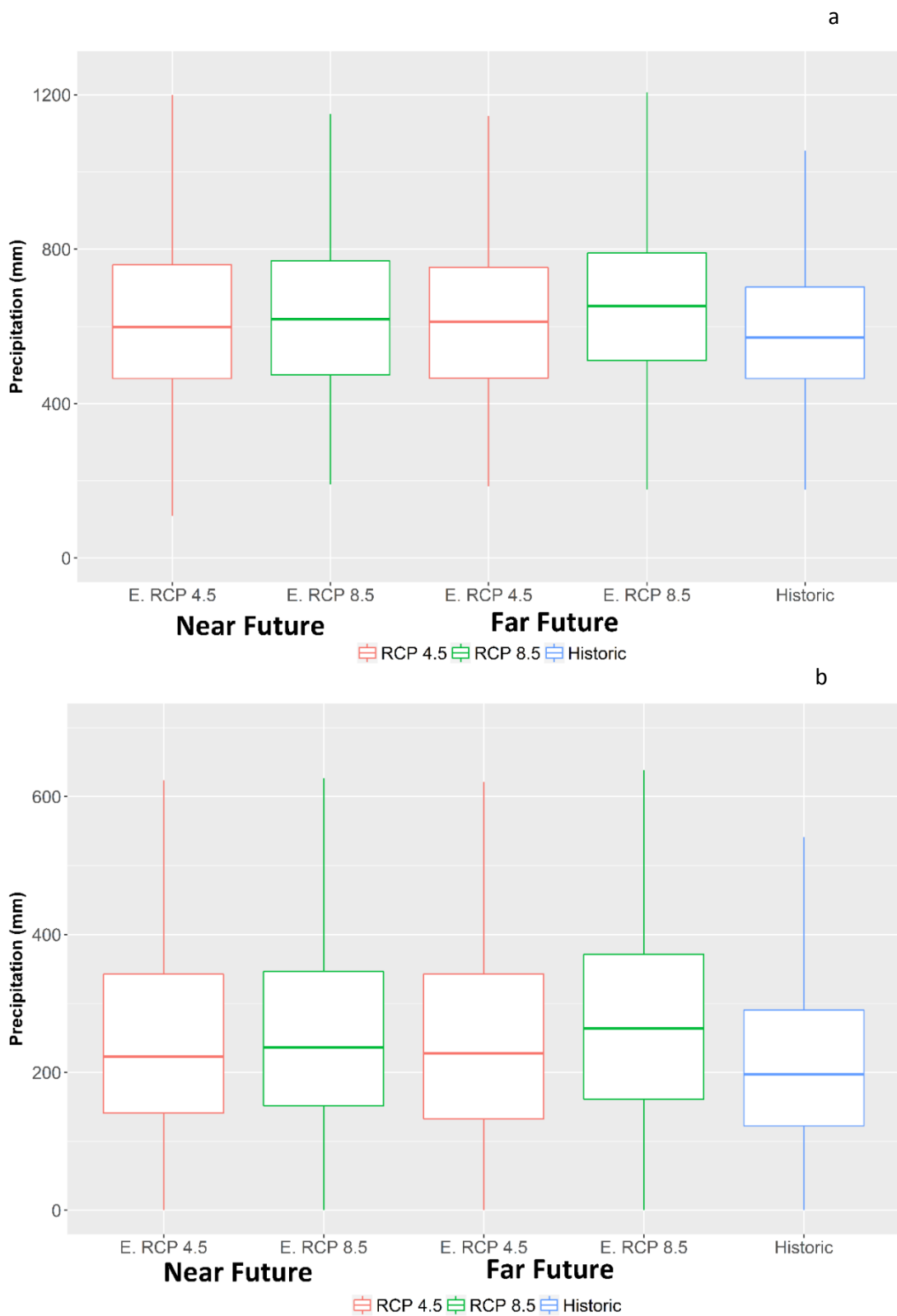
Figure 4.9. Projected annual precipitation ≥ 95th percentile (a) and annual sum of total precipitation ≥ 99th percentile (b) presented as ensemble for two RCPs (E. RCP 4.5 and E. RCP8.5) scenarios and its comparison with historic data
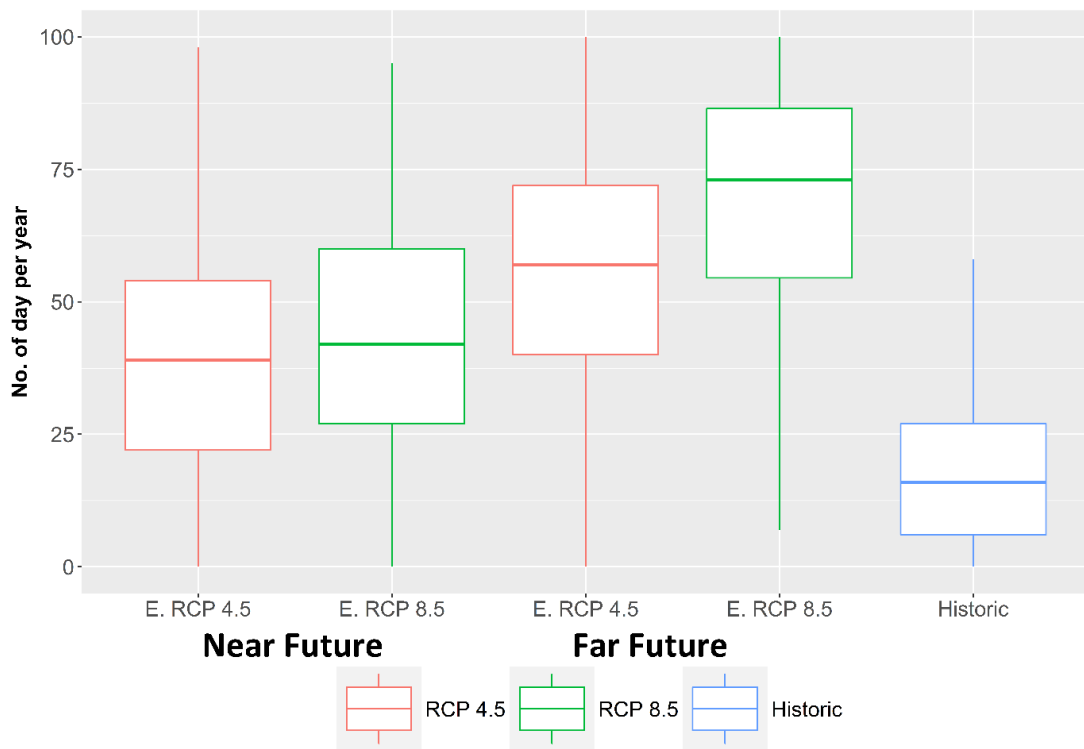
Figure 4.10. Projected annual count of number of warm spell duration days presented as ensemble for two RCPs (E. RCP 4.5 and E. RCP8.5) scenarios and its comparison with historic data

CHAPTER 5

ASSESSING THE MANAGEMENT AND CLIMATE CHANGE IMPACTS ON HYDROLOGIC COMPONENTS: A CASE STUDY ON A FIELD LOCATED AT CENTRAL MISSOURI

ABSTRACT

Runoff and water quality are influenced by management decisions at the field-scale within a watershed. Simulation studies are crucial for quantifying impacts of management and climate change on hydrologic components at field scales where management practices are applied. This study was conducted to evaluate the impact of management and climate change on water quality and quantity. The specific objective was to compare Business-As-Usual (BAU) and Aspirational (ASP) management systems under current and future climate to understand how climate change alone could affect hydrology and determine if the ASP management interventions could mitigate the impacts of climate. Twelve different Global Climate Models (GCMs) under two Representative Concentration Pathways (RCP 4.5 and RCP 8.5) were used for future projection. This study was congruent to Central Mississippi River Basin (CMRB)-Long-Term Agroecosystems Research (LTAR) common experiment. This study was conducted to evaluate the impact of best management practices, specifically cover crop planting, longer crop rotation, and no-till practices over historic and future timeframes, within the experimental field (Field 1) located at Goodwater Creek Experimental Watershed (GCEW), Missouri. GCEW is within the Central Mississippi River Basin site of the USDA's Long Term Agroecosystems Research program. The Agricultural Policy Environmental eXtender (APEX), a field scale hydrologic model was used for the simulation. The APEX model was calibrated and validated for runoff and water quality using data collected at the edge of field and management scenarios in combination with climate scenarios were compared. The change in management

alone from BAU to ASP during the historic period (1981-2010) resulted in 25% less annual median runoff. The median annual runoff loss was reduced by 16.5% and 18.8% in ASP scenario compared to BAU for ensemble of RCP 8.5 for near (2016-2045) and far future (2046-2075) respectively. The average ensemble annual soluble nitrogen in watershed outflow was 14 kg/ha for BAU compared to 12 kg/ha for ASP management for the baseline historic period. The results indicate the inclusion of no-till and winter cover crop resulted in increased subsurface flow. The results indicate the environmental benefit of crop rotation and cover crop with reduction in runoff and nutrient losses. The ASP management provides surface cover all year round and improves soil water properties resulting in lower runoff. Although, there is a benefit of ASP for reduction of nitrogen in water there is higher denitrification and volatilization loss of nitrogen under ASP compared to BAU.

Keyword: APEX, Climate, Runoff, Nitrate

Introduction

Conventional agricultural practices have been shown to result in a variety of negative environmental impacts due to runoff and nutrient losses in surface water bodies (Andraski et al., 2003; Ghidey and Alberts, 1998; Johnson et al., 1979). In response to the need to mitigate the negative impacts of agriculture while ensuring sufficient production of food to meet the needs of growing populations, a variety of best management practices (BMPs) have been studied over the past few decades. BMPs have been shown to help decrease surface runoff, improve water quality, e.g., through nutrient retention, and improve long-term soil health. Increasing pressure on agricultural systems due to climate change creates an increasing need for impact assessment under multiple future climate scenarios in order to plan for mitigation and adaptation as needed. Agriculture systems are a key focus due to the direct connection

to climatic conditions and corresponding potential for significant impacts to human life and the economy (Schlenker and Roberts, 2009).

Anticipating impacts to agricultural systems due to future climate via model simulation is often limited by lack of data and resources required to properly calibrate and validate models. As more data are collected, it becomes possible to simulate the performance of BMPs in a field or watershed to assess current performance as well as to identify or rule out risks under future climate conditions. The projected increase in temperature and variable precipitation patterns associated with future climate are expected to impact the volume of surface runoff and soil erosion (Zhang et al., 2012) and ultimately crop production (Lobell and Field, 2007; Rosenzweig et al., 2013; Rosenzweig et al., 2002). Increased runoff can result in induced erosion, which can transport sediment and soil organic carbon, impacting soil health (Novara et al., 2018) and ultimately impact crop production. In addition, increased runoff can result in increased nitrate loss, which is of major concern for Midwestern watersheds. However, there are many complex and dynamic interactions among climate, vegetation, hydrology, and other biogeochemical cycles that are important in relation to evaluating the productivity and environmental performance of agricultural systems under both current and changing future climate. Alternative management system can be a viable alternative to combat future climate change impacts on agriculture.

BMPs such as crop rotation and conservation tillage have been shown to improve soil physical and biological properties resulting in increased water retention, increased carbon sequestration, runoff reduction, pest and disease control, and improve water quality (Hoorman, 2009; Poeplau and Don, 2015). Introducing cover crops in rotation are found to improve soil water retention properties due to increased

118

soil organic matter (Mills et al., 1988). Other benefits of crop rotation, cover crops and tillage include their capacity to influence soil water movement by inducing physical changes in soil macro and micro-pore structure, which significantly influence the surface and subsurface flow (Baker, 1987). Earlier studies have reported greater reductions in runoff and increased ground water recharge from no-till systems compared to conventional tillage (Edwards et al., 1990; Plaster, 2013) as no-till improves soil structure and soil organic matter. Increased surface residue, water infiltration, and improved soil aggregate stability are found to be major benefits of application of BMPs (Reeves, 1997).

Simulation models can be used as a cost effective tool to assess the impacts of climate and management change on hydrology. With increased climate-driven risk to hydrology and crop production, simulation models are useful tools to better understand benefits of BMPs and adoption need under climate change. Simulation models have been widely used for accessing long-term management and climate change impact on hydrologic components. Past studies have used process-based hydrologic models (e.g., SWAT and APEX) to simulate management and climate change impact on hydrologic components. Unlike simple water balance models, process-based hydrologic models take into consideration many key processes and spatial heterogeneity to better replicate cause and effect relations (Graeff et al., 2012). There have been many studies using the SWAT model to simulate impact on alternative management and climate change impact on hydrology (Ficklin et al., 2013a; Ficklin et al., 2013b; Tuppad et al., 2010; Ullrich and Volk, 2009), which report the benefits of alternative management systems on runoff and nutrient loading reductions. Earlier simulation studies conducted using APEX report the benefits of

inclusion of BMPs (e.g., cover cop and crop rotation) on runoff reduction compared to continuous corn under climate change (Gautam et al., 2015).

This study was conducted on a field located within Goodwater Creek Experimental Watershed (GCEW) and is unique due to the extensive data available to characterize hydrology, soil and weather for the long term. Future precipitation and ultimately runoff is projected to increase for Salt River Basin and GCEW (Gautam et al., 2018). The GCEW is part of a Central Mississippi River Basin (CMRB)-Long Term Agroecosystems Research (LTAR) network, and long-term measured data include flow data since 1971 and runoff and water quality data from fields and plot since 1992.This makes it a unique site for impact assessment using simulation models. Details regarding the measured long-term data for the study watershed including weather, water quality and quantity have been described by Baffaut et al. (2015); Lerch et al. (2015); Sadler et al. (2015a); Sadler et al. (2015b). Projected increase in future precipitation is a major challenge for this study watershed, where the majority of the soils include a claypan layer at a fairly shallow depth. Runoff is projected to increase in GCEW based on simulation model projections (Gautam et al., 2018). Claypan soils have very slow vertical movement of water due to the restrictive clay in subsoil. As a result, the thin layer of top soil can quickly saturate resulting in runoff. Alternative management systems on these restrictive layer soils should aim to increase infiltration by improving surface cover and crop residue incorporation. In this study, APEX simulations were used to assess the impact of management on runoff, soluble nitrogen yield in watershed outflow and evapotranspiration. The management scenarios include the typical cropping system that represents management in the region (Business As Usual (BAU)) and an improved management scenario

(Aspirational (ASP)), which includes cover cropping, a more diverse crop rotation, and no tillage.

Materials and Methods

Description of Study Watershed

The study was conducted in a 35 ha agricultural field (Field 1) located in GCEW (figure 5.1). This study area is managed by the USDA Agricultural Research Service Cropping System and Water Quality Research Unit in Columbia, Missouri. The study watershed is characteristic of the Central Claypan Major Land Resource Area, which encompasses around 3 million ha in Missouri and Illinois. Management on Field 1 during 1991-2003 included a corn-soybean rotation and mulch tillage (Lerch et al., 2005). An aspirational management system that includes a corn-soybean-wheat rotation with cover crop between main crops and no tillage was started after 2004. Historically, the northern three-fourths of the field were managed with corn, soybean, wheat and grain sorghum using plow and disk till (intensive tillage) and the southern one-fourth was under pasture until 1981 when this pasture was converted to cropland (Mudgal et al., 2012). The soils in the watershed are silt loam type with 0% to 3% slope, and contain a claypan found 15 cm below surface in the most eroded zone to 100 cm in deposit zones (Mudgal et al., 2012). The study area received an average annual precipitation of 974 mm between1969 and 2010, with maximum and minimum annual rainfall of 1580 and 465 mm, in 2008 and 1971 respectively. The daily average maximum and minimum temperatures during the 42-year (1969-2010) period were 17.2°C and 6.5°C, respectively.

APEX model Calibration, Validation and Evaluation Criteria

APEX is a field-scale model that is designed to simulate the impact of change in agricultural management systems on water quality and quantity (Williams and

Izaurralde, 2006). This model has also been used to simulate the potential impacts of climate change (Gautam et al., 2015). The APEX model (version 808) was used for this study. Measured weather data (daily precipitation and daily maximum and minimum temperature) were used for simulating the hydrology of Field 1 during the historic period (Sadler et al., 2015b). Measured soil properties including soil texture, cation exchange capacity, organic carbon content, and soil pH (Sudduth et al., 2003; Sudduth et al., 2005), soil hydraulic properties including soil water parameters (field capacity and wilting point) (Jiang et al., 2007) and saturated hydraulic conductivity and bulk density were used to describe soil in the watershed (Mudgal et al., 2010). Elevation data previously collected using kinematic global positioning system survey on 10-m transects were used in this study (Fraisse et al., 2001). The field was divided into 35 subareas based on slope, depth of claypan and soil mapping units. Details on model setup can be found in Mudgal et al. (2012).

The modification in APEX model setup was made to improve its utility for climate change impact assessment. The crop management operations, including planting and other operations were scheduled based on heat units (HU) accumulated since the beginning of the year or since planting. This is based on heat unit theory, which is used to predicting development stage of crops in relation to heat unit accumulated (Cross and Zuber, 1972). With HU based management, scheduling of any operations are triggered based on accumulated temperature. The HU based crop management scheduling was used to represent the change in planting dates in the future because of projected increased temperatures. In APEX, HU based crop operation scheduling can coincide with precipitation events as it is solely based on temperature, which is not a true replication of farmer decision-making practice.

The APEX model was calibrated using historic observations with a two-year warmup period (1991-1992). Data from 1993-1998 were used for calibration and 1999-2003 data were used for validation. Model calibration was conducted for runoff, nitrate, phosphorus and atrazine. APEX being a daily time step model, daily runoff and pollutant transport of successive days were combined when those belonged to the same event based on hydrograph dynamics. Sensitivity analysis was conducted using one parameter at a time and sensitive parameters were changed to maximize model evaluation criteria. The model performance was tested using the coefficient of determination (r^2) and Nash-Sutcliffe efficiency (NSE). The r^2 value above 0.60 and NSE values above 0.50 during the calibration and validation periods were set as a criterion for satisfactory model performance during the model simulation of daily streamflow as defined by Moriasi et al. (2015).

Long-Term Simulation Scenarios

Two different management scenarios and output from twelve GCMs including two different RCPs were used for simulation. Details of the management and climate scenarios are presented in sections below.

Management scenarios

Management Scenario 1. *Business as usual (BAU).* This scenario included a 2-year corn-soybean rotation using conventional tillage. For BAU, nitrogen was applied at the rate of 190 kg/ha when corn was planted resulting in a total application of 2850 kg nitrogen per hectare over a 30-year period. This was the dominant crop rotation scenario in the study region.

Management Scenario 2. *Aspirational scenario (ASP).* This scenario included a 3-year crop rotation (corn-soybean-wheat) with the addition of cover crops, rye grass or clover in the winter under no-till management. In this scenario, nitrogen fertilizer was applied at the rate of 161 kg-N/ha during the first year while planting of corn and cover crop and 122 kg-N/ha was applied as split dose during planting and during wheat emergence (spring) for winter wheat during the three-year rotation period. The resulting total nitrogen application was 2830 kg nitrogen per hectare over a 30-year period. The goal of this management system was to build soil health by increasing species diversity and carbon sequestration.

Climate scenarios and future projection

Climate data from the CMIP5 project available at 12 km^2 horizontal resolution for GCM models were obtained (Maurer et al., 2007). These data were downscaled using observed P and T data over the years from the local weather station located in Field 1. The bias in temperature and precipitation were corrected using delta and quantile mapping, respectively. Details for each of the bias correction approach can be found in Gautam et al. (2018). The ensemble of multiple model projection of precipitation and temperature is presented in figure 5.2. The potential for future advancements in crop cultivators was not simulated in the present study due to lack of a clear understanding of potential future crop cultivars.

The long-term scenario was run for 60 years (2016-2075) for each of the 12 GCM models under two RCPs (RCP 4.5 and RCP 8.5) under the two management scenarios (BAU and ASP). The comparisons between BAU and ASP during the historic period (1981-2010) represents the impact of management change alone on hydrologic components as the climate data were similar across the baseline historic

period for all the climate models. Only two RCPs were used to represent the worst and moderate case scenarios, which are based on the projected radiative forcing of 4.5 and 8.5 W/m^2, respectively. RCP 2.6 had already been surpassed when we conducted this study and RCP 6.0 is intermediate to RCP 4.5 and RCP 8.5. All the results are presented as the ensemble median of hydrologic parameters and water quality parameters simulated with APEX using 12 GCM model datasets. The Q1 and Q3 values were used to represent the uncertainty of values for simulated components, when using precipitation and temperature data form the multiple GCM models.

Results and Discussions

Model Calibration and Validation

The default and adjusted model parameter values are presented in table 5.1. The calibration objective was to maximize the model evaluation criteria for all the output variables considered for calibration of the model. Model parameters, including the curve number and associated parameters, hydraulic conductivity, evapotranspiration related parameters and depth of claypan were determined to be sensitive to runoff based on an earlier study (Mudgal et al., 2012). The model parameters controlling surface runoff, atrazine, biological processes, and nutrient runoff were important parameters considered during the calibration-validation process. Daily streamflow simulation at the field outlet resulted in r^2 of 0.94 and NSE of 0.94 during calibration (1993–1998), and r^2 of 0.86 and NSE of 0.0.86 during the validation. Other output variables including pesticide and nutrients were considered during calibration and validation (table 5.2). Calibration of a model using multiple outputs increased confidence of the model.

Management and climate change impacts on hydrology and water quality

Water Yield and Surface Runoff

Simulation of management change from BAU to ASP during the historic period resulted in 7% (223 mm to 206 mm) reduction in annual median simulated water yield. Future climate simulation results indicated a 5.9% (254 mm to 239 mm) and 7.6% (242 mm to 223 mm) decrease in annual median ensemble water yield from application of the aspirational scenario instead of business as usual for near future and far future for model forced with RCP 4.5 climate models (Table 5.3). Results indicated that the majority of the water yield reduction occurred during April, May, and June (figure 5.3a). For RCP 8.5, overall results indicated around 0.9% and 0.2% decrease in annual median ensemble water yield from application of aspirational scenario instead of business as usual for near and far future (Table 5.3). Similarly, the RCP 4.5 results indicated the majority of water yield reduction was simulated to occur during April, May and June (figure 5.3b). The reduction in water yield was due to the application of no-till and cover crops. The comparison of simulated soil organic content under BAU and ASP indicated around 13% increase under ASP management compared to BAU. Previous studies also report the benefit of no-till on improving soil organic content and ultimately soil water properties (Huang et al., 2010; Kumar et al., 2012).

Simulation of management change from BAU to ASP during the historic period resulted in 25% (162 mm to 120 mm) reduction in annual median simulated surface runoff. A recent experimental study in Iowa reported a 15% increase in soil organic matter for top soil after nine year from inclusion of cover crop (rye) to a no-till corn silage-soybean rotation (Moore et al., 2014). The runoff reduction after

application of aspirational management practices was attributed to increased organic matter and decreased curve number due to no-till management and cover crop. Future simulation results for surface runoff indicate a 21.9% (185 mm to 144 mm) and 23.6% (178 mm to 135 mm) decrease in the RCP4.5 near and far future, respectively, based on the annual median ensemble surface runoff due to the application of ASP scenario instead of BAU (Table 5.3). Results indicate that the median ensemble surface runoff decreases in most months of the year (figure 5.4a). For RCP 8.5 overall the results indicate around 16.5% (192 mm to 160 mm) and 18.8% (203 mm to 164 mm) decrease in annual median ensemble surface runoff from application of the ASP scenario instead of BAU for near future and far future for model forced with RCP 8.5 climate models (Table 5.3). For extreme scenarios (RCP 8.5), the ASP management can at best achieve the highest median annual runoff observed in the past. Even with the addition of this management change (BAU to ASP), climate change will increase surface runoff. Similar to RCP 4.5, results indicated surface runoff reduction in almost all months of the year due to management change (figure 5.4b). Previous studies also indicated improvement of soil water properties due to decreased bulk density, increased water-aggregate stability, and improved soil porosity after the introduction of a cover crop in the rotation (Hatfield and Sauer, 2011). Smaller changes in water yield compared to surface runoff in the study are attributed to the fact that ASP management increased the subsurface flow. Calculation based on historic median results presented for BAU and ASP indicate around 25 mm increase in subsurface flow after implementation of ASP. Improved water infiltration can be attributed to increased crop residue, increased available water content, decreased curve number, and improved soil organic matter provided by cover crop and no-till management system. Cover crops provide soil cover and are also known for

improving soil organic matter; 9% to 85% increases in soil organic matter are reported for different soil and climatic conditions (Hatfield and Sauer, 2011). The ensemble median water yield and surface runoff values including Q1 and Q3 value based on multi-model projection for field 1 for both RCPs under BAU and ASP is presented in Supplement fig 5.1 and Supplement fig 5.2.

Evapotranspiration

Simulation of management change from BAU to ASP during the historic period resulted in 1.5% (723 mm to 712 mm) reduction in annual median simulated evapotranspiration. Higher ET occurs during June, July, and August for BAU as the crop grown (Corn and Soybean) in this management system reaches optimum growth during these months (Supplement fig 5.3). For the ASP scenario, ET is also higher during April and May due to inclusion of winter wheat in the rotation which reach optimum growth during these months (Supplement fig 5.3). The comparison of ET response between the two management systems indicates higher monthly peak for BAU management compared to ASP management where cultivation of cover crop and winter wheat flatten monthly ET response. Future simulation results indicate around 1.58% (730 mm to 718 mm) and 1.89% (725 mm to 711 mm) decrease in annual median ensemble evapotranspiration from application of ASP instead of BAU for near future and far future for model forced with RCP 4.5 climate models (Table 5.3). Results indicate an increase in ET during March, April and May (figure 5.5a). For RCP 8.5 overall the results indicate around 3% (729 mm to 707 mm) and 3.47% (735 mm to 710 mm) decrease in annual median ensemble evapotranspiration from application of ASP instead of BAU for near future and far future for model forced with RCP 8.5 climate models (Table 5.3). Result indicates the increase in ET during March, April and May (figure 5.5b). Results indicate increase in ET in summer

months and decrease in fall ET for future for model forced with both RCPs. The increase in summer ET is the result of projected increase in summer temperature.

<u>Soluble Nitrogen</u>

The median annual simulated soluble nitrogen loss was 8 kg/ha for BAU compared to 3.9 kg/ha for ASP management for the historic period, which indicates benefit of management change on reduction of nitrogen loss. The ensemble soluble nitrogen values including Q1 and Q3 values based on multi model projection for Field 1 for both RCPs under BAU and ASP is presented in Supplement fig 5.4. The wide range of Q1 and Q3 for monthly soluble nitrogen yield indicates the sensitivity of nitrogen loss to precipitation (Supplement fig 5.4). Future simulation results indicate a decrease in annual median ensemble soluble nitrogen yield from application of ASP scenario compared to the BAU scenario for models forced with both RCP 4.5 and RCP 8.5 climate data. Median annual values of soluble nitrogen loss based on the ensemble of multiple models was simulated to be 7.8 kg/ha for BAU management compared to 4.7 kg/ha for ASP for models forced with RCP 8.5 for 60-year future period. Similar reduction of nitrogen was simulated for RCP 4.5 models. Studies indicate benefit of cover crop on reduction of nitrogen loss by 1% to 89% based on results across 10 studies (Tellatin and Myers, 2017). In addition to annual reduction potential, it is very important to know the seasonal behavior of nitrate loss. The hypoxic zone in the Gulf of Mexico occurs annually during early spring and summer (Rabalais et al., 2002). Results indicate that the majority of soluble nitrogen yield was simulated to reduce during February through August for models forced with both RCP 4.5 and RCP 8.5 climate data (figure 5.6a and figure 5.6b) after application of ASP. The main reason for reduction of soluble nitrogen yield during February through August is caused by runoff reduction from application of cover crop and no-till

(figure 5.4 and Supplement fig 5.4). Another reason for reduction of soluble nitrogen yield during spring for the ASP scenario is due to application of fertilizer in split dose compared to BAU where majority of nutrients are applied during April and May during Corn years. Increase in the soluble nitrogen yield during September through December after application of ASP scenario is due to loss of N-fertilizer applied for winter wheat and cover crop. Note that the nitrogen loss during winter is very small. Decreased loss of nitrogen in outflow is due to decrease in surface runoff and increased loss of nitrogen via denitrification and ammonia volatilization after the application of aspirational management. A previous study shows higher volatilization loss due to surface application of fertilizer (Rochette et al., 2009). In addition, residue from no-till in ASP has increased supply of energy material available to denitrification organism and increased soil moisture content favoring denitrification (Aulakh et al., 1984). Note that the overall amount of nitrogen applied over the period of comparison is similar, as presented in section 2.3. A previous study also reports benefits of improved cropping management system, a simulation study conducted at Southwestern Minnesota using soil-plant-atmosphere simulation reports reduced in Nitrogen loss by 11.1 kg N/ha for corn-soybean rotation (Feyereisen et al., 2006). Cover crops affect the hydrologic balance, lower soil NO_3-N level and provide cover for fallow period between summer crops. The major benefit of having soil cover year round includes uptake of soil NO_3-N by crop leachable, and its conversion to organic nitrogen in plant biomass (Hoyt and Mikkelsen, 1991).

Conclusions

A calibrated APEX model was used to simulate the effect of climate change and management change on hydrologic components using downscaled T and P data from GCMs under two emission scenarios. Management change alone resulted in 25% (162

mm to 120 mm) decrease in median annual simulated surface runoff and 4.1 kg/ha (8 kg/ha to 3.9 kg/ha) reduction on annual simulated soluble nitrogen yield. Comparison of two management scenarios, business as usual (two year corn-soybean rotation) and aspirational scenario (three year corn-soybean-wheat rotation with no-till), demonstrate the benefits of aspirational management system under the future projected by RCP 4.5 and RCP 8.5 scenarios. Overall the results for surface runoff indicate around 21.9% (185 mm to 144 mm) and 23.6% (178 mm to 135 mm) decrease in annual median ensemble surface runoff in with application of aspirational scenario instead of business as usual for near future and far future for model forced with RCP 4.5 climate models. Similarly, for RCP 8.5 overall the results indicate around 16.5% (192 mm to 160 mm) and 18.8% (203 mm to 164 mm) decrease in annual median ensemble surface runoff from application of aspirational scenario instead of business as usual for near future and far future. Aspirational scenarios resulted in reduction in average annual soluble nitrogen yield. Median annual values of soluble nitrogen loss based on ensemble of multiple model was simulated to be 7.8 kg/ha for BAU management compared to 4.7 kg/ha for ASP for model forced with RCP 8.5 for 60-year future period. Decreased loss of nitrogen is due to decrease in surface runoff and increase loss of nitrogen via denitrification and ammonia volatilization.

References

Andraski, T. W., Bundy, L. G., and Kilian, K. C. (2003). Manure History and Long-Term Tillage Effects on Soil Properties and Phosphorus Losses in Runoff. *Journal of Environmental Quality* **32**, 1782-1789.

Aulakh, M., Rennie, D., and Paul, E. A. (1984). The Influence of Plant Residues on Denitrification Rates in Conventional and Zero Tilled Soils 1. *Soil Science Society of America Journal* **48**, 790-794.

Baffaut, C., Sadler, E. J., and Ghidey, F. (2015). Long-Term Agroecosystem Research in the Central Mississippi River Basin: Goodwater Creek Experimental Watershed Flow Data. *Journal of Environmental Quality* **44**, 18-27.

Baker, D. (1987). "Overview of Rural Nonpoint Pollution in the Lake Erie Basin." Heidelberg Coll., Tiffin, OH (USA). Water Quality Lab.

Cross, H., and Zuber, M. (1972). Prediction of Flowering Dates in Maize Based on Different Methods of Estimating Thermal Units 1. *Agronomy Journal* **64**, 351-355.

Edwards, W., Shipitalo, M., Owens, L., and Norton, L. (1990). Effect of Lumbricus Terrestris L. Burrows on Hydrology of Continuous No-Till Corn Fields. *Geoderma* **46**, 73-84.

Feyereisen, G.W., Wilson, B.N., Sands, G.R., Strock, J.S. and Porter, P.M. (2006). Potential for a Rye Cover Crop to Reduce Nitrate Loss in Southwestern Minnesota. *Agronomy Journal* **98**, 1416-1426.

Ficklin, D., Stewart, I., and Maurer, E. (2013a). Effects of Projected Climate Change on the Hydrology in the Mono Lake Basin, California. *Climatic Change* **116**, 111-131.

Ficklin, D. L., Stewart, I. T., and Maurer, E. P. (2013b). Climate Change Impacts on Streamflow and Subbasin-Scale Hydrology in the Upper Colorado River Basin. *PLoS ONE* **8**, e71297.

Fraisse, C., Sudduth, K., and Kitchen, N. (2001). Delineation of Site-Specific Management Zones by Unsupervised Classification of Topographic Attributes and Soil Electrical Conductivity. *Transactions of the ASABE* **44**, 155.

Gautam, S., Baffaut, C., Thompson, A., Svoma, B., Phung, Q., and Sadler, E. (2018). Assessing Long-Term Hydrological Impact of Climate Change Using an Ensemble Approach and Comparison with Global Gridded Model-a Case Study on Goodwater Creek Experimental Watershed. *Water* **10**, 1-25.

Gautam, S., Mbonimpa, E., Kumar, S., Bonta, J., and Lal, R. (2015). Agricultural Policy Environmental Extender Model Simulation of Climate Change Impacts on Runoff from a Small No-Till Watershed. *Journal of Soil and Water Conservation* **70**, 101-109.

Ghidey, F., and Alberts, E. (1998). Runoff and Soil Losses as Affected by Corn and Soybean Tillage Systems. *Journal of Soil and Water Conservation* **53**, 64-70.

Graeff, T., Zehe, E., Blume, T., Francke, T., and Schröder, B. (2012). Predicting Event Response in a Nested Catchment with Generalized Linear Models and a Distributed Watershed Model. *Hydrological Processes* **26**, 3749-3769.

Hatfield, J. L., and Sauer, T. J. (2011). "Soil Management: Building a Stable Base for Agriculture," American Society of Agronomy, Madison, Wisconsin, 409.

Hoorman, J. J. (2009). Using Cover Crops to Improve Soil and Water Quality. *Agriculture and Natural Resources. The Ohio State University.*

Hoyt, G., and Mikkelsen, R. (1991). Soil Nitrogen Movement under Winter Cover Crops and Residues. Cover crops for clean water. Soil Water Conservation Society, Ankeny, IA, 91-94.

Huang, S., Sun, Y.-N., Rui, W.-Y., Liu, W.-R., and Zhang, W.-J. (2010). Long-Term Effect of No-Tillage on Soil Organic Carbon Fractions in a Continuous Maize Cropping System of Northeast China. *Pedosphere* **20**, 285-292.

Jiang, P., Anderson, S. H., Kitchen, N. R., Sudduth, K. A., and Sadler, E. J. (2007). Estimating Plant-Available Water Capacity for Claypan Landscapes Using Apparent Electrical Conductivity. *Soil Science Society of America Journal* **71**, 1902-1908.

Johnson, H., Baker, J., Shrader, W., and Laflen, J. (1979). Tillage System Effects on Sediment and Nutrients in Runoff from Small Watersheds. *Transactions of the ASABE* **22**, 1110-1114.

Kumar, S., Kadono, A., Lal, R., and Dick, W. (2012). Long-Term No-Till Impacts on Organic Carbon and Properties of Two Contrasting Soils and Corn Yields in Ohio. *Soil Science Society of America Journal* **76**, 1798-1809.

Lerch, R., Baffaut, C., Sadler, E., and Kremer, R. (2015). Long-Term Agroecosystem Research in the Central Mississippi River Basin: Goodwater Creek Experimental Watershed and Regional Herbicide Water Quality Data. *Journal of Environmental Quality* **44**, 28-36.

Lerch, R., Kitchen, N., Kremer, R., Donald, W., Alberts, E., Sadler, E., Sudduth, K., Myers, D., and Ghidey, F. (2005). Development of a Conservation-Oriented Precision Agriculture System: Water and Soil Quality Assessment. *Journal of Soil and Water Conservation* **60**, 411-421.

Lobell, D. B., and Field, C. B. (2007). Global Scale Climate–Crop Yield Relationships and the Impacts of Recent Warming. *Environmental Research Letters* **2**, 014002.

Maurer, E. P., Brekke, L., Pruitt, T., and Duffy, P. P. (2007). Fine-Resolution Climate Projections Enhance Regional Climate Change Impact Studies. *Eos, Transactions of American Geophysical Union* **88**, 504.

Mills, W., Thomas, A., and Langdale, G. (1988). Rainfall Retention Probabilities Computed for Different Cropping-Tillage Systems. *Agricultural Water Management* **15**, 61-71.

Moore, E., Wiedenhoeft, M., Kaspar, T., and Cambardella, C. (2014). Rye Cover Crop Effects on Soil Quality in No-Till Corn Silage–Soybean Cropping Systems. *Soil Science Society of America Journal* **78**, 968-976.

Moriasi, D. N., Gitau, M. W., Pai, N., and Daggupati, P. (2015). Hydrologic and Water Quality Models: Performance Measures and Evaluation Criteria. *Transactions of the ASABE* **58**, 1763-1785.

Mudgal, A., Anderson, S., Baffaut, C., Kitchen, N., and Sadler, E. (2010). Effects of Long-Term Soil and Crop Management on Soil Hydraulic Properties for Claypan Soils. *Journal of Soil and Water Conservation* **65**, 393-403.

Mudgal, A., Baffaut, C., Anderson, S., Sadler, E., Kitchen, N., Sudduth, K., and Lerch, R. (2012). Using the Agricultural Policy/Environmental Extender to Develop and Validate Physically Based Indices for the Delineation of Critical Management Areas. *Journal of Soil and Water Conservation* **67**, 284-299.

Novara, A., Pisciotta, A., Minacapilli, M., Maltese, A., Capodici, F., Cerdà, A., and Gristina, L. (2018). The Impact of Soil Erosion on Soil Fertility and Vine Vigor. A Multidisciplinary Approach Based on Field, Laboratory and Remote Sensing Approaches. *Science of The Total Environment* **622**, 474-480.

Plaster, E. (2013). "Soil Science and Management," Cengage Learning, Boston, MA.

Poeplau, C., and Don, A. (2015). Carbon Sequestration in Agricultural Soils Via Cultivation of Cover Crops – a Meta-Analysis. *Agriculture, Ecosystems & Environment* **200**, 33-41.

Rabalais, N. N., Turner, R. E., and Wiseman Jr, W. J. (2002). Gulf of Mexico Hypoxia, Aka "the Dead Zone". *Annual Review of Ecology and Systematics* **33**, 235-263.

Reeves, D. (1997). The Role of Soil Organic Matter in Maintaining Soil Quality in Continuous Cropping Systems. *Soil and Tillage Research* **43**, 131-167.

Rochette, P., Angers, D. A., Chantigny, M. H., MacDonald, J. D., Bissonnette, N., and Bertrand, N. (2009). Ammonia Volatilization Following Surface Application of Urea to Tilled and No-Till Soils: A Laboratory Comparison. *Soil and Tillage Research* **103**, 310-315.

Rosenzweig, C., Jones, J. W., Hatfield, J. L., Ruane, A. C., Boote, K. J., Thorburn, P., Antle, J. M., Nelson, G. C., Porter, C., Janssen, S., Asseng, S., Basso, B., Ewert, F., Wallach, D., Baigorria, G., and Winter, J. M. (2013). The Agricultural Model Intercomparison and Improvement Project (Agmip): Protocols and Pilot Studies. *Agricultural and Forest Meteorology* **170**, 166-182.

Rosenzweig, C., Tubiello, F. N., Goldberg, R., Mills, E., and Bloomfield, J. (2002). Increased Crop Damage in the Us from Excess Precipitation under Climate Change. *Global Environmental Change* **12**, 197-202.

Sadler, E. J., Lerch, R. N., Kitchen, N. R., Anderson, S. H., Baffaut, C., Sudduth, K. A., Prato, A. A., Kremer, R. J., Vories, E. D., and Myers, D. B. (2015a). Long-

Term Agroecosystem Research in the Central Mississippi River Basin: Introduction, Establishment, and Overview. *Journal of Environmental Quality* **44**, 3-12.

Sadler, E. J., Sudduth, K. A., Drummond, S. T., Vories, E. D., and Guinan, P. E. (2015b). Long-Term Agroecosystem Research in the Central Mississippi River Basin: Goodwater Creek Experimental Watershed Weather Data. *Journal of Environmental Quality* **44**, 13-17.

Schlenker, W., and Roberts, M. J. (2009). Nonlinear Temperature Effects Indicate Severe Damages to Us Crop Yields under Climate Change. *Proceedings of the National Academy of Sciences* **106**, 15594-15598.

Sudduth, K., Kitchen, N., Bollero, G., Bullock, D., and Wiebold, W. (2003). Comparison of Electromagnetic Induction and Direct Sensing of Soil Electrical Conductivity. *Agronomy Journal* **95**, 472-482.

Sudduth, K., Kitchen, N., Wiebold, W., Batchelor, W., Bollero, G., Bullock, D., Clay, D., Palm, H., Pierce, F., and Schuler, R. (2005). Relating Apparent Electrical Conductivity to Soil Properties across the North-Central USA. *Computers and Electronics in Agriculture* **46**, 263-283.

Tellatin, S., and Myers, R. (2017). Cover Crops at Work: Keeping Nutrients out of Waterways. *In* "Cover Crop Resource Series". SARE and the University of Missouri.

Tuppad, P., Kannan, N., Srinivasan, R., Rossi, C. G., and Arnold, J. G. (2010). Simulation of Agricultural Management Alternatives for Watershed Protection. *Water Resources Management* **24**, 3115-3144.

Ullrich, A., and Volk, M. (2009). Application of the Soil and Water Assessment Tool (Swat) to Predict the Impact of Alternative Management Practices on Water Quality and Quantity. *Agricultural Water Management* **96**, 1207-1217.

Williams, J. R., and Izaurralde, R. (2006). "Watershed Model," CRC Press, Boca Raton, FL.

Zhang, Y., Hernandez, M., Anson, E., Nearing, M., Wei, H., Stone, J., and Heilman, P. (2012). Modeling Climate Change Effects on Runoff and Soil Erosion in Southeastern Arizona Rangelands and Implications for Mitigation with Conservation Practices. *Journal of Soil and Water Conservation* **67**, 390-405.

Table 5.1. Parameters and selected value used in simulation of runoff and water quality using APEX model for field 1.

Parameter ID	Parameter name	Parameter range	Selected value
Parameter that affect runoff			
12	Soil evaporation coefficient	1.5-2.5	1.5
16	Expands CN retention parameter	1-1.5	1.5
17	Plant cover factor for evaporation	0-0.5	0.05
20	CN initial abstraction	0.05-4	0.2
34	Hargreaves equation exponent	0.5-0.6	0.6
46	RUSLE C-factor coefficient	0.5-1.5	0.5
51	Water stored in residue coefficient	0.1-0.9	0.9
Parameters that affect atrazine fate and transport			
24	Pesticide leaching ratio	0.1-1	0.15
Parameters that affect biological processes (e.g., microbial degradation)			
29	Biological mixing efficiency	0.1-0.5	0.10
31	Maximum depth for biological mixing	0.1-0.3	0.30
69	Microbial activity adjustment	0.1-1	0.2
70	Microbial decay rate coefficient	0.5-1.5	0.5
Parameters that affect dissolved nitrogen fate and transport			
4	Water storage N leaching	0-1	0.55
14	Nitrate leaching ratio	0.1-1	0.20
28	Upper nitrogen fixation limit	0.1-20	2
54	N enrichment ratio coefficient	0.3-0.9	0.6
80	Upper limit of nitrification-volatilization	0-0.5	0.1
86	N upward movement by evaporation coefficient	0.001-20	1
Parameters that affect dissolved phosphorus fate and transport			
8	Soluble P runoff coefficient	10-20	13
30	Soluble P runoff exponent	1-1.5	1.3
58	P enrichment ratio exponent	0.3-0.9	0.6
59	P upward movement by evaporation coefficient	1-20	1
84	P mineralization coefficient	0.001-20	0.2

Table 5.2. Calibration and validation of daily runoff and water quality parameters

Variable	Calibration (1993-1998)			Validation (1999-2003)		
	r^2	NSE	RSR	r^2	NSE	RSR
Runoff	0.94	0.94	0.25	0.86	0.86	0.37
Atrazine	0.81	0.79	0.46	0.85	0.57	0.66
Nitrate	0.5	0.49	0.72	0.5	0.47	0.73
Phosphorus	0.54	0.52	0.66	0.47	0.47	0.73

Table 5.3. Ensemble median and quartiles of annual simulated water yield, surface runoff and evapotranspiration

Water Yield (% Change due management change BAU to ASP)				
	RCP 4.5		RCP 8.5	
	Near Future	Far Future	Near Future	Far Future
Median	-5.9	-7.6	-0.9	-0.2
1st Quartile	-14.2	-3.2	-7.9	-6.8
3rd Quartile	-13.1	2.9	2.9	1.7
Surface Runoff				
Median	-21.9	-23.6	-16.5	-18.8
1st Quartile	-37.9	-30.0	-29.6	-24.4
3rd Quartile	-17.3	2.9	-10	-10
Evapotranspiration				
Median	-1.6	-1.9	-3	-3.5
1st Quartile	0.9	0.5	-0.4	-1.1
3rd Quartile	-2	-3.2	-5.9	-3.8
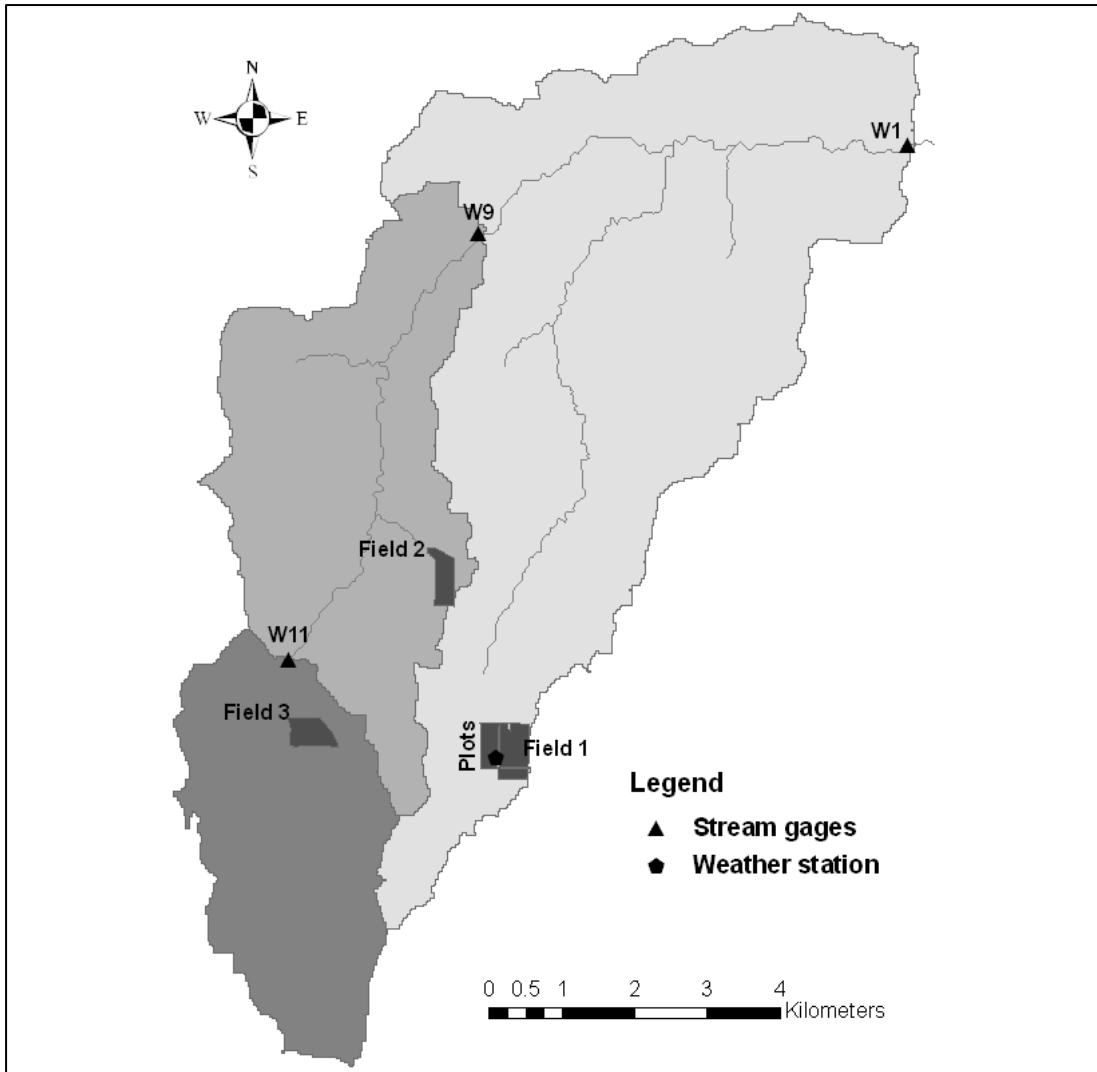
Figure 5.1. Location of Field 1 and weather station within Goodwater Creek
Experimental Watershed.
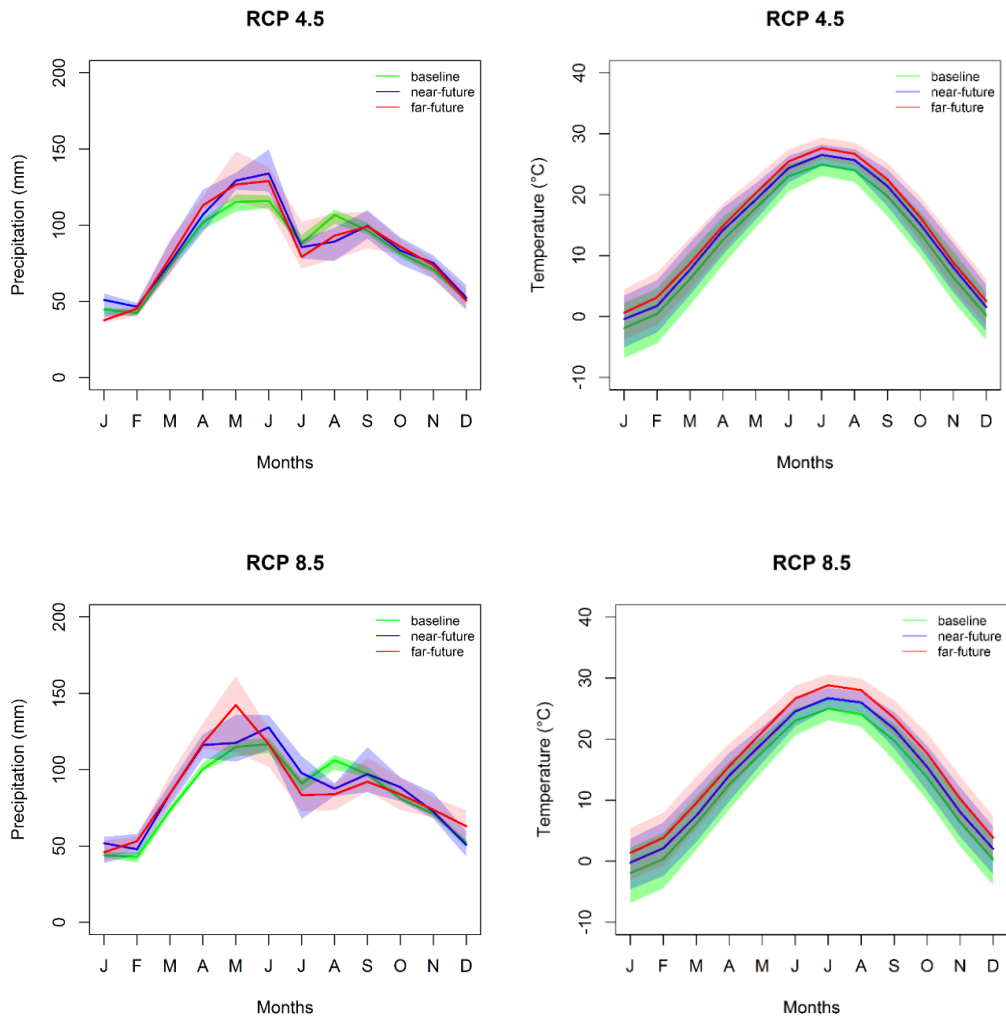
Figure 5.2. Monthly ensemble median and quartile of downscaled monthly precipitation and temperature for historic and future projections in field 1. The median is represented by the solid line with Q1 represented by the lower bound of the shaded region and Q3 represented by the upper bound of the shaded region.
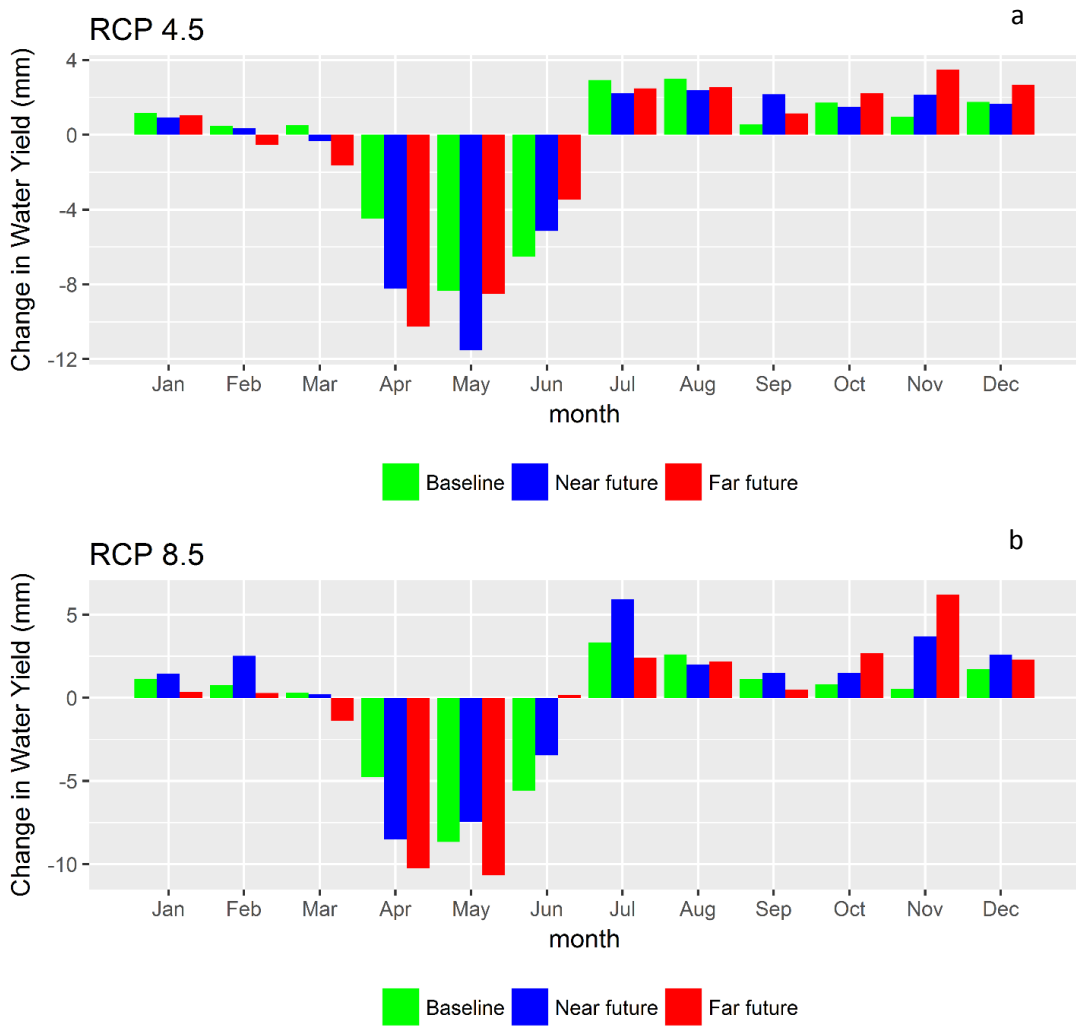
Figure 5.3. Monthly change in ensemble median water yield (mm) after implementation of aspirational management scenario a) model forced RCP 4.5 models and b) model forced with RCP 8.5 climate models
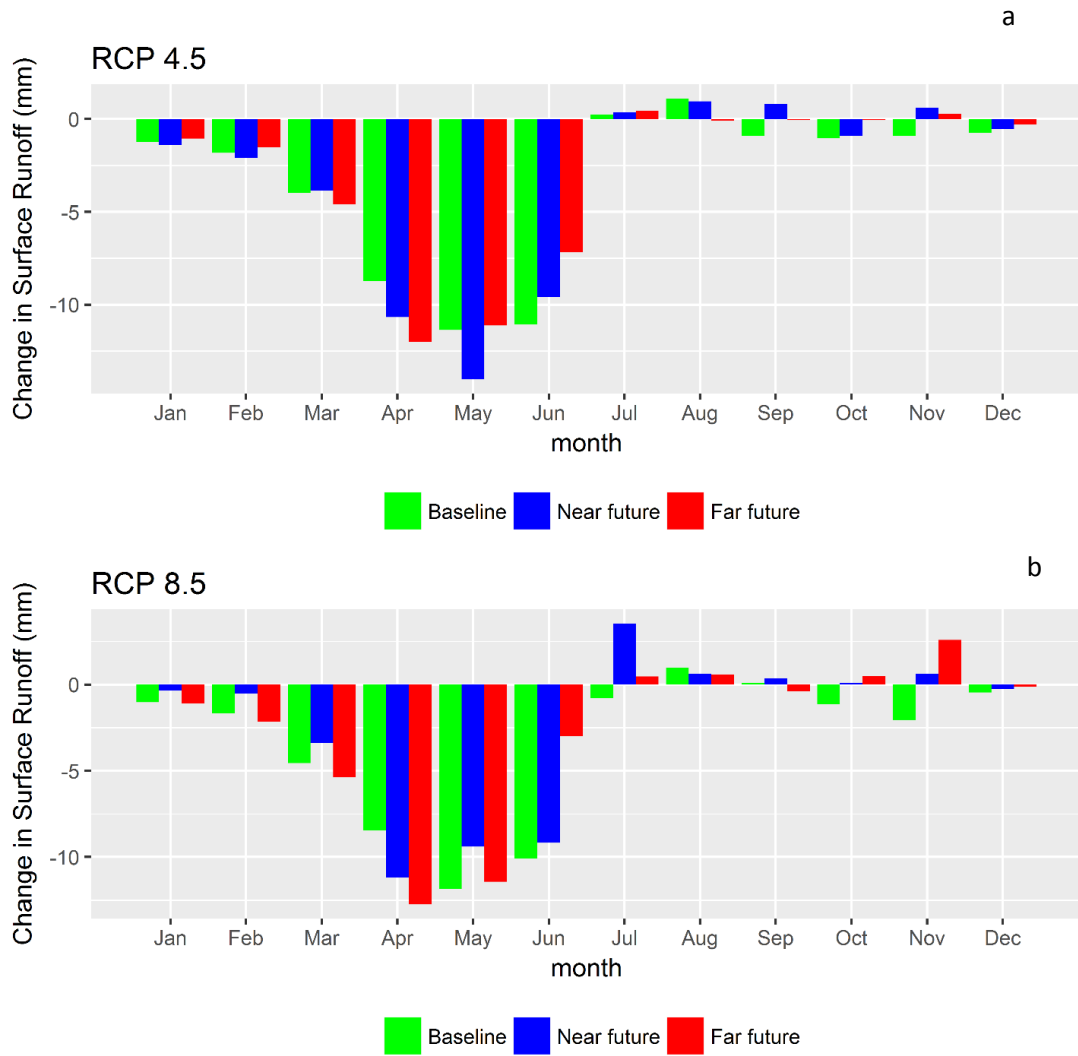
Figure 5.4. Monthly change in ensemble median surface runoff (mm) after implementation of aspirational management scenario a) model forced with RCP 4.5 climate data and b) model forced with RCP 8.5 climate data.
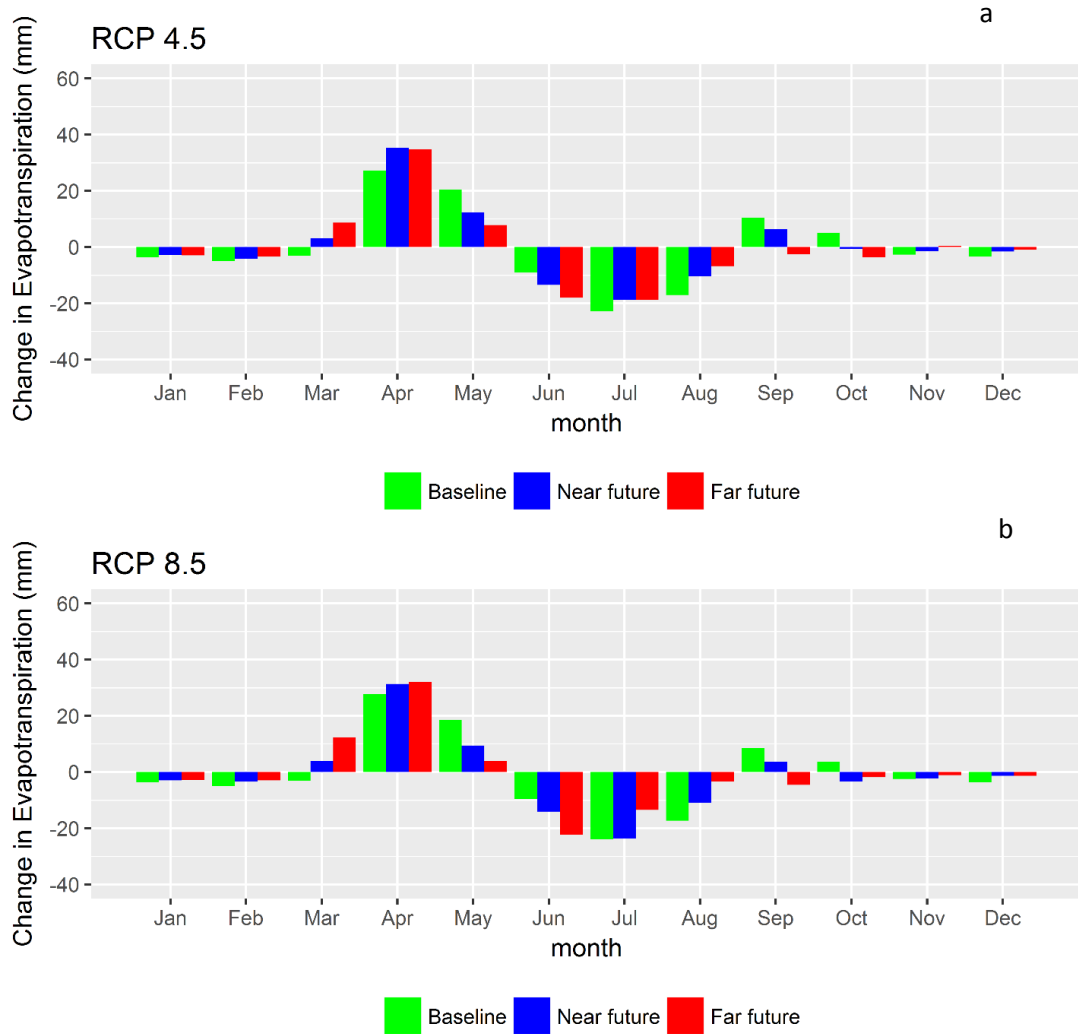
Figure 5.5. Monthly change in ensemble median evapotranspiration (mm) after implementation of Aspirational management scenario a) model forced RCP 4.5 models and b) model forced with RCP 8.5 climate models
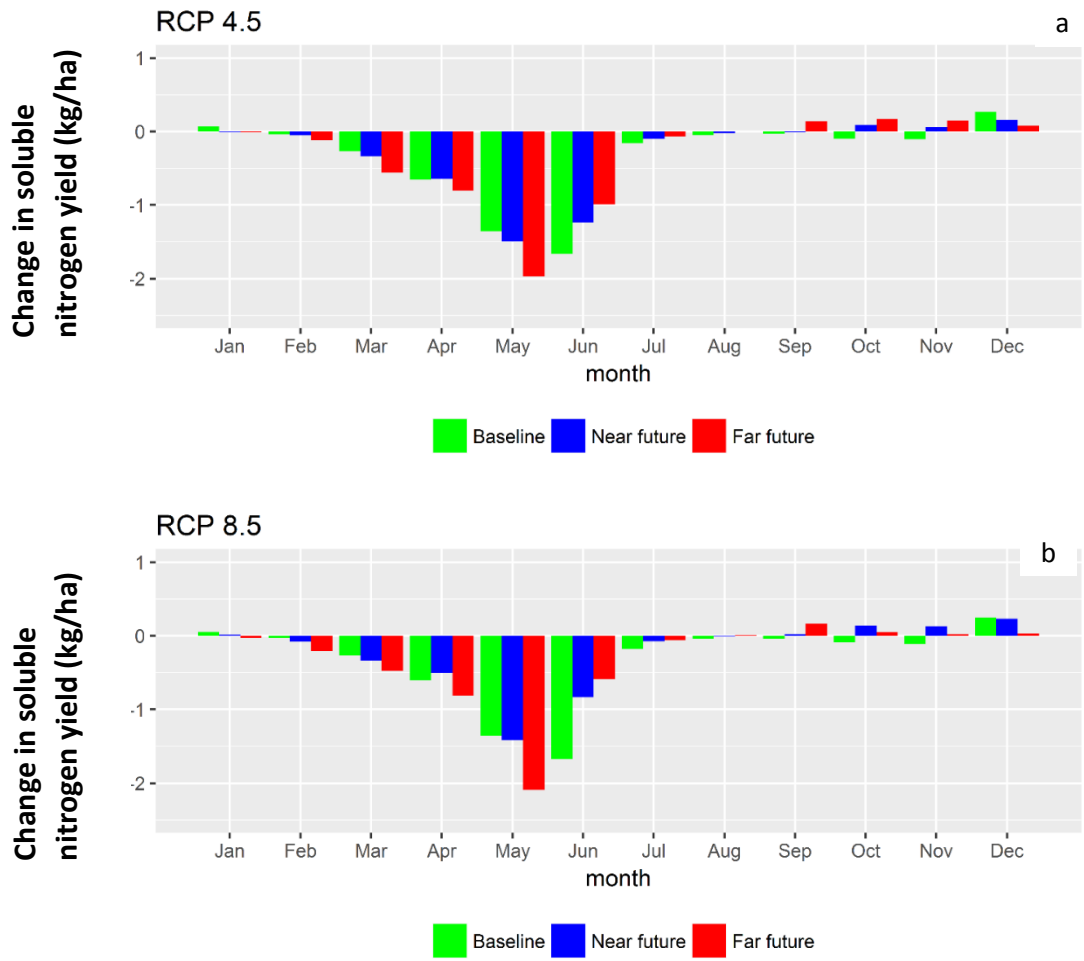
Figure 5.6. Monthly change in ensemble median soluble nitrogen yield (kg/ha) after implementation of Aspirational management scenario a) model forced RCP 4.5 models and b) model forced with RCP 8.5 climate models

CHAPTER 6

CONCLUSIONS

Future impacts of climate change on hydrologic components of Goodwater Creek Experimental Watershed (GCEW) and experimental field (Field 1) were simulated using watershed and field scale hydrologic model Soil and Water Assessment Tool (SWAT) and Agricultural Policy Environmental eXtender (APEX), respectively. Multiple climate model predictions from the Coupled Model Intercomparison Project (CMIP5) were statistically downscaled and used for SWAT simulation. Climate model output and future SWAT simulated hydrology data were used to predict future occurrence of drought and extreme events. Further, Field scale study was focused to simulate alternative management scenarios.

The following conclusions are determined from three simulation studies:

Study 1- Hydrological impact of climate change over GCEW

1. Downscaled climate model projections suggested an increase in spring precipitation and increased temperatures in the future for the study region, with the magnitude varying with the GCM model and emission scenarios. The change in precipitation for the extreme scenario (RCP 8.5) ranged from −7% to 16% for near future, and from −10% to 28% for far future scenarios.

2. Results showed increased water yield, surface runoff during spring months, and a shift in ET for all the RCPs except RCP 2.6 in the far future. The greatest increase in the median water yield and surface runoff (29% and 30%) compared to the baseline was for the far future of the most extreme future climate scenario, i.e., RCP 8.5.

3. The shift in the peak ET from July to June for RCP 4.5, RCP 6.0, and RCP 8.5 indicated the probable impact of increased CO_2 concentration and temperature

145

on planting dates and seasonality, which may ultimately impact future crop yields.

4. The comparison with gridded model output indicated that hydrological modeling at larger scales fails to capture peak and minimum runoff, which may be very important for adaptation responses at local scales. Average annual surface runoff during 2016–2075 was over-estimated by 6–8% using LPJmL and under-estimated by 5–30% using JeDi-DGVM, compared to the simulated SWAT results. Global gridded data with coarse spatial resolution does not capture small-scale details that are necessary for agricultural management decisions.

5. Simulation using higher spatial resolution, as well as additional downscaling of weather data provided by CMIP5, helps to adequately represent the hydrological components of small watersheds. This may be particularly important in watersheds with problematic soils, such as claypan soils found in GCEW and the surrounding region, which have a very thin top-soil layer above a claypan to hold and supply water to plants.

Study 2- Multi-index evaluation of future drought and extreme over GCEW

1. The results from meteorological drought indicate increased frequency of dry months for both RCPs for winter, summer, and fall seasons for both near and far future. Hydrologic drought indicates increase in the frequency of hydrologic drought for all four seasons. The results from agricultural drought indicate increased frequency of dry months for all RCPs for both spring and summer months for future.

2. The results from the precipitation-based indices indicates an increase in heavy precipitation days and amount for the spring season and decrease in heavy precipitation days and amount for summer season. The results based on the warm spell duration indicator indicates significant increase in WSDI days for future for all the RCPs.

3. The results based on both drought and extreme indices indicate extreme summer with dry and hot condition. In addition, projected increase in heavy precipitation days and amount during spring may lead to more frequent wet field conditions during planting time hindering agricultural management. Future studies should focus on building mitigation scenarios to combat the impact of these changes.

Study 3- Management and climate change impact assessment at field scale

1. Comparison of two management scenarios, business as usual (two year corn-soybean rotation) and aspirational scenario (three year corn-soybean-wheat rotation with no-till), demonstrate the benefits of aspirational management system on runoff and nitrogen loss reduction for both historic and future period.

2. The change in management alone from BAU to ASP during the historic period (1981-2010) resulted in 25% less annual median simulated runoff. The median annual runoff loss was reduced by 16.5% and 18.8% in ASP scenario compared to BAU for ensemble of RCP 8.5 for near (2016-2045) and far future (2046-2075) respectively.

3. Aspirational scenarios resulted in reduction in average simulated annual soluble nitrogen yield. Average annual values of simulated soluble nitrate loss based on ensemble of multiple models were simulated to be 15.7 kg/ha for

147

BAU management compared to 13.8 kg/ha for ASP for models forced with

RCP 8.5 for 60-year future period. Although, there is a benefit of ASP for

reduction of nitrogen in water there is higher denitrification and volatilization

loss of nitrogen under ASP compared to BAU.

APPENDICES

APPENDIX 1

Supplemental Table 3.S1. List of the model used for impact assessment.

SN	Model	SN	Model
1	bcc-csm1-1.1.rcp26	25	ipsl-cm5a-mr.1.rcp26
2	bcc-csm1-1.1.rcp45	26	ipsl-cm5a-mr.1.rcp45
3	bcc-csm1-1.1.rcp60	27	ipsl-cm5a-mr.1.rcp60
4	bcc-csm1-1.1.rcp85	28	ipsl-cm5a-mr.1.rcp85
5	ccsm4.1.rcp26	29	miroc-esm.1.rcp26
6	ccsm4.2.rcp26	30	miroc-esm.1.rcp45
7	ccsm4.1.rcp45	31	miroc-esm.1.rcp60
8	ccsm4.2.rcp45	32	miroc-esm.1.rcp85
9	ccsm4.1.rcp60	33	miroc-esm-chem.1.rcp26
10	ccsm4.2.rcp60	34	miroc-esm-chem.1.rcp45
11	ccsm4.1.rcp85	35	miroc-esm-chem.1.rcp60
12	ccsm4.2.rcp85	36	miroc-esm-chem.1.rcp85
13	gfdl-esm2g.1.rcp26	37	miroc5.1.rcp26
14	gfdl-esm2g.1.rcp45	38	miroc5.1.rcp45
15	gfdl-esm2g.1.rcp60	39	miroc5.1.rcp60
16	gfdl-esm2g.1.rcp85	40	miroc5.1.rcp85
17	gfdl-esm2m.1.rcp26	41	mri-cgcm3.1.rcp26
18	gfdl-esm2m.1.rcp45	42	mri-cgcm3.1.rcp45
19	gfdl-esm2m.1.rcp60	43	mri-cgcm3.1.rcp60
20	gfdl-esm2m.1.rcp85	44	mri-cgcm3.1.rcp85
21	ipsl-cm5a-lr.1.rcp26	45	noresm1-m.1.rcp26
22	ipsl-cm5a-lr.1.rcp45	46	noresm1-m.1.rcp45
23	ipsl-cm5a-lr.1.rcp60	47	noresm1-m.1.rcp60
24	ipsl-cm5a-lr.1.rcp85	48	noresm1-m.1.rcp85

Supplemental Table 3.S2. Monthly additive factor used for the bias correction of maximum temperature using delta method for all the models

Model SN.	Jan	Feb	Mar	Apr	May	Jun	Jul	Aug	Sep	Oct	Nov	Dec
1	-0.90	-0.31	0.91	-1.04	-1.12	-1.11	-1.64	-1.50	-2.09	-2.31	-0.19	-0.34
2	-1.24	-0.82	0.58	-1.04	-1.04	-1.04	-1.89	-1.49	-1.99	-2.37	-0.87	-0.55
3	-1.27	-0.46	0.67	-0.91	-1.36	-1.18	-1.95	-1.49	-1.95	-2.75	-0.69	-0.57
4	-0.97	-0.45	0.38	-1.27	-1.09	-1.15	-1.95	-1.69	-2.06	-2.41	-0.37	-0.28
5	-0.64	-1.01	-0.76	-1.19	-1.80	-1.29	-1.66	-1.37	-1.65	-1.49	-0.56	-1.42
6	-0.84	-0.96	-0.53	-1.37	-1.75	-1.40	-2.04	-1.68	-1.70	-1.89	-1.12	-1.35
7	-0.62	-0.84	-0.50	-1.09	-1.94	-1.33	-1.91	-1.47	-1.85	-1.81	-0.65	-1.30
8	-0.76	-0.39	-0.24	-1.11	-1.91	-1.28	-2.04	-1.57	-1.87	-1.77	-1.13	-1.05
9	-1.04	-1.05	-1.05	-1.09	-1.95	-1.19	-1.72	-1.50	-1.64	-1.54	-0.79	-1.59
10	-0.65	-0.03	-0.22	-1.15	-1.91	-1.47	-2.18	-1.76	-1.82	-1.93	-0.81	-1.13
11	-1.24	-1.32	-0.63	-1.15	-1.90	-1.26	-1.87	-1.41	-1.67	-1.78	-0.64	-1.48
12	-0.64	-0.23	-0.23	-1.17	-1.96	-1.62	-2.07	-1.73	-1.93	-1.93	-1.12	-1.35
13	-0.21	-0.99	-0.05	-1.29	-1.71	-1.25	-1.91	-1.43	-1.59	-2.25	-0.84	-1.32
14	-0.39	-1.21	-0.33	-1.18	-1.65	-1.24	-1.70	-1.27	-1.67	-2.42	-0.89	-0.83
15	-0.36	-1.26	0.26	-1.13	-1.62	-1.42	-1.84	-1.23	-1.59	-2.06	-0.91	-1.14
16	-0.37	-0.96	-0.11	-1.27	-1.77	-1.25	-1.75	-1.23	-1.60	-2.17	-0.82	-1.02
17	-0.64	-0.86	-0.06	-0.81	-1.66	-1.22	-1.64	-1.23	-1.62	-1.97	-1.07	-1.13
18	-0.21	-0.83	-0.03	-0.80	-1.64	-1.09	-1.61	-1.18	-1.46	-1.87	-0.76	-1.43
19	-0.45	-1.11	-0.26	-0.76	-1.49	-1.23	-1.66	-1.15	-1.73	-1.82	-0.84	-1.28
20	-0.27	-1.25	-0.07	-0.73	-1.76	-1.30	-1.78	-1.19	-1.62	-1.98	-0.65	-1.11
21	-0.70	-1.70	0.21	-1.25	-2.01	-1.80	-2.06	-1.45	-1.66	-2.02	-1.39	-1.11
22	-0.99	-1.78	0.25	-1.41	-2.09	-1.79	-2.08	-1.51	-1.66	-1.97	-1.63	-1.35
23	-0.87	-1.55	0.06	-1.23	-2.04	-1.74	-2.05	-1.41	-1.57	-2.13	-1.20	-1.18
24	-0.93	-1.47	0.56	-1.01	-1.94	-1.69	-2.05	-1.51	-1.77	-2.00	-1.12	-1.06
25	-0.88	-0.40	-0.26	-1.06	-1.84	-1.65	-1.58	-1.49	-1.84	-1.50	-0.65	-0.66
26	-0.69	-0.36	-0.30	-0.84	-1.79	-1.48	-1.43	-1.33	-1.81	-1.14	-0.60	-0.70
27	-0.74	-0.64	-0.34	-1.03	-2.00	-1.60	-1.65	-1.44	-1.74	-1.44	-0.65	-0.79
28	-0.79	-0.46	-0.19	-1.13	-1.73	-1.52	-1.54	-1.46	-1.69	-1.45	-0.61	-0.46

29	-1.01	-0.84	-0.28	-1.25	-1.25	-1.32	-1.60	-1.42	-1.70	-1.32	-0.52	-1.12
30	-1.44	-0.87	-0.06	-1.20	-1.24	-1.36	-1.75	-1.76	-2.06	-1.47	-0.73	-1.28
31	-1.03	-1.07	-0.32	-1.18	-1.21	-1.37	-1.66	-1.47	-1.93	-1.33	-0.36	-0.96
32	-1.05	-0.70	-0.26	-1.30	-1.30	-1.28	-1.69	-1.60	-1.90	-1.47	-0.47	-1.36
33	-0.35	0.02	0.38	-1.01	-1.57	-1.08	-1.43	-1.36	-1.36	-1.56	-0.37	-1.50
34	-0.41	-0.17	0.32	-0.57	-1.44	-1.13	-1.40	-1.27	-1.39	-1.50	-0.48	-1.13
35	-0.38	0.00	0.50	-0.87	-1.65	-1.08	-1.40	-1.36	-1.60	-1.71	-0.58	-1.06
36	-0.30	-0.10	0.58	-0.77	-1.71	-1.15	-1.49	-1.38	-1.29	-1.47	-0.56	-1.19
37	-0.53	0.19	0.17	-0.89	-1.41	-1.25	-1.73	-1.43	-1.57	-1.93	-0.91	-0.93
38	-0.92	-0.17	-0.03	-1.19	-1.56	-1.23	-1.68	-1.52	-1.69	-2.15	-0.89	-1.17
39	-0.59	0.13	0.14	-1.06	-1.53	-1.34	-1.74	-1.48	-1.83	-2.00	-0.76	-0.86
40	-0.83	-0.35	-0.07	-1.15	-1.47	-1.23	-1.70	-1.47	-1.68	-2.10	-0.95	-0.99
41	-0.91	-0.89	0.38	-1.09	-1.21	-1.13	-1.48	-1.29	-0.71	-0.97	0.02	-0.86
42	-0.64	-0.66	0.00	-0.88	-1.32	-1.11	-1.48	-1.31	-0.83	-0.98	-0.20	-0.65
43	-0.93	-0.80	0.21	-0.94	-1.33	-0.98	-1.38	-1.24	-0.85	-1.05	-0.10	-0.75
44	-0.77	-0.66	-0.16	-1.06	-1.26	-1.21	-1.39	-1.22	-0.75	-1.18	-0.21	-0.90
45	-0.57	-0.89	-0.24	-0.57	-1.51	-1.26	-1.60	-1.35	-1.70	-1.38	-0.64	-0.69
46	-0.37	-0.84	-0.48	-0.61	-1.22	-1.24	-1.58	-1.52	-1.80	-1.57	-0.58	-0.43
47	-0.62	-0.92	-0.36	-0.51	-1.42	-1.23	-1.69	-1.62	-1.81	-1.63	-0.54	-0.55
48	-0.22	-0.75	-0.34	-0.56	-1.44	-1.17	-1.55	-1.41	-1.82	-1.58	-0.54	-0.26

Supplemental Table 3.S3. Monthly additive factor used for the bias correction of minimum temperature using delta method for all the models

Model SN	Jan	Feb	Mar	Apr	May	Jun	Jul	Aug	Sep	Oct	Nov	Dec
1	0.36	0.83	1.95	0.54	0.62	0.30	-0.03	-0.08	-0.68	-0.44	0.91	0.95
2	0.11	0.54	1.84	0.56	0.72	0.34	-0.23	-0.10	-0.47	-0.35	0.46	0.76
3	-0.02	0.74	1.88	0.60	0.44	0.25	-0.27	-0.11	-0.61	-0.61	0.65	0.75
4	0.27	0.83	1.69	0.34	0.57	0.27	-0.32	-0.27	-0.60	-0.42	0.74	0.96
5	0.27	0.83	1.69	0.34	0.57	0.27	-0.32	-0.27	-0.60	-0.42	0.74	0.96
6	0.77	0.55	1.09	0.24	0.20	0.00	-0.36	-0.26	-0.27	0.00	0.48	0.18
7	0.98	0.44	1.11	0.49	-0.09	0.06	-0.33	-0.17	-0.47	0.22	0.84	0.20
8	0.76	0.99	1.36	0.47	0.05	0.10	-0.38	-0.17	-0.37	0.21	0.27	0.38
9	0.65	0.38	0.66	0.53	-0.10	0.18	-0.22	-0.18	-0.22	0.49	0.85	-0.02
10	0.94	1.40	1.42	0.42	0.07	-0.02	-0.45	-0.29	-0.38	-0.02	0.66	0.37
11	0.48	0.13	1.02	0.44	-0.06	0.13	-0.32	-0.07	-0.24	0.19	1.03	0.11
12	0.93	1.13	1.35	0.38	0.02	-0.18	-0.43	-0.31	-0.54	-0.04	0.40	0.16
13	1.23	0.57	1.15	0.14	-0.01	0.14	-0.30	0.01	0.16	0.02	0.93	0.37
14	1.04	0.43	1.01	0.11	0.01	0.17	-0.13	0.13	0.02	0.04	0.82	0.73
15	1.01	0.42	1.41	0.19	0.02	0.01	-0.27	0.17	0.05	0.30	0.83	0.49
16	1.05	0.56	1.10	0.05	-0.10	0.16	-0.13	0.15	0.10	0.14	0.83	0.66
17	0.74	0.26	1.34	0.55	0.05	0.33	-0.12	0.13	-0.01	0.19	0.80	0.25
18	1.13	0.31	1.34	0.56	0.15	0.46	-0.12	0.20	0.04	0.17	1.07	0.03
19	0.94	0.15	1.16	0.64	0.25	0.29	-0.10	0.28	-0.14	0.36	1.03	0.10
20	1.09	0.04	1.33	0.64	0.05	0.23	-0.18	0.24	-0.04	0.06	1.14	0.23
21	0.76	-0.09	1.41	0.49	-0.21	-0.28	-0.41	-0.02	-0.19	-0.08	0.19	0.45
22	0.49	-0.17	1.48	0.37	-0.29	-0.26	-0.44	-0.08	-0.18	0.06	0.01	0.30
23	0.62	0.10	1.37	0.52	-0.27	-0.23	-0.38	0.03	-0.07	-0.09	0.24	0.33
24	0.54	0.15	1.72	0.71	-0.16	-0.19	-0.41	-0.09	-0.28	-0.01	0.36	0.36
25	0.88	0.97	1.37	0.51	-0.02	-0.06	0.10	-0.01	-0.31	0.34	0.81	0.80
26	1.03	0.97	1.30	0.63	-0.01	0.00	0.20	0.08	-0.33	0.60	0.88	0.75
27	0.92	0.71	1.22	0.48	-0.18	-0.08	0.00	-0.04	-0.18	0.48	0.85	0.72
28	0.88	0.90	1.29	0.41	0.02	-0.01	0.13	-0.04	-0.21	0.36	0.91	1.00
29	0.48	0.55	1.11	0.22	0.41	0.04	-0.09	-0.08	-0.45	0.48	0.89	0.44

30	0.25	0.64	1.43	0.26	0.39	0.05	-0.20	-0.27	-0.62	0.38	0.76	0.33
31	0.47	0.39	1.17	0.24	0.43	0.04	-0.19	-0.13	-0.55	0.53	1.04	0.62
32	0.42	0.72	1.21	0.18	0.37	0.06	-0.18	-0.16	-0.58	0.42	0.99	0.29
33	1.04	1.15	1.64	0.45	0.17	0.31	-0.03	-0.10	-0.10	0.32	1.31	0.26
34	1.08	0.95	1.52	0.77	0.23	0.22	0.00	-0.02	-0.14	0.30	1.17	0.51
35	1.13	1.12	1.73	0.53	0.03	0.31	0.04	-0.07	-0.26	0.17	1.15	0.60
36	1.22	1.14	1.73	0.64	0.04	0.21	-0.03	-0.11	-0.06	0.35	1.19	0.49
37	1.19	1.31	1.45	0.48	0.20	0.18	-0.21	-0.09	-0.08	0.16	0.69	0.72
38	0.78	0.98	1.24	0.31	0.11	0.20	-0.18	-0.17	-0.28	-0.10	0.74	0.45
39	1.08	1.31	1.42	0.42	0.10	0.11	-0.23	-0.16	-0.29	0.05	0.72	0.73
40	0.87	0.86	1.28	0.32	0.12	0.23	-0.18	-0.14	-0.15	0.00	0.65	0.65
41	0.60	0.42	1.60	0.47	0.50	0.30	0.05	0.01	0.64	0.90	1.54	0.64
42	0.91	0.67	1.27	0.70	0.38	0.32	0.05	0.01	0.59	0.92	1.24	0.77
43	0.58	0.42	1.44	0.60	0.36	0.51	0.13	0.07	0.54	0.82	1.39	0.74
44	0.71	0.59	1.15	0.50	0.45	0.24	0.11	0.12	0.63	0.73	1.28	0.66
45	1.17	0.65	1.10	0.73	0.17	0.23	-0.03	-0.06	-0.26	0.53	0.80	0.81
46	1.35	0.80	0.79	0.72	0.48	0.26	-0.05	-0.20	-0.33	0.31	0.84	0.99
47	1.18	0.61	1.04	0.79	0.26	0.27	-0.14	-0.25	-0.27	0.28	0.80	0.82
48	1.48	0.76	0.96	0.80	0.31	0.30	-0.03	-0.11	-0.38	0.44	0.89	1.17

Supplemental Table 3.S4. Monthly scaling factor used for the bias correction of precipitation using quantile mapping for gage25 datasets for all the models

Model SN.	Jan	Feb	Mar	Apr	May	Jun	Jul	Aug	Sep	Oct	Nov	Dec
1	1.35	2.17	1.72	1.58	1.20	1.87	2.23	2.71	1.64	0.98	0.85	2.87
2	1.35	2.17	2.08	1.58	1.20	2.33	1.31	2.59	1.64	0.98	0.85	2.87
3	1.35	2.17	2.08	1.58	1.20	2.33	2.23	2.71	1.64	0.98	0.85	2.87
4	1.35	2.17	1.71	1.35	1.20	2.33	2.23	2.71	1.64	0.98	0.85	2.87
5	1.73	2.37	1.95	2.48	1.17	2.70	2.49	2.67	2.23	1.43	1.20	4.72
6	1.87	1.76	1.92	1.89	1.14	2.88	2.70	2.66	2.16	1.38	1.23	2.69
7	1.73	2.37	1.95	2.48	1.17	2.70	2.49	2.67	2.23	1.43	1.32	4.72
8	2.03	1.76	1.65	2.27	1.14	2.88	2.70	2.66	2.16	1.38	1.23	2.69
9	1.73	2.37	1.95	2.48	1.17	2.70	2.49	2.67	2.23	1.43	1.32	4.40
10	2.03	1.76	1.31	2.27	1.14	2.88	2.70	2.66	2.16	1.38	1.12	2.69
11	1.73	2.37	1.95	2.48	1.17	2.28	2.25	2.67	2.23	1.43	1.32	4.72
12	2.03	1.76	1.92	2.27	1.14	2.24	2.70	2.66	2.16	1.38	1.23	2.69
13	1.69	3.66	1.61	2.24	1.21	2.74	2.36	2.89	2.31	1.66	1.38	3.03
14	1.69	3.04	1.53	2.24	1.13	2.74	2.36	2.89	2.31	1.85	1.38	3.03
15	1.69	2.40	1.61	2.24	1.21	2.74	2.36	2.89	2.31	1.38	1.15	3.03
16	1.69	2.69	1.61	2.24	1.21	2.74	2.36	1.71	2.31	1.22	0.79	3.03
17	1.49	2.60	1.52	1.71	1.48	2.07	1.89	3.42	1.96	1.51	0.91	2.88
18	1.49	2.60	1.52	1.71	1.48	2.07	1.89	3.42	1.96	1.51	0.91	2.88
19	1.49	2.60	1.52	1.71	1.48	2.07	1.89	3.42	1.96	1.51	0.86	2.88
20	1.49	2.60	1.52	1.71	1.48	2.07	1.89	2.62	1.96	1.51	0.91	2.88
21	1.46	2.79	1.33	1.95	1.42	2.89	2.40	2.79	1.45	1.13	0.99	2.74
22	1.46	2.79	1.33	1.95	1.42	2.89	2.44	2.79	1.28	1.13	0.99	2.74
23	1.46	2.79	1.33	1.95	1.42	2.49	2.44	2.79	1.45	1.13	0.99	2.74
24	1.46	2.79	1.17	1.95	1.42	2.43	2.44	2.79	1.45	1.13	0.99	2.74
25	1.89	2.03	1.89	2.55	1.87	2.95	1.52	3.02	2.15	1.58	1.17	3.62
26	1.94	2.03	1.82	2.55	1.87	2.95	1.52	3.02	2.15	1.58	1.17	3.62
27	1.43	2.03	1.94	1.45	1.40	2.95	1.52	3.02	1.91	1.58	1.17	3.62

|												
28	2.06	2.03	1.94	2.55	1.30	2.95	1.52	3.02	2.15	1.58	1.17	3.62
29	1.83	1.93	1.52	1.62	1.47	3.04	2.40	3.19	1.62	1.17	1.27	2.54
30	1.83	1.93	1.52	1.62	1.47	3.04	2.40	3.19	1.62	1.17	1.41	2.54
31	1.83	1.93	1.52	1.62	1.47	3.04	2.40	3.05	1.62	1.17	1.01	2.54
32	1.83	1.93	1.52	1.62	1.47	3.04	1.84	3.19	1.62	1.17	1.27	2.50
33	1.76	2.84	1.67	2.58	1.18	2.95	2.18	2.65	1.82	1.53	1.10	3.42
34	1.76	1.84	1.75	2.58	1.18	2.95	2.18	2.65	1.82	1.53	1.05	3.42
35	1.47	2.84	1.75	2.58	1.18	2.77	2.18	2.65	1.82	1.53	1.07	2.19
36	1.55	2.84	1.75	2.51	1.18	2.95	2.18	2.65	1.82	1.53	1.10	3.42
37	1.70	3.29	1.55	2.95	1.08	2.73	2.69	2.89	2.09	1.35	0.93	3.34
38	1.70	3.29	1.55	3.20	1.08	2.73	2.69	2.89	2.09	1.35	0.93	3.34
39	1.70	3.29	1.55	3.10	1.08	2.73	2.57	2.89	2.09	1.35	0.93	2.98
40	1.70	3.29	1.55	3.20	1.08	2.73	2.69	2.89	2.09	1.35	0.93	3.34
41	1.54	1.75	1.64	2.12	1.27	3.06	2.45	3.34	2.05	2.08	1.03	4.23
42	1.54	1.75	1.64	2.12	1.27	3.88	2.45	3.26	2.05	1.60	1.11	4.23
43	1.54	1.75	1.64	2.12	1.27	3.88	2.45	2.67	2.05	2.21	1.11	4.23
44	1.54	1.75	1.64	2.12	1.27	3.88	2.45	3.34	2.05	2.21	1.11	3.87
45	1.84	2.13	1.81	1.95	1.74	2.75	1.77	2.52	2.21	1.76	1.41	3.87
46	1.84	2.13	1.81	1.95	1.74	2.75	1.77	2.52	2.21	1.76	1.37	3.87
47	1.24	2.13	1.81	1.95	1.74	2.49	1.77	2.52	2.21	1.76	1.41	3.87
48	1.84	2.13	1.81	1.95	1.74	2.75	1.77	2.52	2.05	1.74	1.39	3.87

Supplemental Table 3.S5. Monthly precipitation threshold (mm) used for the bias correction of precipitation using quantile mapping for gage25 datasets for all the models

Model SN.	Jan	Feb	Mar	Apr	May	Jun	Jul	Aug	Sep	Oct	Nov	Dec
1	1.32	1.81	2.10	1.93	2.71	3.55	3.57	2.46	2.27	1.20	1.84	1.60
2	1.50	1.86	2.01	2.02	2.68	3.54	3.24	2.63	2.09	1.04	1.90	1.66
3	1.32	1.87	2.07	2.10	2.62	3.55	3.23	2.69	2.43	0.98	1.83	1.57
4	1.37	1.86	2.03	1.94	2.85	3.27	3.08	2.44	2.12	1.17	2.09	1.64
5	1.27	2.26	2.12	2.49	3.27	3.87	3.86	3.33	2.84	1.97	2.09	1.73
6	1.34	2.13	2.41	2.49	2.99	4.00	3.13	3.14	3.34	1.84	1.99	1.92
7	1.25	1.88	2.18	2.48	3.32	3.75	3.41	3.34	2.88	1.90	2.00	1.56
8	1.40	1.92	2.36	2.41	2.84	4.26	3.13	3.17	3.24	1.70	2.04	1.63
9	1.31	2.11	2.18	2.58	3.35	3.91	3.91	3.29	2.59	1.83	2.07	1.66
10	1.38	1.92	2.41	2.36	2.78	4.00	3.03	3.03	3.15	1.70	2.14	1.92
11	1.09	2.09	2.34	2.44	3.31	3.73	3.75	3.31	2.72	2.03	2.13	1.59
12	1.49	1.97	2.36	2.33	2.92	4.04	3.19	3.03	3.42	1.86	1.91	1.75
13	1.39	1.48	2.10	2.61	2.67	4.14	3.69	2.64	2.14	1.12	1.97	1.89
14	1.44	1.55	2.04	2.61	2.72	3.81	3.69	2.84	2.31	0.94	2.23	1.75
15	1.38	1.48	2.23	2.61	2.76	4.24	3.69	2.85	2.41	1.09	2.06	1.99
16	1.43	1.71	2.30	2.60	2.67	4.20	3.76	2.85	2.31	1.21	2.19	1.99
17	1.33	1.99	1.94	2.67	2.87	3.84	3.70	3.61	2.29	1.23	2.02	1.69
18	1.33	1.70	2.00	2.73	2.48	3.73	3.87	3.70	2.61	1.36	1.88	1.70
19	1.34	2.07	1.94	2.75	2.56	3.47	3.76	3.37	2.53	1.24	1.96	1.70
20	1.38	1.87	1.84	2.64	2.51	3.55	3.70	3.72	2.44	1.34	1.96	1.70
21	1.39	1.50	2.70	1.97	2.59	2.79	3.74	2.69	2.59	1.90	1.59	1.46
22	1.36	1.56	2.88	1.87	2.87	2.65	3.34	2.74	2.78	1.80	1.60	1.39
23	1.26	1.52	2.63	2.05	2.62	2.79	3.35	2.74	2.78	1.76	1.72	1.58
24	1.19	1.47	2.84	1.97	2.73	2.69	3.72	2.77	2.69	1.88	1.73	1.56
25	0.89	1.98	1.62	1.90	2.48	3.35	4.03	2.68	2.93	1.59	1.82	1.89
26	0.94	1.99	1.72	2.06	2.68	3.58	4.12	2.66	3.13	1.79	1.61	1.94
27	0.98	1.97	1.73	2.00	2.62	3.57	3.96	2.82	2.63	1.66	1.64	1.90
28	0.91	2.08	1.75	1.93	2.57	3.35	3.88	2.82	2.90	1.68	1.59	1.87
29	1.28	1.94	2.19	2.32	2.87	3.43	3.40	2.68	2.54	1.99	1.83	1.69
30	1.26	2.15	1.99	2.27	2.90	3.14	3.39	2.40	2.29	1.99	1.88	1.65

31	1.19	1.97	2.12	2.39	3.02	3.23	3.40	2.68	2.28	1.77	1.83	1.68
32	1.28	1.96	2.04	2.34	2.75	3.33	3.55	2.48	2.51	1.86	1.82	1.62
33	1.41	1.48	2.14	2.51	2.56	4.11	3.27	2.48	2.30	1.66	1.65	1.68
34	1.31	1.47	2.20	2.64	2.86	4.18	3.30	2.48	2.28	1.78	1.82	1.82
35	1.30	1.67	2.19	2.70	2.87	4.11	3.30	2.59	2.36	1.58	1.90	1.57
36	1.44	1.43	2.26	2.51	2.74	4.27	3.25	2.43	2.48	1.72	1.56	1.68
37	1.21	2.03	1.99	2.62	2.73	3.11	3.25	2.89	2.62	1.62	2.22	1.63
38	1.21	2.00	2.00	2.38	2.58	3.17	3.26	2.68	2.68	1.70	2.04	1.56
39	1.22	1.99	1.99	2.48	2.70	2.96	3.08	2.77	2.18	1.64	2.50	1.65
40	1.23	2.27	1.97	2.43	2.82	3.09	3.08	2.90	2.35	1.62	2.45	1.52
41	1.25	2.11	2.20	2.44	2.89	3.21	3.98	2.87	2.95	1.89	1.72	1.83
42	1.24	2.11	2.21	2.33	2.91	3.25	3.73	3.13	2.64	1.83	1.98	1.83
43	1.13	2.30	2.22	2.31	2.92	3.11	3.73	3.19	2.69	1.74	2.02	1.85
44	1.16	2.16	2.22	2.39	2.92	3.17	3.79	2.89	2.63	1.89	2.00	1.93
45	1.21	1.84	2.11	2.73	2.94	3.36	3.30	3.37	2.56	1.70	2.27	1.57
46	1.23	1.61	2.46	2.65	2.79	3.49	3.37	3.01	2.38	1.92	2.09	1.59
47	1.18	1.87	2.33	2.82	2.94	3.41	3.31	2.91	2.35	1.79	2.39	1.38
48	1.23	1.83	2.21	2.56	2.79	3.52	3.32	3.17	2.44	1.62	2.10	1.44

a
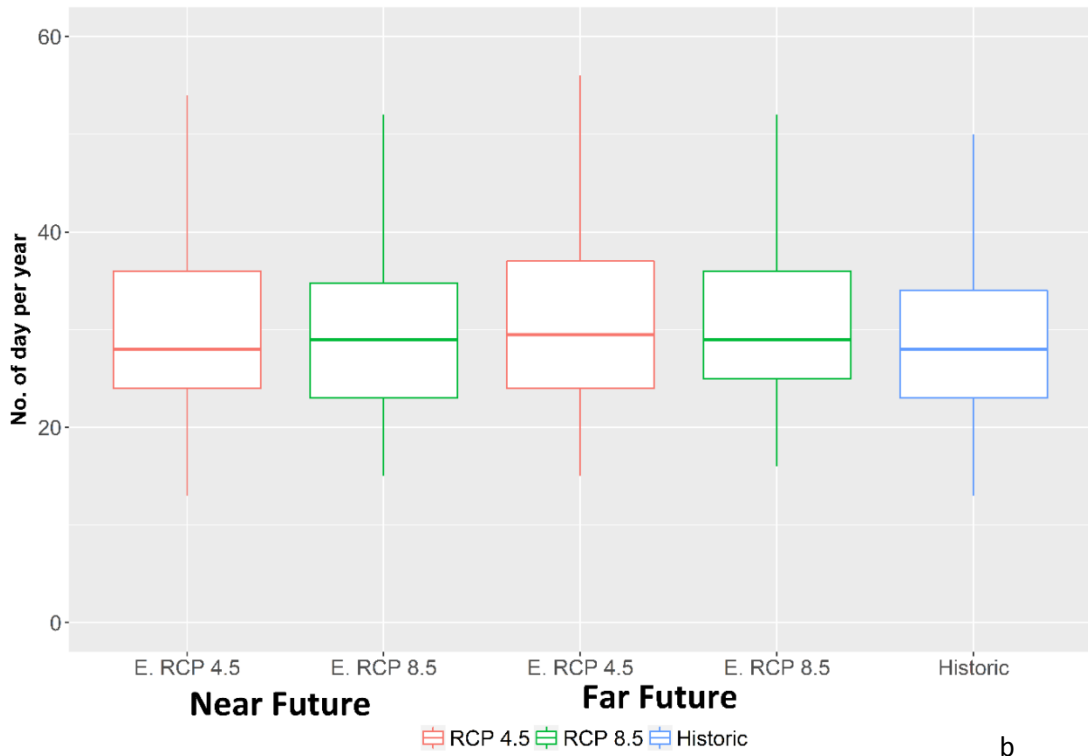
b
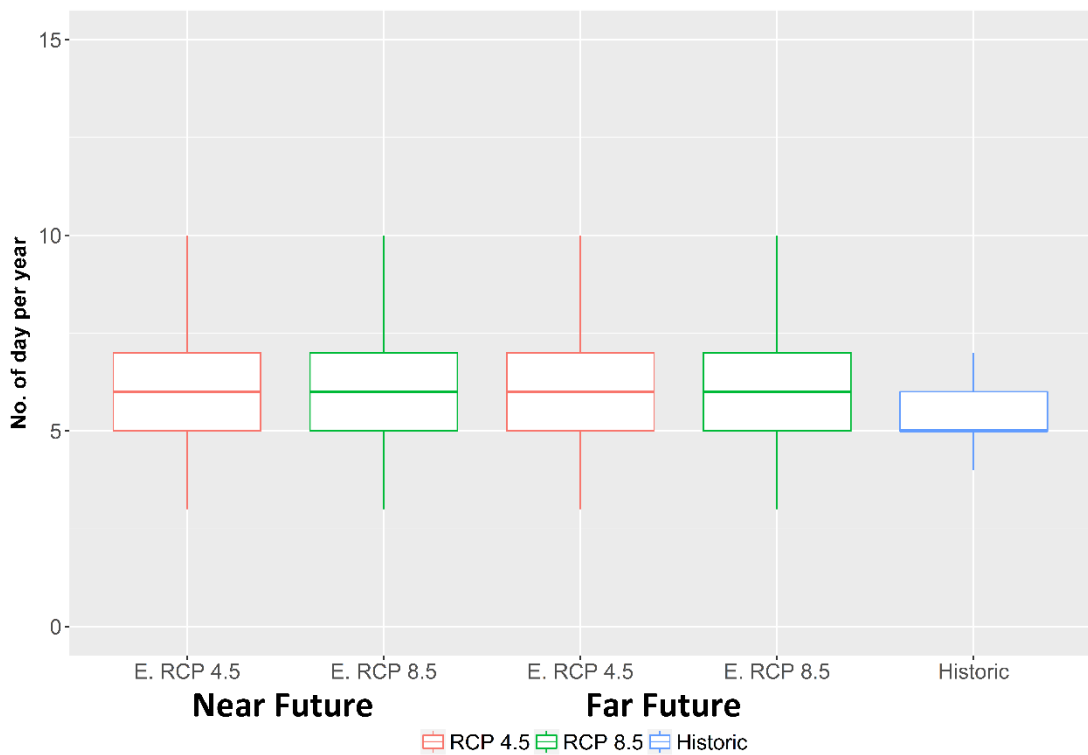
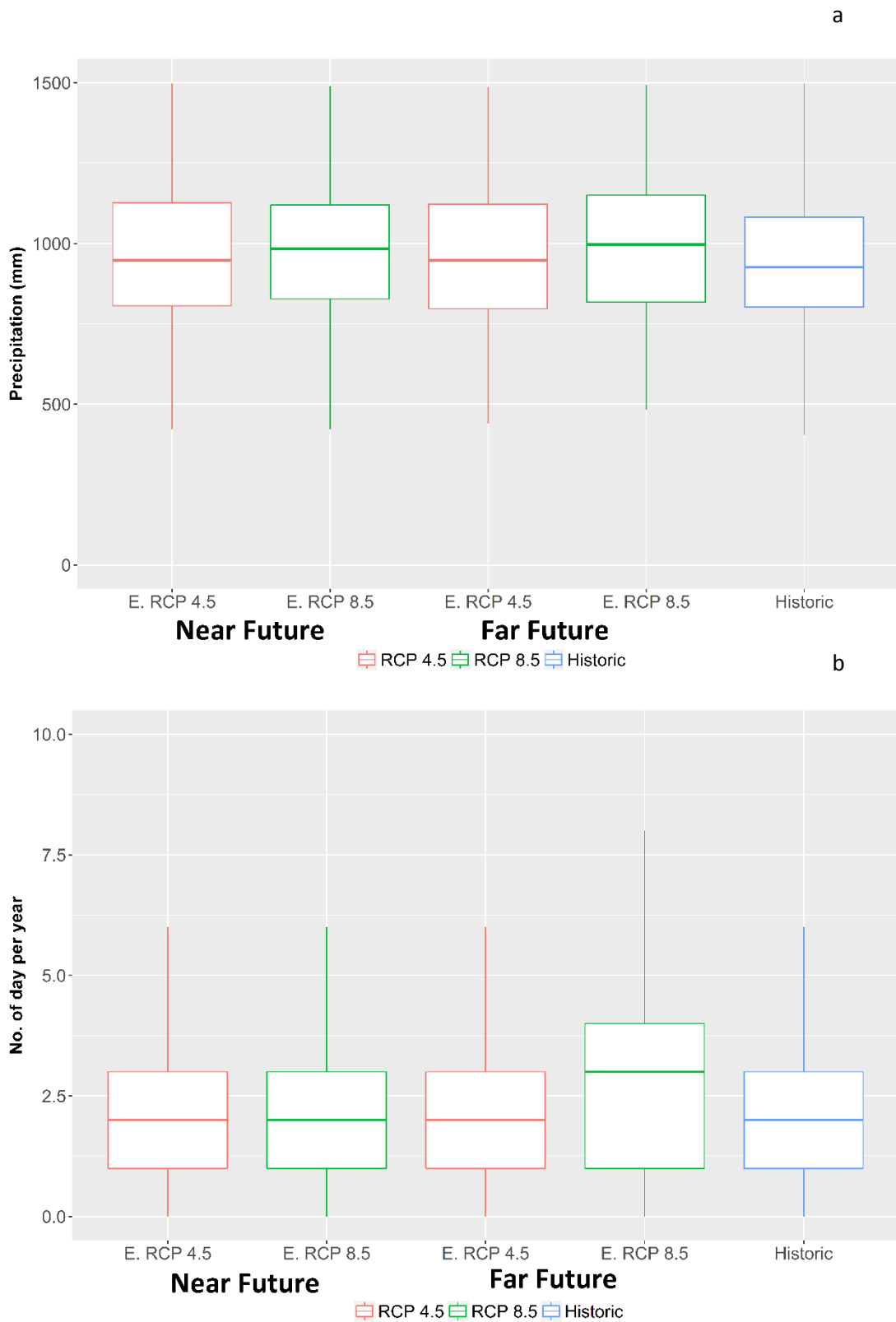Supplement fig 4.1. Projected annual count of consecutive dry days (a) and consecutive wet days (b) presented as ensemble of each of four RCP scenarios and its comparison with historic data

Supplement fig 4.2 Projected annual total precipitation (a) and annual count of days with ≥ 50 mm precipitation (b) presented as ensemble of each of four RCP scenarios and its comparison with historic data.

Supplement table 4.1. Monthly soil water (mm) threshold values that define drought classes based on Soil Moisture Index (SMI) calculation using simulate historic soil datasets for Adco soil

Month	SD	MD	Nor	MW
Jan	173	221	264	290
Feb	191	221	261	284
Mar	209	226	269	288
Apr	182	227	269	291
May	176	222	266	291
Jun	121	176	243	270
Jul	78	114	199	239
Aug	16	106	208	253
Sep	14	118	234	267
Oct	78	140	248	295
Nov	116	179	265	299
Dec	151	212	265	284

SD= Severely dry; MD= Moderately dry; Nor=Normal; MW= Moderately wet.

Soil moisture value smaller or equal to SD are considered severely dry; values greater than SD and smaller than or equal than MD is considered moderately dry; value greater than MD and smaller than or equal to Nor are consider normal and values greater than Nor and smaller than or equal to MW are considered moderately wet and values greater than MW are severely wet.

Supplement table 4.2. Monthly soil water (mm) threshold values that define drought classes based on Soil Moisture Index (SMI) calculation using simulate historic soil datasets for Armstrong soil

Month	SD	MD	Nor	MW
Jan	169	233	265	281
Feb	216	239	260	270
Mar	220	237	264	269
Apr	204	230	265	275
May	193	224	261	281
Jun	159	199	247	261
Jul	159	180	232	244
Aug	123	191	241	274
Sep	100	185	265	272
Oct	101	184	260	285
Nov	122	214	266	279
Dec	146	229	271	277

SD= Severely dry; MD= Moderately dry; Nor=Normal; MW= Moderately wet.

Soil moisture value smaller or equal to SD are considered severely dry; values greater than SD and smaller than or equal than MD is considered moderately dry; value greater than MD and smaller than or equal to Nor are consider normal and values greater than Nor and smaller than or equal to MW are considered moderately wet and values greater than MW are severely wet.

Supplement table 4.3. Monthly soil water (mm) threshold values that define drought classes based on Soil Moisture Index (SMI) calculation using simulate historic soil datasets for Belknap soil

Month	SD	MD	Nor	MW
Jan	428	493	561	594
Feb	474	498	556	580
Mar	482	510	564	589
Apr	477	514	572	602
May	477	512	578	609
Jun	427	481	560	586
Jul	410	461	539	580
Aug	400	467	538	570
Sep	370	464	556	592
Oct	348	460	557	593
Nov	390	480	564	591
Dec	406	492	561	592

SD= Severely dry; MD= Moderately dry; Nor=Normal; MW= Moderately wet.

Soil moisture value smaller or equal to SD are considered severely dry; values greater than SD and smaller than or equal than MD is considered moderately dry; value greater than MD and smaller than or equal to Nor are consider normal and values greater than Nor and smaller than or equal to MW are considered moderately wet and values greater than MW are severely wet.

Supplement table 4.4. Monthly soil water (mm) threshold values that define drought classes based on Soil Moisture Index (SMI) calculation using simulate historic soil datasets for Leonard soil

Month	SD	MD	Nor	MW
Jan	176	242	313	350
Feb	210	259	317	344
Mar	232	273	316	340
Apr	225	268	327	353
May	223	269	328	356
Jun	208	241	318	338
Jul	163	213	292	331
Aug	124	199	293	321
Sep	115	195	294	343
Oct	107	182	298	340
Nov	136	208	313	355
Dec	157	233	315	354

SD= Severely dry; MD= Moderately dry; Nor=Normal; MW= Moderately wet.

Soil moisture value smaller or equal to SD are considered severely dry; values greater than SD and smaller than or equal than MD is considered moderately dry; value greater than MD and smaller than or equal to Nor are consider normal and values greater than Nor and smaller than or equal to MW are considered moderately wet and values greater than MW are severely wet.

Supplement table 4.5. Monthly soil water (mm) threshold values that define drought classes based on Soil Moisture Index (SMI) calculation using simulate historic soil datasets for Mexico soil

Month	SD	MD	Nor	MW
Jan	314	361	394	416
Feb	352	367	390	400
Mar	345	365	396	402
Apr	322	356	394	406
May	316	352	388	412
Jun	259	314	375	392
Jul	229	274	347	366
Aug	202	283	362	405
Sep	175	284	395	407
Oct	216	310	392	421
Nov	243	335	400	411
Dec	293	355	400	408

SD= Severely dry; MD= Moderately dry; Nor=Normal; MW= Moderately wet.

Soil moisture value smaller or equal to SD are considered severely dry; values greater than SD and smaller than or equal than MD is considered moderately dry; value greater than MD and smaller than or equal to Nor are consider normal and values greater than Nor and smaller than or equal to MW are considered moderately wet and values greater than MW are severely wet.

Supplement table 4.6. Monthly soil water (mm) threshold values that define drought classes based on Soil Moisture Index (SMI) calculation using simulate historic soil datasets for Putnam soil

| Month	SD	MD	Nor	MW
Jan	321	344	374	384
Feb	331	344	372	383
Mar	327	343	377	389
Apr	307	337	375	385
May	303	334	372	379
Jun	228	285	344	371
Jul	184	229	315	349
Aug	135	232	343	382
Sep	122	259	376	386
Oct	186	288	373	399
Nov	223	317	381	400
Dec	302	339	379	390

SD= Severely dry; MD= Moderately dry; Nor=Normal; MW= Moderately wet.

Soil moisture value smaller or equal to SD are considered severely dry; values greater than SD and smaller than or equal than MD is considered moderately dry; value greater than MD and smaller than or equal to Nor are consider normal and values greater than Nor and smaller than or equal to MW are considered moderately wet and values greater than MW are severely wet.
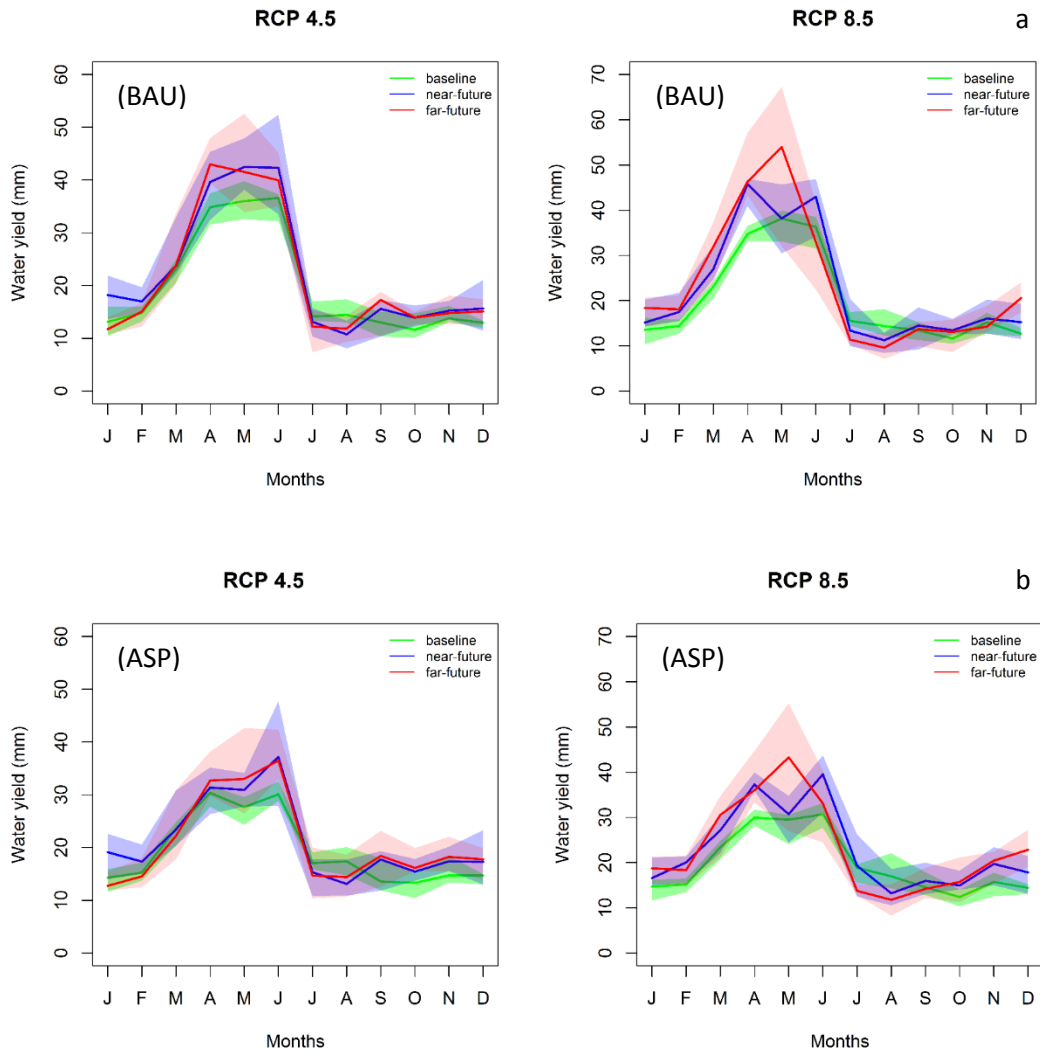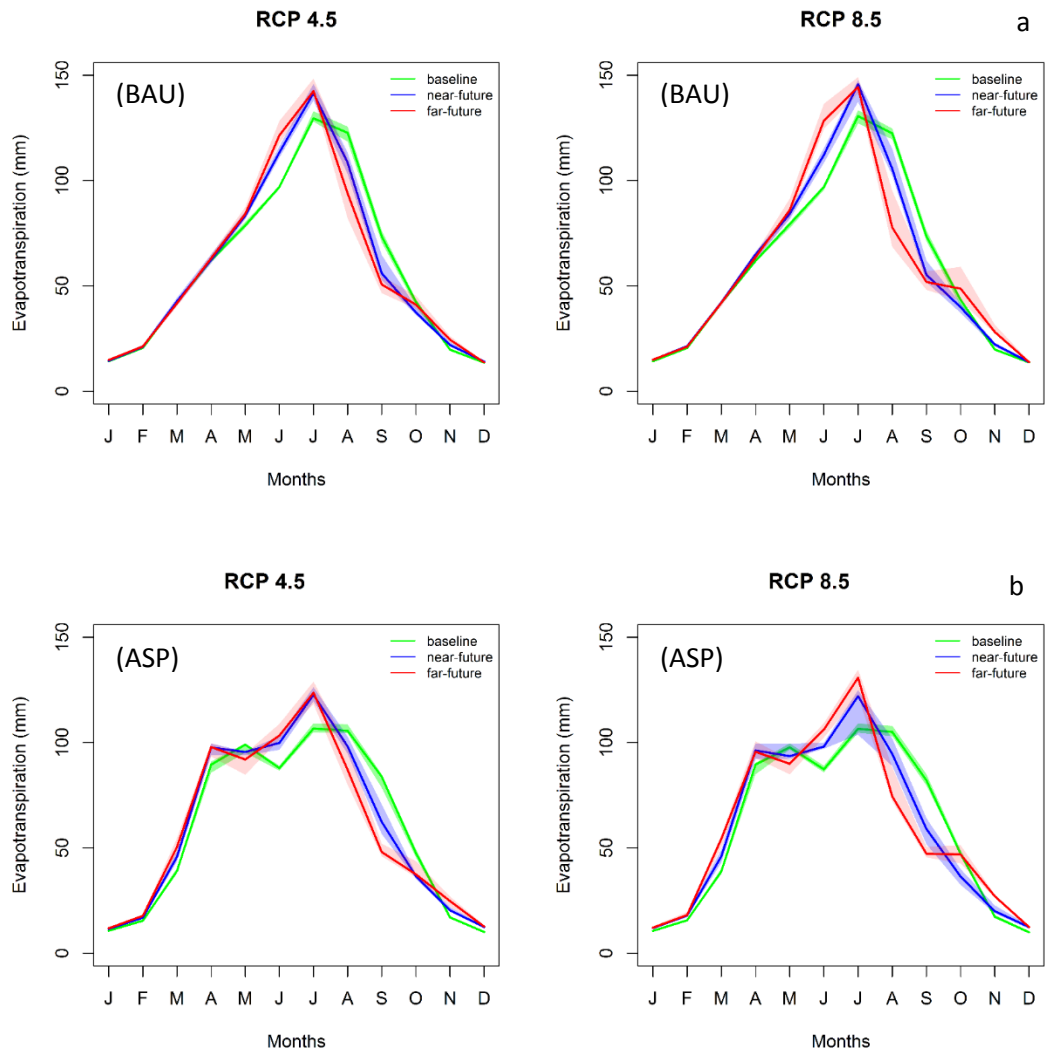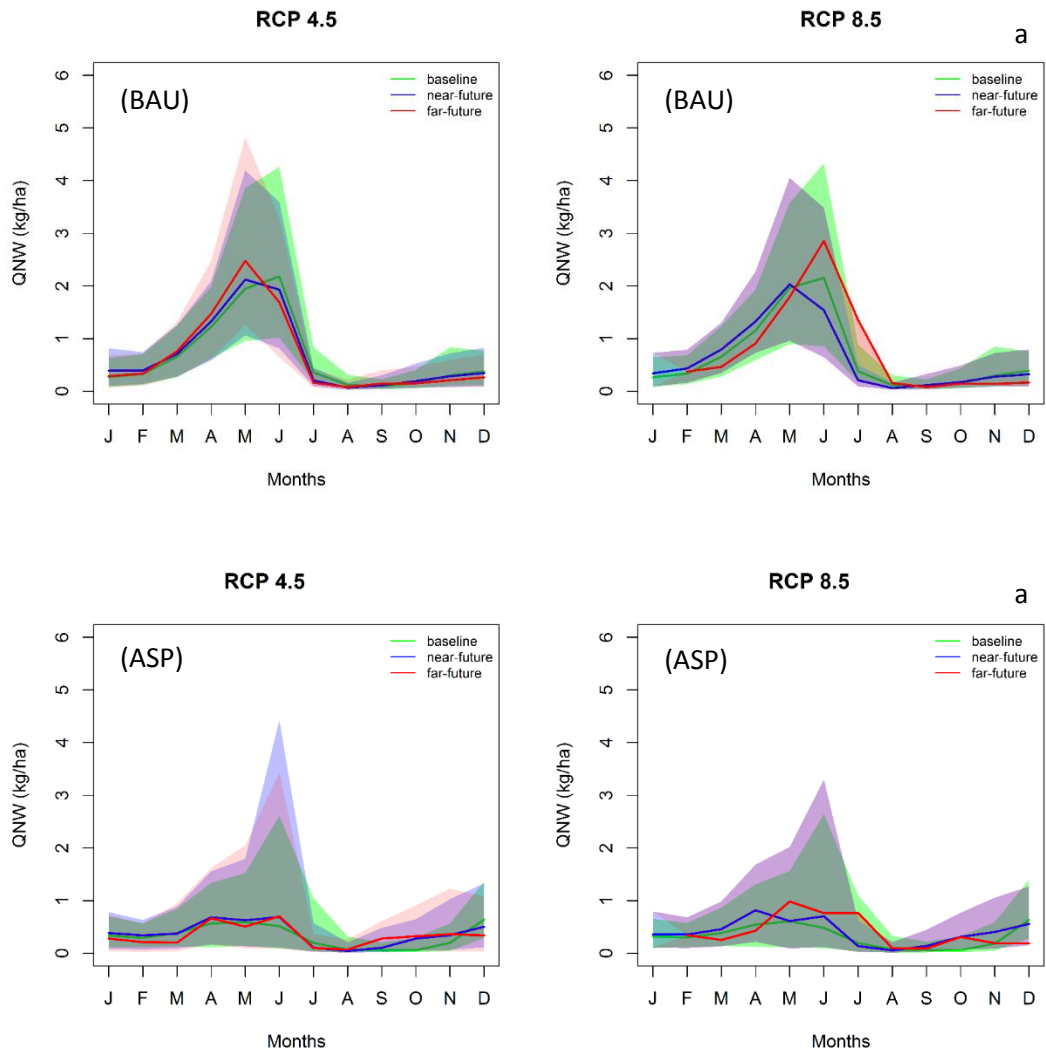
Supplement fig 5.1. Monthly ensemble median and quartile of water yield projections for Field1 for BAU (a) and ASP (b). The median is represented by the solid line with Q1 represented by the lower bound of the shaded region and Q3 represented by the upper bound of the shaded region.
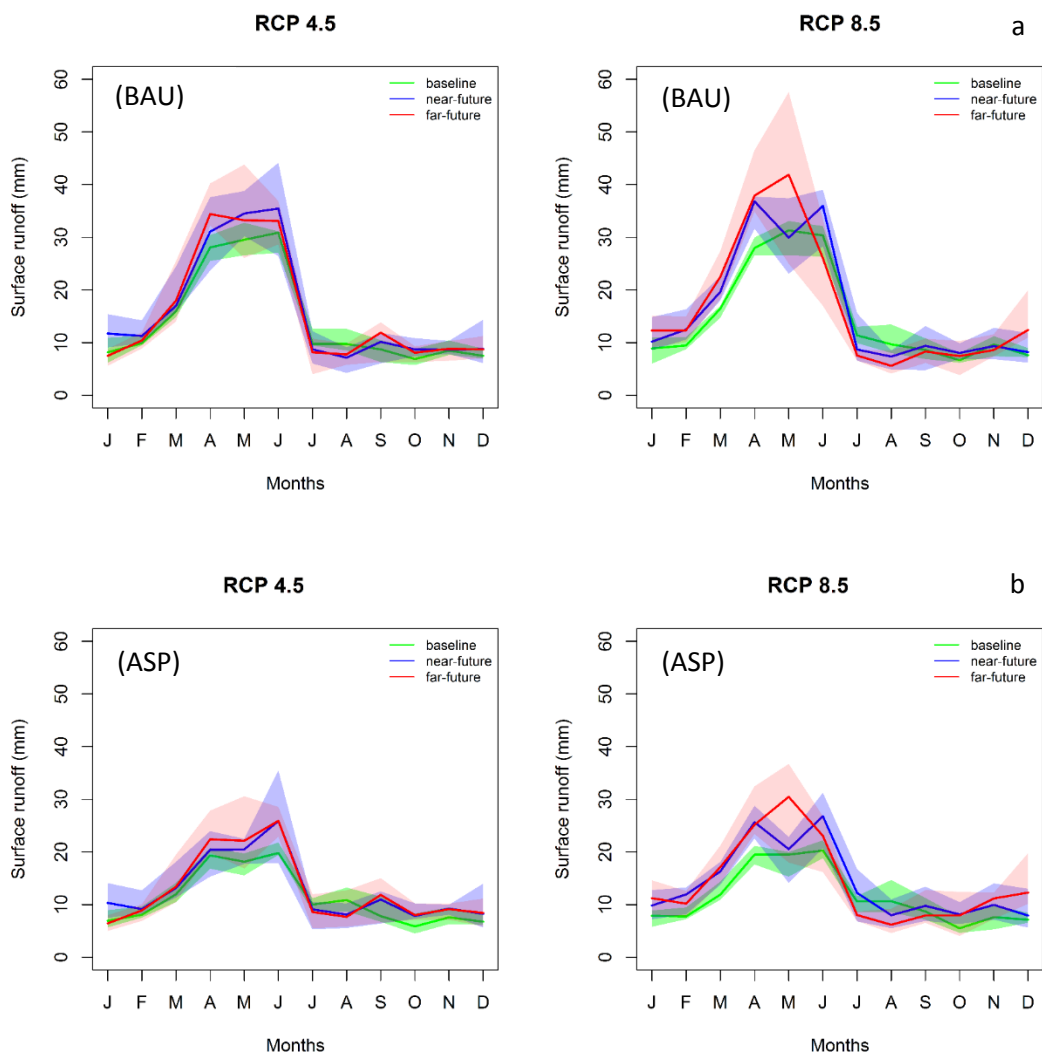
Supplement fig 5.2. Monthly ensemble median and quartile of surface runoff projections for Field1 for BAU (a) and ASP (b). The median is represented by the solid line with Q1 represented by the lower bound of the shaded region and Q3 represented by the upper bound of the shaded region.

Supplement fig 5.3. Monthly ensemble median and quartile of evapotranspiration projections for Field1 for BAU (a) and ASP (b). The median is represented by the solid line with Q1 represented by the lower bound of the shaded region and Q3 represented by the upper bound of the shaded region

Supplement fig 5.3. Monthly ensemble median and quartile of soluble nitrogen yeild for Field1 for BAU (a) and ASP (b). The median is represented by the solid line with Q1 represented by the lower bound of the shaded region and Q3 represented by the upper bound of the shaded region

VITA

Sagar Gautam was born on December 19, 1989 at Butwal, Nepal to Mrs. T.N Gautam and Mrs. M Gautam. He received his B.S. (Agriculture) in 2012 from Banaras Hindu University, Varanasi (India). He joined South Dakota State University in 2013 and received the MS in Soil Science in 2014 under the supervision of Dr. Sandeep Kumar. For his PhD, he joined University of Missouri-Columbia in 2015 and received the doctorate degree in Bioengineering in 2018 under the supervision of Dr. Christine Costello. He has accepted a Research Scientist position at Minnesota Pollution Control Agency, Saint Paul, Minnesota where he will be moving after his graduation.